CORTICAL CONNECTIVITY IN ALCOHOLISM

Evgeny Jenya Chumin

Submitted to the faculty of the University Graduate School
in partial fulfillment of the requirements
for the degree
Doctor of Philosophy
in the Program of Medical Neuroscience,
Indiana University

September 2019

Accepted by the Graduate Faculty of Indiana University, in partial fulfillment of the requirements for the degree of Doctor of Philosophy.

Doctoral Committee

David A. Kareken, Ph.D., ABPP, Chair

Mario Dzemidzic, Ph.D.

July 9, 2019

Joaquín Goñi, Ph.D.

Jaroslaw Harezlak, Ph.D.

Christopher C. Lapish, Ph.D.

Karmen K. Yoder, Ph.D.

ACKNOWLEDGEMENT

This work was supported by: funding to Dr. Karmen K. Yoder (KKY) from the Indiana University School of Medicine (IUSM) Department of Radiology and Imaging Sciences; the National Institute on Alcohol Abuse and Alcoholism (NIAAA; 5P60AA007611-25 (pilot P50 to KKY), NIAAA R21AA016901 (KKY), NIAAA R01AA018354 (KKY)); ABMRF/The Foundation for Alcohol Research (KKY); and the Indiana Clinical and Translational Sciences Institute (NIH TR000006, Indiana Clinical Research Center). Additional support was provided to Dr. Peter Finn (NIAAA AA13650) and to Dr. Hu Cheng from the Indiana Clinical and Translational Sciences Institute at Indiana University Bloomington, IN. Support for education for Mr. Chumin was provided by the IUSM Indiana Biomedical Gateway Program, the Stark Neurosciences Research Institute, NIAAA alcohol research training grant (T32AA07462, PI: Dr. Cristine Czachowski), and the NIAAA Ruth L. Kirschstein Predoctoral Individual National Research Service Award (F31AA025518).

The author gratefully acknowledges the support of his primary mentor, Karmen K. Yoder, PhD, as well as members of his dissertation committee: David A. Kareken, PHD, ABPP (chair); Mario Dzemidzic, PhD; Joaquín Goñi, PhD; Jaroslaw Harezlak, PhD; and Christopher C. Lapish, PhD. Additionally, the author would like to thank the following individuals for their assistance and support throughout the author's graduate career as well as with the included works: Daniel Albrecht, PhD; James Walters, MS; Karen Hile; Tammy Graves; Morgan Mrotek; Christine Herring; Lauren Federici; Cari Cox Lehigh; Elizabeth Patton; Meredith Halcomb, PhD; Gregory Grecco; Tarah Collins; Emma Caress; Michelle Chu; Brandon Oberlin, PhD; Claire Carron, MS; Zikai Lin, MS;

Enrico Amico, PhD; Joey Contreras, PhD; Timothy Durazzo, PhD; Sharlene Newman, PhD; Olaf Sporns, PhD; John West, MS; Rachael Deardorff, MS; Pratik Gandhi, MS; Michelle Dragoo; Courtney Robbins; Traci Day; Robert Bryant; Wendy Territo; Heather Polson; Brooke Rennie; Larry Corbin, AS; Gerry Oxford, PhD; Andy Hudmon, PhD; Ted Cummins, PhD; Gary Landreth, PhD; Nasstassia Belton; Sarah Dolan; Cristine Czachowski, PhD; Robert Steward, PhD; Gary Hutchins, PhD; Mark Green, PhD; Qi-Huang Zheng, PhD; Yu-Chen Wu, PhD; Sourajit Mustafi, PhD; Ulrike Dydak, PhD; David Edmondson, PhD.

Finally, the author thanks his family and friends for their support and encouragement, which helped make the undertaking of this work possible. The author thanks his parents Katerina Wooldridge and Gennadi Andrejev, his wife Abby Chumin, MS, and his in-laws Jay, Sherri, and Emily Hackett for their continued love and support.

Evgeny Jenya Chumin

CORTICAL CONNECTIVITY IN ALCOHOLISM

Alcoholism carries significant personal and societal burdens, and yet we still lack effective treatments for alcohol use disorders. Several lines of research have demonstrated disruption of major white matter (WM) tracts in the brains of detoxified alcoholics. Additionally, there are several reports of alterations in the dopaminergic system of alcoholics. A better understanding of the relationships of brain structure and function in the alcoholic brain is necessary to move toward more efficacious pharmacological interventions. In this dissertation, there are three main chapters. First, reduced WM integrity was reported in a sample of individuals with active alcohol use disorder (AUD). This is a relatively understudied population, which is believed to represent a less severe phenotype compared to the in-treatment samples that are typically studied. Second, higher WM integrity was reported in a sample of college-age, active AUD. In a subsample of these individuals, graph theory measures of structural brain network connectivity were shown to be altered in cigarette-smoking social-drinking controls and smoking AUD subjects, compared to nonsmoking healthy individuals. Finally, a novel multimodal approach that combines diffusion weighted imaging and [^{11}C]raclopride positron emission tomography identified differential relationships between frontostriatal connectivity and striatal dopamine tone in active AUD versus social-drinking controls. This suggests that aberrations in frontostriatal connectivity may contribute to reported differences in dopaminergic function in AUD. In summary, these results show that similar to detoxified/in-treatment alcoholics, active AUD samples

present with WM integrity alterations, and changes in both structural connectivity and frontostriatal structure/function relationships.

David A. Kareken, Ph.D., ABPP, Chair

TABLE OF CONTENTS

LIST OF TABLES

LIST OF FIGURES

LIST OF ABBREVIATIONS

γ	Gamma modularity resolution parameter
ρ	Spearman's rho
ω	Omega modularity coupling parameter
[^{11}C]PHNO	[^{11}C]-(+)-4-propyl-3,4,4a,5,6,10b-hexahydro-2H-naphtho[1,2b][1,4]oxazin-9-ol
[^{18}F]L-DOPA	3,4-dihydroxy-6-[^{18}F]fluoro-l-phenylalanine
A	ambidextrous
AA	African American
AD	axial diffusivity
ADNI	Alzheimer's Disease Neuroimaging Initiative
ADS	Alcohol Dependence Scale
AMPA	alpha-3-hydroxy-5-methyl-4-isoxazoleproprionic acid
ANOVA	analysis of variance
AUC	area under the curve
AUD	alcohol use disorder
BBR	boundary-based registration
BET	brain extraction tool
BP	binding potential
BP_{ND}	nondisplaceable binding potential
BrAC	breath alcohol concentration
CA	co-classification
CH2	Colin 27 MNI brain
CON	controls
CSF	cerebrospinal fluid
cyclic AMP	cyclic adenosine monophosphate
DA	dopamine
DAergic	dopaminergic
DSM-IV	Diagnostic and Statistical Manual of Mental Disorders IV
DSM-V	Diagnostic and Statistical Manual of Mental Disorders V
DTI	diffusion tensor imaging
DWI	diffusion weighted imaging
EEG	electroencephalogram
F	female
FA	fractional anisotropy
FACT	fiber assignment by continuous tracking
FAL	[^{18}F]fallypride
FAST	FMRIB's Automated Segmentation Tool
FDG	2-deoxy-2-[^{18}F]-fluoro-D-glucose
FDR	false discovery rate
FH	family history
FIRST	FMRIB's subcortical segmentation tool
FLIRT	FMRIB's Linear Registration Tool
fMRI	functional magnetic resonance imaging
FNIRT	FMRIB's Nonlinear Registration Tool

FSL	Functional MRI of the Brain Software Library
FWE	family-wise error
GABA	gamma-aminobutyric acid
GLU	glutamate
GLUergic	glutamatergic
GM	gray matter
GRAPPA	Generalized Autocalibrating Partially Parallel Acquisition
HL	Hispanic Latino
IV	intravenous
L	left
LTD	long-term depression
LTP	long-term potentiation
M	male
mCi	millicuries
MD	mean diffusivity
mGluR	metabotropic glutamate receptor
mm	millimeter
ms	milliseconds
MNI	Montreal Neurological Institute
MP-RAGE	magnetization prepared rapid gradient echo
MRI	magnetic resonance imaging
MRTM	Multilinear Reference Tissue Model
MSNs	medium spiny neurons
n/a	not applicable
NAc	nucleus accumbens
NBS	Network Based Statistics
NMDA	N-methyl-D-aspartate
n.s.	not significant
NSDUH	National Survey on Drug Use and Health
NTS	nontreatment-seeking alcoholics
PET	positron emission tomography
RAC	[^{11}C]raclopride
R	right
RD	radial diffusivity
ROI	region of interest
s	seconds
SD	social drinking controls
SMK	cigarette smokers
SNTS	smoking nontreatment-seeking alcoholics
SPECT	single-photon emission computerized tomography
SPM	Statistical Parametric Mapping
SSAGA	Semi-Structured Assessment for the Genetics of Alcoholism
SSRI	selective serotonin reuptake inhibitor
TBSS	Tract-Based Spatial Statistics
TE	echo time
TFCE	threshold-free cluster enhancement

TLFB	Timeline Follow-Back
VST	ventral striatum
VTA	ventral tegmental area
WM	white matter

Introduction

Alcohol is a widely consumed substance throughout the modern world. At low to moderate levels of consumption of 1-2 drinks/day or less (Department of Health and Human Services, 2015a), its effects on health are marginal. However, in a proportion of the population whose drinking levels far exceed those, alcohol use disorders become a significant risk. The American Psychiatric Association in its Diagnostic and Statistical Manual (DSM-V) defines alcohol use disorder (AUD) as a brain disease characterized by loss of control over one's alcohol use despite consequences (APA, 2013). Within the United States, 15.1 million of individuals over 18 had an AUD in 2015 (Department of Health and Human Services, 2015b). Worldwide, 3 million deaths annually are attributed to alcohol misuse, which makes up 5.3% of all reported deaths (WHO, 2014). It is estimated that 88,000 deaths annually are related to alcohol, which makes it the third leading preventable cause of death in the United States (CDC, 2013). Additionally, alcohol misuse was estimated to cost the United States economy $249 billion in 2010 (Sacks et al., 2015). All this poses AUD as a significant problem that must be addressed in research, to increase our understanding of this disease and to improve treatment outcomes.

Chronic AUD has been linked to various types of cancers, as well as liver and cardiac disorders (CDC, 2013). In the brain, AUD is associated with atrophy, as well as executive, memory, and other cognitive deficits (Sullivan et al., 2010). In the most severe cases, AUD can lead to neurological conditions such as Wernicke-Korsakoff syndrome, cerebellar degeneration, or Marchiafava-Bignami disease (Zahr and Pfefferbaum, 2017).

While these diseases present with varying symptomatology, in terms of brain regions affected and presence of cognitive symptoms, at their core they are all related to poor nutrition that is a consequence of chronic alcohol misuse. Additionally, cessation of alcohol use after prolonged dependence will lead to a state of withdrawal. In a majority of cases, the symptoms are mild; however, they are collinear with severity of prior use and can require in-patient treatment for what is referred to as the alcohol withdrawal syndrome. Symptoms may include nausea/vomiting, delirium tremens, seizure, and possibly hallucinations (Goodson et al., 2014). For individuals in a state of withdrawal, treatment is centered on mitigation of presented symptoms and close observation of the patient. Unfortunately, treatment options for post-withdrawal recovery and relapse prevention are few and are of limited efficacy.

The most commonly thought of model for AUD treatment has been one of complete abstinence, endorsed by support groups such as Alcoholics Anonymous. However, the success of these groups is difficult to assess due to the anonymity within them. There are also behavioral intervention treatments, such as cognitive behavioral therapy, which involves working with a mental health professional to develop skills and support systems to help stop or reduce one's alcohol habits. In recent years medications have also become available that can help reduce craving (e.g. Naltrexone, Acamprosate) or aid in alcohol avoidance by blocking the body's ability to metabolize alcohol (Disulfiram). According to the National Institute on Alcohol Abuse and Alcoholism, not all treatment options are equally effective for all patients and the ideal approach should be a combination of treatments tailored to the individual by a health professional. Yet despite the treatment resources available, over 50% of AUD individuals will relapse in

the short-term, with that number increasing to as high as 80% over long-term (Moos and Moos, 2006). Research into the neurobiology of AUD can facilitate a better understanding of the mechanisms involved in the maintenance of addiction, which can in turn lead to informed development of novel treatments. In this report, we investigated understudied clinical populations with AUD, in order to increase our understanding of the neurobiological consequences of early/middle adulthood AUD and to inform future intervention development efforts.

Neurocircuity of Reward

Dopamine (DA) releasing neurons located in the ventral tegmental area (VTA), play a major role in reward from natural (e.g. food) as well as non-appetitive (e.g. monetary) reinforcers. Most drugs of abuse are believed to exert their pharmacological effect in a way that modulates DA function. The anatomical dopaminergic (DAergic) projections from the VTA to the striatum (predominantly the ventral portion (VST)) and the frontal cortex, along with a reciprocal VST to VTA Gamma-Aminobutyric acid (GABA) projection and cortical glutamatergic (GLUergic) inputs to both the VST and the VTA form the mesocorticolimbic circuit that has been widely implicated in alcohol dependence (Alasmari et al., 2018). The earliest research that hinted at the involvement of this circuit in reward was done by Olds and Milner (1954), which showed that rats will self-administer electrical stimulation when the electrodes were placed in the general area of the VST. Since then, a plethora of research has shown that mammals will self-administer drugs of abuse (for review see Clemens and Holmes (2018)), such as alcohol

(Samson et al., 1988, Stangl et al., 2017, Matson and Grahame, 2013) and that this behavior is in part modulated by activity of the VST (Samson et al., 1992, Hodge et al., 1997, Doyon et al., 2003, Boileau et al., 2003).

In recent decades, the neurocircuitry of reward and addiction has been expanded, as our understanding of its underlying mechanisms evolved. It is now believed to involve processes related to motivation, decision-making, salience, and habit formation (Kalivas and Volkow, 2005, Haber and Behrens, 2014, Tang et al., 2015). The mesocorticolimbic circuit is positioned within a larger, basal ganglia circuit, which includes the amygdala, hippocampus, thalamus, globus pallidus, and midbrain nuclei (Haber and Knutson, 2010, Haber, 2014, Parent and Hazrati, 1995). Together this circuitry is necessary for goal-directed actions, with the striatum serving as the input of the basal ganglia regions such as the amygdala and hippocampus, to integrate information about emotion and environment, as well as cortical and thalamic inputs, which relay motivation and behavioral adaptation related information (Haber and Behrens, 2014).

The striatum has been classically subdivided into the dorsal striatum (caudate and putamen) and the VST, which encompasses the nucleus accumbens (NAc) and ventral portions of the precommissural caudate and putamen. It contains predominantly GABAergic medium spiny neurons (MSNs), which receive excitatory GLUergic inputs from the aforementioned cortical and thalamic regions, modulatory DAergic connections from the VTA (Gerdeman et al., 2003), and local inhibitory inputs from GABAergic interneurons and other MSNs (Bolam and Izzo, 1988). The terminal fields of these projections are arranged in a partially overlapping topographical manner, further supporting its role in integrative processing (Haber et al., 2006, Choi et al., 2017, Haber

and Behrens, 2014). Additionally, drugs of abuse have been shown to modify the morphology of MSNs (Robinson and Kolb, 1997, Robinson et al., 2001), a likely neuroadaptation that may lead to sensitization and habit formation. In summary, the mesocorticolimbic and cortico-basal ganglia circuitry are key in motivation and control in response environmental stimuli, such as drugs of abuse. While nonhuman research has been able to tease out the circuitry with great detail, neuroimaging studies in humans with AUD have focused on global white matter or regional gray matter disruption. Integration of information from nonhuman studies into hypotheses that can be tested *in vivo* in humans has tremendous translational potential. The following section will focus on alcohol and its effects on the two major neurotransmitter systems (DA and glutamate (GLU)) within the frontostriatal portion of this circuitry, as a basis for Chapter 4 of this report that addresses, the structure/function relationship disruption in human subjects with AUD.

Alcohols Effects on Reward-Related Neurotransmitter Systems

The DAergic system is one that is most frequently associated with alcoholism and reward/addiction in general. Generally referred to as the DAergic reward system, it includes the VTA/substantia nigra neurons that terminate in the striatum, and to a lesser extent in the cortex. There are five metabotropic DA receptor types in the mammalian brain. The D1-like receptors (D1, D5) are stimulatory in nature and upon the binding of DA increase the activity of adenylyl cyclase, which leads to increased levels of cyclic adenosine monophosphate (cyclic AMP). Conversely, the D2-like receptors (D2, D3, and

D4), are inhibitory and lead a reduction in cyclic AMP and activation of potassium channels. In the striatum, these receptors are found on dendritic branches of MSNs, where D1 activation makes them more excitable via a protein kinase-A dependent modulation of ionotropic GLU receptor expression, and D2 activation reduces excitability through mechanisms that internalize alpha-3-hydroxy-5-methyl-4-isoxazoleproprionic acid (AMPA) receptors and release intracellular calcium stores. Additionally, DA reduces the amount of GLU released into the synapse by binding to D2 autoreceptors on the presynaptic DAergic neuron axons (Surmeier et al., 2007). The relative distribution of DA receptors is such that D1 receptors are more prevalent in the cortex, while both D1 and D2 receptors show similar densities in the striatum, with some exceptions such as the pallidum, where regional specificity exists (Hall et al., 1994, Palacios et al., 1988). Additionally, within the striatum, two MSN subtypes exist, the striatonigral, which express high levels of D1 receptors, and striatopallidal, which have high D2 expression (Surmeier et al., 2007). Both human and animal research has shown that DA is elevated in response to alcohol (Doyon et al., 2003, Yoder et al., 2016, Oberlin et al., 2015b, Gonzales et al., 2004). Additionally, in human positron emission tomography studies, the role of D2 receptors in the striatum in alcoholism is well established (see section below on *Human Neuroimaging in Alcohol Use Disorder*).

In line with other drugs of abuse, alcohol enhances DAergic function in the striatum. However, unlike cocaine, which directly increases synaptic DA by blocking its reuptake, alcohols actions are indirect. Administration of alcohol increases levels of extracellular DA in the NAc of rodents, but not through direct actions in the NAc (Yim et al., 1998) nor through actions of its first metabolite acetaldehyde (Clarke et al., 2014).

Rather, alcohol decreases the activity of N-methyl-D-aspartate (NMDA) receptors (Lovinger et al., 1989) and enhances the activity of GABA and glycine, both of which contribute the observed increase in DA seen after alcohol administration (Vengeliene et al., 2008). One theory is that DA in the mesocorticolimbic circuitry plays a role of salience attribution to rewarding environment stimuli (Berridge, 2006, Berridge and Robinson, 2016, Gonzales et al., 2004, Oliva and Wanat, 2019) and that alcohol and other drugs of abuse sensitize this system (Gerdeman et al., 2003). At the neuronal level, transition from an initial seeking behavior to a habitual and even compulsive use is likely to involve a complex system of cascading feedback loops (Melis et al., 2002, Haber and Behrens, 2014), competing DAergic activity (Grace and Bunney, 1985), as well as the interaction of DA and other neurotransmitter systems.

One such neurotransmitter system that is modulated by DAergic activity, especially in the striatum, is the GLUergic neurotransmitter system. GLU is the major excitatory neurotransmitter in the mammalian brain, with both ionotropic (NMDA, AMPA) and metabotropic (mGluR) receptors. Activation of ionotropic receptors leads to conformational changes that allow cation influx into the cell, depolarizing it. Binding of GLU to mGluRs leads to signaling cascades that are mGluR type dependent. Type 1 mGluRs are coupled to G-proteins that initiate phospholipase C, insositol 1,4,5-triphosphate, and diacylglycerol signaling cascades, while Type 2,3 receptor types are coupled to inhibitory G-proteins that reduce cyclic AMP levels (Willard and Koochekpour, 2013, Meldrum, 2000). The striatum receives multiple GLUergic inputs from throughout the brain, which makes it key in information integration. The NAc receives GLUergic inputs from the frontal cortex, amygdala, hippocampus, and thalamus

(Everitt and Robbins, 2005). These connections terminate primarily onto the dendritic branches of MSNs, which express variable subunit composition AMPA receptors depending on MSN subtype (Stefani et al., 1998). In addition, both NMDA ionotropic and mGluR metabotropic receptors are found on MSNs. One of the roles of mGluRs in the striatum is to modulate AMPA activity via changes in phosphorylation (Dell'Anno et al., 2013). The receptor type and subunit distribution of GLU receptors can be altered in an activity dependent manner, e.g. through trafficking/membrane cycling of AMPA receptor subtypes (Werner et al., 2017), and these receptor alterations are believed to play a major role in transition to addiction (Alasmari et al., 2018).

It has been well established that alcohol alters GLUergic transmission, as first shown in hippocampal neurons (Lovinger et al., 1989). Subsequent research has shown that alcohol exposure increased AMPA activity of D1 expressing MSNs (Xiao et al., 2008), as well as NMDA-dependent LTP/LTD in D1+/D1- MSNs, respectively (Renteria et al., 2017). *In vivo*, long-term vapor exposure to alcohol increased choline and GLU in the basal ganglia of rodents (Zahr et al., 2008) and it has been shown that GLU signaling in the NAc is tied to alcohol reinforcement (Vengeliene et al., 2008). Additionally, AMPA and NMDA receptors on MSNs as well as on DA neurons from the VTA influence alcohol response after a period of deprivation, but not in cue-induced reinstatement (Eisenhardt et al., 2015). In summary, the GLUergic and DAergic systems are heavily involved in alcoholism, suggesting that GLU dependent plasticity is involved in transition to addiction behaviors such as habitual and compulsive drinking (Alasmari et al., 2018). With a large GLUergic input from the frontal area to the striatum, understanding the frontostriatal connectivity disruptions as a consequence of alcoholism

could offer meaningful insight into the neurobiology of alcoholism and contribute to novel treatment interventions. We are unable to directly investigate connectivity and neurotransmitter function *in vivo* in humans. However, noninvasive neuroimaging techniques that are presented in the subsequent sections and utilized in this report, can offer indirect metrics of white matter structural integrity and receptor availability that may serve as proxy for the underlying neurobiology of interest.

Human Neuroimaging in Alcohol Use Disorder

The above-mentioned research has advanced our understanding of the neurocircuitry and mechanisms underlying alcoholism and addiction a great deal. Unfortunately, nonhuman research of alcoholism often suffers the limitation of a lack of generalizability. Therefore, in order to achieve a comprehensive understanding of the mechanisms and consequences of alcoholism, a complementary body of research involving human subjects is necessary. Since the late 1970's, research that utilizes the noninvasive magnetic resonance imaging (MRI) as well as minimally invasive positron emission tomography (PET) techniques has aimed to understand the mechanisms of alcoholism in human subjects. The following two subsections will provide an overview of how these imaging techniques have contributed to our increased understanding of the consequences of alcoholism in humans.

Positron Emission Tomography (PET)

PET imaging offers an ability to noninvasively investigate the neurochemical underpinnings of the human brain. Radiotracers (so named because they are delivered in trace amounts) are compounds that are radioactively labeled and injected into the body. These radiotracers are continuously undergoing decay, emitting β particles, which annihilate with electrons to produce γ rays that are detected by the PET scanner. Two commonly used elements for labeling are carbon ([^{11}C]) and fluorine ([^{18}F]), which have half-lives of approximately 20.3 and 109.8 minutes, respectively, and are ideal for PET studies of a single bolus tracer injection.

Early studies which applied PET to alcoholic patients utilized [^{15}O]water, [^{11}C]glucose, and 2-deoxy-2-[^{18}F]-fluoro-D-glucose (FDG). Continuously infused labeled water (due to the short half-life of ^{15}O) was used as an indicator of blood flow and acute alcohol administration was shown to reduce blood flow in cerebellum and increase it in the right temporal and prefrontal regions (Volkow et al., 1988). More recently, ^{15}O water was utilized to show an increase in relative cerebral blood flow in alcoholics who were in a state of early withdrawal (Umhau et al., 2013). Both [^{11}C]glucose and [^{18}F]FDG are used as indices of energy utilization and glucose metabolism. Alcohol dependent individuals have shown decreased glucose metabolism compared to controls (Wang et al., 1993, Volkow et al., 2015) and alcohol administration results in acute reduction in glucose utilization (Volkow et al., 1990, de Wit et al., 1990, Volkow et al., 2006). The interpretation is that administration of alcohol leads to a shift from utilization of glucose to acetate (an alcohol metabolite) as the source of energy in the brain (Volkow et al., 2013, Volkow et al., 2015).

Another unique advantage of PET over other human neuroimaging techniques is the ability to image various receptors systems. Agonist, antagonist, and allosteric modulator drugs have been utilized to image changes in endogenous neurotransmitter levels, receptors number, and responses to pharmacological and behavioral manipulations. In alcohol dependent samples alterations have been reported in both major excitatory and inhibitory neurotransmitter systems. The radioligand [^{11}C]ABP688, has shown altered mGluR5 in the amygdala of recovering alcoholics (Akkus et al., 2018) and the GABAa allosteric site ligand [^{11}C]Ro15 4513 was used to show reduced GABAa alpha 1/5 subunit availability in the NAc, hippocampus, and amygdala of >6wk abstinent alcoholics (Lingford-Hughes et al., 2010). However, studies with [^{11}C]flumazenil (Ro15 1788) a competitive GABAa inhibitor at the benzodiazepine site, as well as [^{123}I]iomazenil single-photon emission computerized tomography (SPECT), have shown in primates, an increase in GABAa availability in early abstinence (Cosgrove et al., 2014, Hillmer et al., 2016). This increase was normalized at 1 month abstinence in primates, and prolonged abstinence from alcohol in humans normalized GABAa in nonsmokers, but not in cigarette users (Cosgrove et al., 2014).

Due to its extensive role in addiction and reward, the DAergic system has been widely investigated in AUD. Majority of research with DAergic PET has utilized the DA receptor type 2/3 antagonists [^{11}C]raclopride (RAC) and [^{18}F]fallypride (FAL). These two tracers offer distinct advantages, with RAC suitable for investigations of striatal DA function and displacement studies (i.e. experimental designs that involve a challenge condition that is meant to increase or decrease DA). Additionally, the relatively short half-life of RAC allows for multi-scan designs to be carried out in a single day.

Alternatively, the half-life of FAL is almost 2 hours, which limits investigator to a single scan session per day, but its increased signal to noise properties allow for quantitation of cortical DA. The most common outcome measure from receptor system PET studies is binding potential (BP_{ND}), which quantifies the ration of specific to nondisplaceable binding in the tissue. Two methods commonly utilized to estimate BP_{ND} are kinetic modeling and the Logan graphical analysis (Innis et al., 2007, Ichise et al., 2003, Logan et al., 1996).

FAL studies that focused on cortical DA have shown no differences in cortical BP_{ND} in saline versus intravenous (IV) ethanol (Pfeifer et al., 2017) in healthy individuals, or versus IV citalopram (a selective serotonin reuptake inhibitor (SSRI)) in alcohol dependent compared to healthy individuals (Zorick et al., 2019). In the former, orbitofrontal, inferior frontal, and prefrontal cortex BP_{ND} correlated with self-reported liking of alcohol (Pfeifer et al., 2017), while in the latter the SSRI condition was associated with reduced self-reported cue-induced craving for alcohol (Zorick et al., 2019). A longitudinal study reported a reduced FAL BP_{ND} in the thalamus, hippocampus, insula, and temporal regions of alcoholics compared to controls. Additionally, at one year follow-up BP_{ND} of recovering alcoholics who abstained or reduced their drinking increased relative to baseline (Rominger et al., 2012).

While Rominger et al. (2012) found no difference in baseline striatal FAL BP_{ND} of alcoholics compared to controls, studies that utilized RAC have shown a reduction in BP_{ND} in the striatum of chronic alcoholics (Martinez et al., 2005, Volkow et al., 2002), that can recover with prolonged abstinence (Volkow et al., 2002). Additionally, alcohol dependent participants showed a diminished DA response to an amphetamine challenge

(Martinez et al., 2005). Family history (FH) of alcoholism has also been implicated in DAergic differences, with higher BP_{ND} in FH positive compared to FH ambiguous and FH negative individuals (Alvanzo et al., 2017), although Munro et al. (2006) found no differences. Furthermore, change in BP_{ND} after amphetamine challenge, showed no differences in FH positive from negative individual in either study. Finally, there is evidence for the role of striatal (specifically the ventral striatum (VST)) DA in acute alcohol and alcohol-related stimulus response. Baseline DA is correlated to perceived intoxication (Yoder et al., 2005, Yoder et al., 2007) and IV alcohol has been shown to increase DA activity in the VST (Aalto et al., 2015, Yoder et al., 2016). Additionally, beer flavor presentation alone was able to elicit a DAergic response in the right VST (Oberlin et al., 2013, Oberlin et al., 2015b). Interestingly, the DA radiotracers 3,4-dihydroxy-6-[^{18}F]fluoro-l-phenylalanine ([^{18}F]L-DOPA; index of DA synthesis capacity) and [^{11}C]-(+)-4-propyl-3,4,4a,5,6,10b-hexahydro-2H-naphtho[1,2b][1,4]oxazin-9-ol ([^{11}C]PHNO; a D3 receptor agonist), did not show any differences between alcoholics and controls (Heinz et al., 2005, Deserno et al., 2015, Erritzoe et al., 2014, Thiruchselvam et al., 2017).

In summary, evidence from PET imaging studies in humans supports animal research findings that alcohol acts to disrupt the function of major neurotransmitter systems. Alterations in DAergic function in acute alcohol administration and in GABA and GLU systems in chronic alcoholism, further lend credence to the animal studies that suggest a shift from alcohol reinforcement (DA related) to compulsive/dependent alcohol consumption. However, the underlying mechanisms of this shift in humans remains unclear. The following section provides an overview of white matter structural

disruptions in AUD, which may influence the observed changes in PET studies, a topic addressed in Chapter 4 of this report.

Diffusion Weighted Imaging (DWI)

DWI is an MRI sequence that takes advantage of the magnetic properties of protons in water in order to model water diffusion in the brain. In cortical white matter (WM), where axons form highly structured bundles referred to as fiber tracts, diffusion of water can be an approximation of WM orientation and coherence. Most commonly a diffusion tensor model is fit to the signal (generally referred to a diffusion tensor imaging (DTI)), which estimates diffusion in a voxel as an ellipsoid (Alexander et al., 2007). A set of diffusion scalar metrics can then be calculated from the eigenvalues and eigenvectors of those ellipsoids. The four commonly used metrics are (1) axonal diffusivity (AD), which is the eigenvalue along the longest axis and is believed to indicate relative axonal health, (2) the average of the two smaller eigenvalues that is related to demyelination called radial diffusivity (RD), (3) the average of all three eigenvalues that is indicative of membrane density called mean diffusivity (MD), and (4) fractional anisotropy (FA), which is a metric of variance of the eigenvalues and is thought to be an indicator of microstructural integrity (Alexander et al., 2007). Several studies have shown that DTI can model structural connectivity in the brain, especially of the major WM tracts (Haber and Knutson, 2010, Draganski et al., 2008, Lehericy et al., 2004, Jarbo and Verstynen, 2015). However, the limitations of DWI, particularly in areas of crossing WM fibers and highly curved tracts (Maier-Hein et al., 2017) need to be considered in the interpretations of DWI results.

Chronic alcohol misuse had been related to alteration in DTI indices of WM (Pfefferbaum et al., 2009, Yeh et al., 2009, Fortier et al., 2014, Pfefferbaum et al., 2014). Measures of WM integrity were also correlated with AUD severity (Yeh et al., 2009, Monnig et al., 2014, Monnig et al., 2015, Pfefferbaum et al., 2006b, Müller-Oehring et al., 2009). Some of these studies did not account for differential cigarette use between alcoholics and controls. Cigarette use has been shown to disrupt WM and affect treatment outcomes in recovering alcoholics (Savjani et al., 2014, Yeh et al., 2009, Durazzo et al., 2014a, Durazzo et al., 2014b) and is highly comorbid in the AUD population, ranging between 60% and 90% (Falk et al., 2006, Kalman et al., 2005). Therefore, comorbid cigarette and alcohol use is carefully considered in subsequent chapters.

DTI investigations in AUD have primarily involved in-treatment/detoxified individuals and to some extent a similar pattern is observed in PET studies. Yet the majority of those with AUD have not sought any treatment and as such represent an understudied, perhaps distinct phenotype of those with AUD. Thus, Chapters 1 and 2 investigate microstructural differences in distinct AUD populations of nontreatment-seekers and college-aged early onset AUD samples, respectively. Additionally, novel approaches from network science were employed (see subsequence section for an overview) in order to relate WM microstructural disruptions in AUD to alterations of structural connectivity.

Applications of Network Science to the Human Brain in Alcoholism

Recent improvements in MRI technology and DWI sequences, as well as tractography algorithms have allowed for estimation of structural connectivity at the whole brain level. This model of whole brain connectivity can be represented as a numeric matrix of NxN brain regions (nodes), referred to as the connectome (Rubinov and Sporns, 2010). Initial models contained binary information of whether a connection (i.e. edge) was present for a particular region pair, but recently the use of weighed edges that represent the strength of connectivity (e.g. number of streamlines or FA) has become increasingly common. This representation of the brain can offer unique insight into brain structure and function. Analytic techniques from the areas of graph theory and network science offer an approach to study conditions such as alcoholism on a systemic level. This is intuitively appealing as alcohol effects are seen throughout the brain.

Graph theory investigations in alcohol-related populations that utilize functional networks (resting state functional MRI (fMRI) and electroencephalogram (EEG) recordings) have observed a varying degree of alterations. Alcohol dependent individuals showed no differences in global fMRI network metrics, however measures of network efficiency and clustering correlated with alcohol dependence duration and severity (Sjoerds et al., 2017), while in EEG-based networks alcoholics had reduced nodal clustering during a cognitive task (Cao et al., 2014). Acute alcohol administration in primate fMRI resulted in altered hub node (a heavily connected regions) and community structure, while healthy human EEG studies under acute alcohol showed alterations in global efficiency, albeit these results were likely due to differences in network density

(Telesford et al., 2013, Lithari et al., 2012). Alterations in functional network structure have also been observed in family history of alcoholism positive high-risk youth and in children with fetal alcohol spectrum disorder (Holla et al., 2017, Wozniak et al., 2012). To my best knowledge, only one investigation examined structural networks in alcoholic individuals compared to unaffected siblings as well as healthy controls and found altered rich club (a group of heavily connected nodes) organization as well as differential local clustering and efficiency of left caudate, right putamen, and left hippocampus among groups (Zorlu et al., 2017). It is not known whether alterations in global graph theory metrics of structural connectivity are present in active AUD. Therefore, the goal of the latter part of Chapter 2 as well as Chapter 3 was to address this in active young/middle adulthood nontreatment-seeking AUD samples.

Possible Role of Frontostriatal Connectivity in AUD

The role of frontostriatal circuitry in neurobiology of alcoholism has been highlighted throughout this introduction. In order to translate preclinical work into humans, it is necessary to employ multimodal neuroimaging studies that combine information about structure and function. Such studies have a great potential to increase our understanding of the consequences of alcoholism, yet these investigations have been extremely limited. One study showed that in healthy individuals, DWI-quantified structural connectivity can be used to parcellate the striatum based on cortical inputs, resulting in a spatially coherent pattern of connectivity (Tziortzi et al., 2014). In addition, the authors found BP changes in response to an amphetamine challenge in [^{11}C]PHNO

and [^{11}C]raclopride to be more homogeneous within connectivity-based than anatomical striatal subdivisions. The second study performed in nonhuman primates, assessed [^{18}F]fallypride PET change in BP after methylphenidate administration in the caudate and found it to be correlated with functional connectivity within the prefrontal cortex (Birn et al., 2019). Thus, the aim of this report, and specifically the fourth chapter was to investigate whether indices of frontostriatal WM integrity and striatal DA function were related and if these metrics were disrupted in AUD.

The above sections provide a review of addiction circuitry and processes as related to AUD, as well as evidence from human structural and functional neuroimaging studies. While there is extensive evidence for functional disruption of the striatal DAergic system and aberrant WM integrity and connectivity, combined structure/function investigations of frontostriatal projections are limited. Frontostriatal connectivity is of special interest as it is involved in transition to compulsive alcohol use and addiction. Network science approaches in combination with multimodal imaging methodologies can offer a novel insight into the neurobiology of alcoholism. Notably, future studies need to be aware of potential confounds of comorbid cigarette use on brain structure in alcoholism as well as of the methodological limitations of network science that can affect the finding (i.e. sufficient sample size, impact of network construction and false-positives, and statistical multiple comparisons problems).

Chapter 1: Differences in White Matter Microstructure and Connectivity in Nontreatment-Seeking Individuals with Alcohol Use Disorder

This chapter describes the use of diffusion weighted imaging (DWI) to assess microstructural differences in the white matter (WM) in alcohol use disorder (AUD). A sample of thirty-eight actively drinking nontreatment-seeking alcoholics (NTS) were compared to nineteen social drinking (SD) controls. This NTS sample is distinct from the predominantly studied detoxified/in-treatment alcoholics. In addition, the sample consists of all cigarette smoking participants, as cigarette use can confound DWI outcome measures. Subjects underwent a DWI and a high-resolution anatomical T1-weigned scan. Fractional anisotropy (FA) data were analyzed with the Tract-Based Spatial Statistics (TBSS) framework. From all participants, recent alcohol consumption was quantified with the Timeline Follow-Back questionnaire.

Results of this study were consistent with existing literature that shows reduced WM integrity, as indexed by FA, in alcoholics compared to controls. Across both groups, average number of drinks per week correlated negatively correlated with FA. Qualitative analysis of tractography modeled WM connections through regions of group difference implicated areas of the frontal, temporal, and parietal regions as possible terminations of those WM projections.

Introduction

An estimated 15 million people in the United States have an alcohol use disorder (AUD) (Department of Health and Human Services, 2015b), which in 2010 cost the nation 249 billion dollars (Sacks et al., 2015). Additionally, in AUD, the prevalence of tobacco use has been estimated to be ~60-90%, as compared to ~10% in a light-drinking population (Falk et al., 2006, Kalman et al., 2005, Romberger and Grant, 2004). Numerous neuroimaging studies have reported deleterious effects of alcohol on regional white matter (WM) microstructure in AUD (Bagga et al., 2014, Müller-Oehring et al., 2009, Pfefferbaum et al., 2006b, Pfefferbaum and Sullivan, 2002, Pfefferbaum et al., 2000, Yeh et al., 2009, Monnig et al., 2013, Pfefferbaum et al., 2014, Segobin et al., 2015). However, this established body of research typically does not address the potential confound of cigarette smoking in abnormalities of brain structure in AUD. There is also a body of literature that indicates cigarette smoking has detrimental effects on WM (Zhang et al., 2011, Savjani et al., 2014, Baeza-Loya et al., 2016, Zou et al., 2017). However, given that up to 85% of alcoholics are also smokers (Durazzo et al., 2007b, Romberger and Grant, 2004), it is still unclear what the relative contribution of chronic alcohol use is to deficits in WM. Some work in nontreatment-seeking (NTS) individuals with AUD has shown differences in brain volumes of NTS compared to light drinking controls (Cardenas et al., 2005), that could be, in part, attributed to smoking status (Durazzo et al., 2007a); but the effects of extensive alcohol misuse alone have not yet been isolated.

While research into WM microstructural abnormalities in detoxified/abstinent AUD is extensive, the same cannot be said for the NTS population. This is important, as

findings from detoxified alcoholics may not generalize to community-dwelling NTS. Only 8.3% of those with an AUD have sought treatment (Department of Health and Human Services, 2015b), which makes the NTS population the majority of individuals with AUD. Additionally, as noted above, the presence of comorbid cigarette use in AUD has been overlooked in neuroimaging studies of the NTS population. Thus, the overarching goal of this work was to determine if there are detectable effects of alcohol dependence on WM microstructure in a currently drinking NTS population, while controlling for cigarette smoking status. Based on existing literature in detoxified AUD subjects, we hypothesized that smoking NTS will have lower WM integrity (assessed with fractional anisotropy, FA) compared to social drinking (SD) controls. To test our hypothesis, we utilized Tract-Based Spatial Statistics (TBSS) to identify areas of compromised WM microstructure in NTS. We also applied a novel, WM tractography-based approach, to objectively identify the gray matter regions that could be targets of cortical projections that pass through any observed WM differences.

Materials and Methods

Subjects

All procedures were approved by the Indiana University Institutional Review Board in accordance with the Belmont Report. Subjects were recruited from the community using advertisements in a local paper and social media. Written informed consent was obtained after confirmation that breath alcohol concentration (BrAC) was zero and study procedures were explained. Subjects were 21-55 years old, and were able

to read, understand, and complete all procedures in English. This study was a retrospective analysis of magnetic resonance imaging (MRI) data from nineteen smoking social drinkers (SD) and thirty-eight smoking nontreatment-seeking (NTS) alcohol dependent participants. MRI data were acquired in subjects who participated in the positron emission tomography (PET) studies designed to investigate the dopamine system; PET data from most subjects in the current work have been published (Albrecht et al., 2013, Yoder et al., 2011b, Oberlin et al., 2015a, Yoder et al., 2016, Yoder et al., 2011a). All subjects included in the present analyses were cigarette smokers. Exclusion criteria were: history or presence of any psychiatric, neurological, or other medical disorder, current use of any psychotropic medication, positive urine pregnancy test, positive urine toxicology screen for illicit substances, and contraindications for safety in the MRI scanner. The Semi-Structured Assessment for the Genetics of Alcoholism was administered to confirm presence or absence of AUD. NTS met DSM-IV criteria for alcohol dependence, had not received treatment within the past year, and were not actively seeking treatment. The following questionnaires were also administered: a medical history and demographics questionnaire, the 90-day Timeline Follow-Back for alcohol use (TLFB), Alcohol Dependence Scale (ADS), Fagerstrom Test for Nicotine Dependence (Pomerleau et al., 1994), Edinburgh Handedness Inventory, and an internally-developed substance use questionnaire.

Imaging

MRI imaging was done on a 3T Siemens Magnetom Trio with a 12-channel head coil array (Siemens, Erlangen, Germany). Diffusion-weighted imaging (DWI) data were

acquired using monopolar Stejskal-Tanner diffusion weighting, single shell (*b*-value = 1000 s/mm^2), and 48 distinct diffusion gradients (eight $b = 0$ images acquired first; GRAPPA with in-plane acceleration of 2). Other parameters were 81ms echo time (TE), 0.7ms echo spacing, scan duration 8:10min, 128x128 matrix, anterior to posterior phase-encoding , 6/8 partial Fourier phase, 68 axial slices, and 2x2x2 mm^3 isotropic voxels. There were minor variations in TE and scan duration, as the DWI sequence was incrementally adjusted over time to minimize bed vibration and image artifacts. A small subset of data ($n = 7$) were collected with one $b = 0$ volume. A high-resolution, T1-weighted, whole-brain magnetization prepared rapid gradient echo (MP-RAGE) image was acquired with the parameters optimized for the Alzheimer's Disease Neuroimaging Initiative (http://adni.loni.usc.edu/): 9:14 min, no GRAPPA, matrix size 240x256, 160 sagittal slices, 2.91ms TE, 1.05x1.05x1.2 mm^3 voxels.

Image Processing

Processing was carried out with an in-house pipeline implemented in Matlab (MathWorks, version 2014b) that incorporated programs from the Oxford Centre for Functional MRI of the Brain (FMRIB) Software Library (FSL version 5.0.9)(Jenkinson et al., 2012) and Camino (Cook et al., 2006) software suites. Figure 1 illustrates the key steps of the image processing.

T1 preprocessing

Preprocessing steps included: (1) Denoising of each subjects' T1-weighted image with an optimized nonlocal means filter for 3D MRI (Coupé et al., 2008), (2) Automated

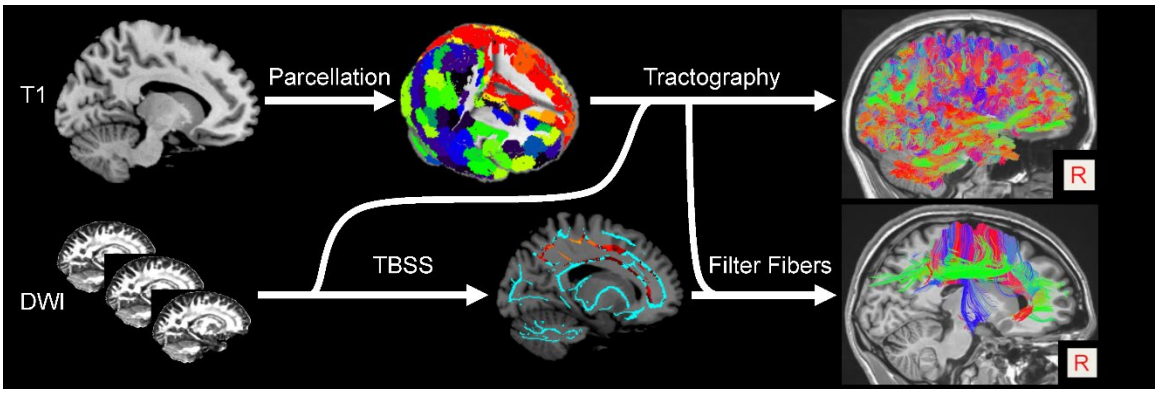

Figure 1. Overall processing scheme for isolating tractography-derived streamlines that passed through regions of significantly different FA in the TBSS group analyses. Each subject's gray matter (derived by segmenting the T1 image; top left) is divided into 278 functionally-derived regions (top middle, GM regions color-coded). Diffusion-weighted image (DWI) data (bottom left) are preprocessed to obtain diffusion tensor information and fractional anisotropy (FA) volumes. Anatomical and DWI data information are combined to perform deterministic tractography (top right). FA data are analyzed with tract-based spatial statistics (TBSS). The TBSS-derived significant clusters (bottom middle; orange-red) are used to "filter" the reconstructed fiber tracts to identify those that passed through the significant clusters (bottom right). The fiber tracts are color-coded to indicate their predominant orientation (left/right in red; anterior/posterior in green; inferior/superior in blue).

cropping and bias field correction (FSL *robustfov* and FAST), (3) Brain extraction (FSL-BET), and (4) Tissue-type (FSL-FAST) and subcortical structure (FSL-FIRST) segmentation.

Both gray and white matter (GM, WM) images from FSL-FAST were enlarged by a single modal dilation. The GM-WM spatial overlap provided an interface region that defined seed regions for tractography. A combined cerebrospinal fluid (CSF; from FSL-FAST) and subcortical GM (from FSL-FIRST) masks were used to minimize erroneous assignment of WM voxels as GM.

DWI preprocessing

Diffusion images were visually inspected for signal dropout and significant head motion artifacts. Only datasets that passed visual inspection were included. DWI images were denoised with a local principal component analysis filter (Manjón et al., 2013). The eight $b = 0$ volumes were spatially registered (FSL-FLIRT dof6) to the first volume and averaged to optimize image quality and minimize effects of head motion. Motion correction of each DWI volume was achieved with linear registration (FLIRT dof6) to the reference $b = 0$ volume. Eddy current correction was performed with FSL *eddy correct* (Jenkinson and Smith, 2001). The $b = 0$ volume was co-registered (dof6 and WM boundary-based registration [BBR]) to the preprocessed T1 image and this transformation was subsequently applied to the DWI data. Voxel-wise calculation of fractional anisotropy (FA) and tensor modeling were conducted using multi-tensor fitting in Camino, where each voxel was classified as either isotropic, single-tensor (anisotropic,

Gaussian), or crossing fibers (anisotropic, non-Gaussian). At multiple points throughout the preprocessing steps, images were visually inspected for quality assurance.

Tract-Based Spatial Statistics (TBSS)

Voxelwise statistical analysis of the FA data was performed with FSL's Tract-Based Spatial Statistics (TBSS) (Smith et al., 2006). Each subject's FA data were aligned into a common space using the nonlinear registration (FNIRT), which uses a b-spline representation of the registration warp field. Next, a mean FA volume was created and thinned to form an FA skeleton that represented the centers of all tracts in the sample. Each subject's aligned FA data were then projected onto the skeleton, and the resultant datasets served as input into the voxelwise statistics algorithm. Group differences were interrogated with FSL's *randomise* permutation testing. Contrasts were generated after 10,000 permutations with Threshold-Free Cluster Enhancement (TFCE) (Smith and Nichols, 2009), and were corrected for multiple comparisons (family-wise error; FWE). The anatomic locations of significant clusters were used as a starting point for post-hoc, qualitative tractography analyses (2.6). Cluster size, peak voxel significance and the corresponding coordinate, as well as the mean FA value of each significant cluster were extracted with the FSL *cluster* tool. Additionally, the mean FA value from each subject's FA skeleton was extracted using Matlab. These extracted average FA values were tested for a relationship with recent alcohol use by nonparametric correlation analysis (Spearman's rho) in SPSS 24. A nonparametric test was chosen because recent alcohol use (drinks/week) was non-normally distributed.

Connectivity Analyses

Deterministic Tractography

Deterministic tractography conducted in Camino with the Fiber Assignment by Continuous Tracking (FACT) algorithm used a single seed per voxel at the GM-WM interface region. Fiber assignment began in a seed voxel, with 1 mm increments (1 step per voxel). Except for two-tensor voxels, fiber tracking followed the major diffusion gradient from voxel-to-voxel except when the turning angle exceeded 45º in 5 steps, which resulted in termination of tracking. Encountering a two-tensor voxel led to fiber duplication, with each of the two fibers following one of the tensor directions. Streamlines were restricted to WM voxels where FA > 0.1, and were terminated when they reached a GM voxel on either end. Very short (< 8 mm) or long (> 180 mm) streamlines were discarded.

Tract (Streamline) Isolation

To isolate fibers passing though voxels with significant group differences in FA, the TBSS output images were transformed into each subject's native space with FSL tbss_deproject. Camino *procstreamlines* projected the cluster maps onto each subject's tractography results, and constrained the tractography data to fibers that passed through the significant clusters (e.g., TBSS *p*-value volumes; Figure 1). To perform quality checks of modeled streamlines, fiber data were converted to trk format for visualization in TrackVis (Wang et al., 2007).

Gray Matter Parcellation

Each subject's gray matter was subdivided into 278 regions based on a functionally-derived parcellation (Shen et al., 2013). This allowed us to locate gray matter sources of streamlines passing through white matter areas of significantly different FA. The parcellation was applied to each subject's data by the following steps: 1) spatial transformation of the native T1 volume into MNI space (FSL: flirt-dof6, flirt-dof12, fnirt); 2) application of the individual inverse transformation parameters to the MNI template parcellation; and 3) masking the resultant native-space parcellation with each subject's GM mask from FSL-FAST. For quality assurance, the final parcellations were overlaid on the respective T1 volumes for visual inspection.

Connectivity Visualization

The number of streamlines that connected any pair of gray matter regions was obtained from a connectivity matrix generated with the Camino *conmat* function. Connections were assessed separately for NTS and SD. For each group, a region-by-region connectivity matrix was generated with the conservative requirement that, to be counted, a given connection must be present in all subjects within that group. GM regions that were connected via the significant cluster areas were visualized by an overlay of the connected GM regions for each group onto a Colin 27 (CH2) MNI brain template.

Other Statistical Analyses

Group differences in sample characteristics were assessed with independent-samples *t*-tests or χ^2 tests (R; version 3.3.0).

Results

Subjects

Subject characteristics are presented in Table 1. NTS and SD were well-matched on all demographic characteristics and tobacco use. NTS reported significantly higher alcohol consumption and scored higher on the Alcohol Dependence Scale (ADS).

TBSS: SD vs. NTS

NTS had lower FA compared to SD, predominantly in the left hemisphere ($p<0.05$ TFCE, FWE-corrected; Figure 2). Thirty-three significant clusters were identified. Data for the largest (exceeding 90 mm^3) and likely most relevant clusters are presented in Table 2.

Correlations of FA with recent alcohol use

Across all subjects, number of drinks per week had a significant negative correlation with average FA from the TBSS skeleton (Spearman's $\rho = -0.348$, $p = 0.008$; Figure 3).

Structural Connectivity

In SD, 42 of the 278 gray matter regions were connected though the significant clusters from the NTS < SD TBSS contrast, while NTS had 40 connected gray matter regions. Spatially, these regions were largely overlapping between groups, with some regions unique to each group. Figure 4 illustrates the connected GM regions for each

Table 1. Subject Characteristics. Data are mean ± standard deviation. TLFB: TimeLine Follow Back. ADS: Alcohol Dependence Scale. SD: social drinkers. NTS: nontreatment-seeking alcoholics. AA: African-American. HL: Hispanic Latino. R: right. A: ambidextrous. n.s.: not significant.

	SD	NTS	*p*-value
N	19	38	
Age	37.8 ± 8.6	38.6 ± 8.1	n.s.
Gender	3 F	7 F	n.s.
Race	6 AA	17 AA	n.s.
Ethnicity	0 HL	0 HL	
Education (years)	12.8 ± 2.3	12.7 ± 1.9	n.s.
Handedness	19 R	36 R; 2 A	
Drinks/DD	3.4 ± 1.4	8.8 ± 3.3	< 0.05
Drinks/Week	6.4 ± 7.5	38.4 ± 18.9	< 0.05
ADS	3.9 ± 2.8	12.5 ± 5.4	< 0.05
Fagerstrom (smokers only)	4.4 ± 1.4	4.3 ± 2.1	n.s.

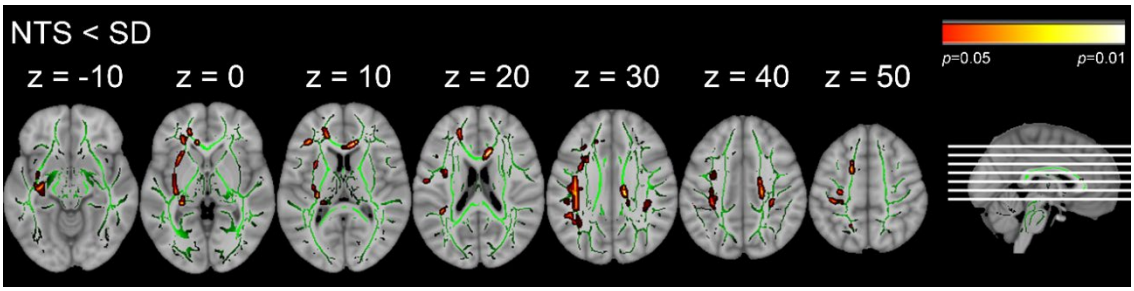

Figure 2. TBSS results. Areas of significant group differences in FA ($p < 0.05$, *FWE*-corrected, red-yellow colors) superimposed on the mean fractional anisotropy (FA) skeleton shown in green. Smoking social drinkers (SD) compared to nontreatment seekers NTS. Axial slice positions are illustrated in the sagittal section. For better visualization, significant voxels within the white matter skeleton were thickened with *tbss_fill*.

Table 2. Characteristics of significant clusters from the NTS < SD TBSS contrast.

***** Eleven clusters (< 90 mm^3) were omitted.

[#] Coordinates are in Montreal Neurological Institute (MNI) space.

TBSS: tract-based spatial statistics. SD: social drinkers. NTS: nontreatment-seekers. FA: fractional anisotropy. FWE: Family-wise error. MNI: Montreal Neurological Institute.

Cluster*	Cluster Size (mm^3)	FA SD	FA NTS	Peak *p*-value (FWE)	Peak MNI coordinates[#] (mm) (x, y, z)
1	1298	0.59 ± 0.07	0.54 ± 0.09	0.028	-39, -12, 28
2	417	0.55 ± 0.10	0.47 ± 0.12	0.045	-31, -24, -7
3	340	0.60 ± 0.09	0.53 ± 0.13	0.044	-19, 42, 4
4	319	0.57 ± 0.10	0.52 ± 0.10	0.045	14, -20, 30
5	296	0.58 ± 0.08	0.53 ± 0.09	0.045	-33, -20, -1
6	282	0.52 ± 0.08	0.44 ± 0.07	0.044	12, 27, 14
7	258	0.35 ± 0.09	0.27 ± 0.10	0.042	34, -38, 33
8	202	0.57 ± 0.07	0.52 ± 0.10	0.044	-45, -46, 30
9	168	0.52 ± 0.09	0.44 ± 0.08	0.046	-30, 8, 5
10	133	0.55 ± 0.08	0.48 ± 0.08	0.048	-36, -54, 26
11	122	0.67 ± 0.06	0.61 ± 0.08	0.046	-30, 12, 32
12	120	0.78 ± 0.08	0.73 ± 0.09	0.042	-27, -3, 42

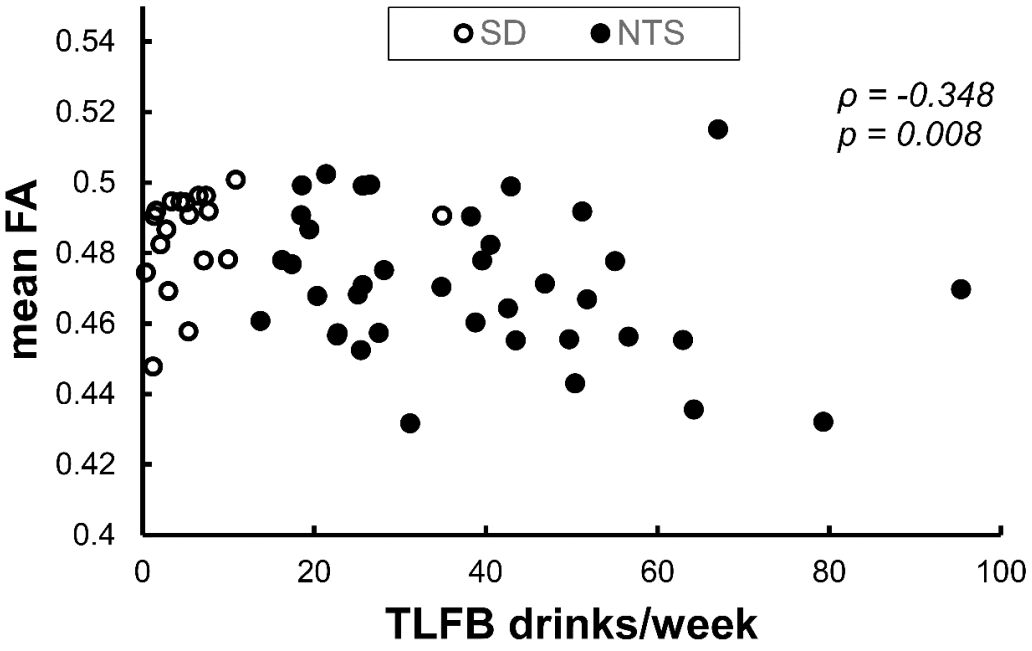

Figure 3. Correlation of mean FA obtained from the TBSS white matter skeleton with self-reported average number of drinks per week in the past 90 days across the full sample. FA: fractional anisotropy. TFLB: Timeline Follow-Back. ρ: Spearman's rho.

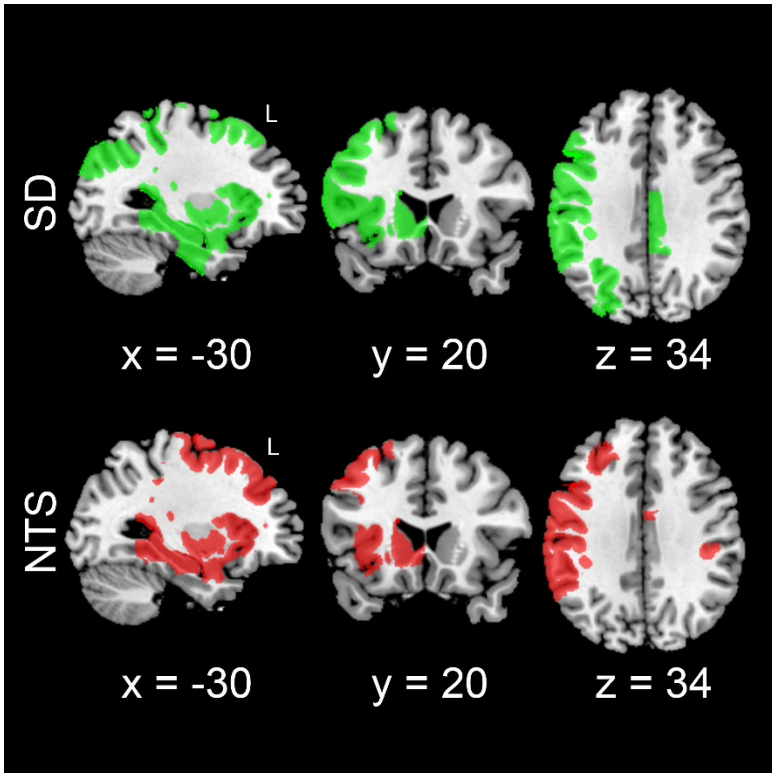

Figure 4. Spatial distribution of gray matter regions connected through TBSS-derived white matter clusters that showed significant group differences in FA. Connected regions are shown for both smoking social drinkers (SD, green) and smoking nontreatment-seeking alcohol use disorder subjects (NTS; red). Note that NTS have a qualitatively distinct yet overlapping spatial distribution of connected GM regions that are also fewer in number compared to SD. Connected gray matter regions are overlaid on a Colin 27 (CH2) MNI template brain, with MNI-coordinates provided below each slice.

group. There were qualitative differences in regional patterns of GM targets between groups (see Discussion).

Discussion

This study found effects of alcohol dependence on WM microstructure in nontreatment-seeking alcohol dependent individuals who had lower FA relative to smoking social drinkers. Importantly, all subjects in both the NTS and SD groups were cigarette smokers. Not matching groups for smoking status is a potentially important confound that is often overlooked in neuroimaging studies of addiction. We used our results as a starting point for implementation of a novel approach to identify gray matter regions that could be the sources of denervation through the areas of compromised white matter (identified via TBSS). We also found that FA values in the whole study sample were negatively associated with recent drinking behavior.

The areas in which NTS had significantly lower FA compared to SD were primarily in the left hemisphere, notably, in the external capsule and the superior longitudinal fasciculus. FA deficits in regions that contain these tracts have been previously reported in AUD (Pfefferbaum et al., 2009, Yeh et al., 2009) and altered WM integrity in the tracts has been associated with altered cognitive function (Bagga et al., 2014, Trivedi et al., 2013). Also, detrimental effects of alcohol on callosal WM have been reported to occur preferentially in the genu of the corpus callosum (Estruch et al., 1997, Pfefferbaum et al., 1996), and anterior WM tracts have also been shown to have greater deficits in FA (Pfefferbaum et al., 2009). Thus, the pattern of WM deficits that we

observed in NTS are consistent with previous findings, and provide additional evidence that anterior WM and longer tracts, such as the superior longitudinal fasciculus, may be more vulnerable to the effects of alcohol. At this time, it is not clear why the results were apparently lateralized; however, it is possible that larger *n* may have revealed bilateral effects.

To begin to understand possible changes in brain function as a consequence of WM disruption, we employed a novel filtered tractography approach, whereupon the putative GM endpoints of compromised WM tracts were identified. There were some regional differences in the connectivity patterns between NTS and SD. Connected GM regions that were only seen in the NTS group included areas in the frontal lobe and anterior cingulate gyrus. Connected regions that were only observed in SD included frontal lobe and middle/posterior cingulate gyrus, as well the left temporal, parietal, and occipital lobes. In NTS, the absence of connections to posterior regions in parietal and occipital lobes may be additional evidence that alcohol has detrimental effects on long WM tracts, such as the superior longitudinal fasciculus.

The observed WM deficits in NTS are likely to have functional ramifications in the brain. Recent research with functional MRI showed that functional connectivity of the cingulate cortex was associated with time to relapse in a recovering AUD sample (Zakiniaeiz et al., 2017). In addition, functional connectivity of the precuneus in response to alcohol cues was associated with severity alcohol dependence (Courtney et al., 2014). Thus, it may be the case that with continued alcohol misuse, structural differences in individuals with AUD may be related to functional deficits that alter brain function. In

turn, this may contribute to the maintenance of AUD, and potentially increase the risk for relapse in those who attempt to quit drinking.

Resting state functional MRI has been used to parse the brain into networks with functional significance (Yeo et al., 2011), which is helpful in interpreting structural connectivity results. In the present study, regions with differential structural connectivity between NTS and SD predominantly belonged to the ventral and dorsal attention networks (Fox et al., 2006), frontoparietal network (Vincent et al., 2008), and the default mode network (Andrews-Hanna et al., 2010). Broadly speaking, these networks are involved in orientation of attention to internal and external stimuli, decision-making, and self-referential processes – all of which are relevant to addictive processes. Indeed, studies of AUD-related populations have reported altered function of these networks (Fryer et al., 2013, Wetherill et al., 2012, Chanraud et al., 2011). Thus, the observed structural differences in NTS in the present work are consistent with these functional findings. However, in this retrospective study, functional MRI data were not available, so we were unable to relate brain function to the observed structural differences.

There are other limitations to consider for this retrospective study. First, we were unable to test for any possible interaction of cigarette and alcohol use because a nonsmoking group was not available in this retrospective sample. We also lacked metrics on lifetime exposure to alcohol as well as continuous metrics of recent and lifetime smoking rates, which could have provided insight as to the putative cumulative effects of alcohol on WM and allowed for a more precise control for cigarette use. However, we believe that the observed negative association between recent drinking history and FA is likely related to lifetime alcohol exposure, as drinking patterns often solidify in early

adulthood. Second, recent research suggests that tractography algorithms may be prone to false positive results (Maier-Hein et al., 2017). The approach we applied here was designed to reduce the likelihood of such effects via application of a conservative, deterministic tracking algorithm and by restriction of the seeding area to the GM/WM interface, rather than utilizing the full extent of all GM voxels in the brain. Finally, this approach only investigated WM connectivity through TBSS skeleton, which represents the center of core WM, and not the full extent of the WM tracts. In addition, no distinctions were made as to which specific regions were connected to one another. However, this approach provided qualitative insight into putative GM connections of compromised WM tracts in AUD. It also sets a premise for future work to investigate specific structural connectivity in AUD with regional- and/or network-based tractography approaches.

In conclusion, we used TBSS to assess the effects of alcohol dependence on WM integrity in currently-drinking subjects with alcohol dependence, while controlling for cigarette smoking status. We also found that recent drinking (a probable proxy for lifetime alcohol exposure) was inversely correlated with WM integrity. Additionally, we employed a novel, qualitative method to identify the GM regions that may be adversely affected by regions of significantly lower FA in NTS, such as the cingulate cortex and precuneus. The results strongly suggest that currently-drinking individuals with alcohol dependence have features of WM microstructural deficits. Presence of these deficits in NTS highlights the need for additional research on consequences of alcohol misuse in currently drinking, community-dwelling AUD populations, who represent the majority of individuals with the disorder.

Chapter 2: Alterations in White Matter Microstructure and Connectivity in Young Adults with Alcohol Use Disorder

This chapter describes the use of diffusion weighted magnetic resonance imaging (DWI) to assess whether alcohol misuse in emergent adulthood is associated with alterations in white matter (WM) microstructure. Twenty-two college-age individuals with alcohol use disorder (AUD) and eighteen social drinking controls (CON) underwent DWI as well as high resolution T1-weighted imaging. Scalar indices of diffusivity in WM, were estimated and compared between groups with the tract-based spatial statistics (TBSS) framework. Additionally, a graph theory-based analysis of structural connectivity was employed to assess for alterations in strength of community association among brain regions.

Results of the voxelwise analysis of group differences revealed that the AUD group had higher fractional anisotropy (FA; and index of WM integrity) in cortical WM as well as lower FA in cerebellar and insular WM. Mean diffusivity was generally lower in AUD compared to CON group. Network analysis of strength of community structure showed lower co-classification of regions between the ventral attention and default mode networks, and higher co-classification between regions of visual, default mode, and somatomotor brain networks of AUD subjects. Additionally, AUD had higher fiber density between an adjacent pair of regions within the default mode network.

Introduction

Alcohol use disorder (AUD) is the most common addictive disorder and is associated with significant morbidity, mortality, social, and economic burden (WHO, 2014). Despite decades of research, a complete understanding of the disease processes remains incomplete, which hinders the development of successful treatments for AUD. One strategy to aid in our knowledge is to study younger individuals with AUD in order to better characterize the brain during the earliest stages of the disorder. Additionally, AUD is a significant health problem in young adults. According to the 2016 National Survey on Drug Use and Health (NSDUH), 12% of individuals aged 21- 25 years old report heavy alcohol use (binge drinking on five or more days in the past month), yet only 5.6% of those 35 and older report heavy alcohol use (Department of Health and Human Services, 2015b). Furthermore, among college aged students (age 18-25), studies show that between 10 - 20% meet the criteria for an alcohol use disorder; however, in the general population, only around 5% meet the criteria for AUD (Blanco et al., 2008, Department of Health and Human Services, 2015b). These epidemiological reports demonstrate that AUD in young adults is already a significant problem. Although a growing body of literature exists on the effects of drinking (and risk for AUD) on adolescent (age 13-17) brains (Nguyen-Louie et al., 2018, Tapert et al., 2003) (also, see below), little is known about brain structure in young adults (~18-25 years old) with AUD. Late adolescence/emerging adulthood is a critical neurodevelopmental window that involves maturation of reward-related regions and cortical areas involved with executive function (for review see Bava and Tapert (2010)). As this age group enters a

collegiate environment, the potential for greater exposure to alcohol increases. In turn, this increases the vulnerability for development of AUD and potential concomitant adverse consequences on brain development during this time period. Thus, there is a critical need to better understand the effects of AUD on the brain in younger individuals, as this may ultimately facilitate the ability to identify those at risk for sustained AUD. In turn, such knowledge could permit development of interventions to prevent extensive damage and/or persistence of AUD throughout adulthood.

Diffusion weighted imaging (DWI) is a neuroimaging technique that allows a non-invasive investigation of white matter (WM) microstructure. In preclinical studies, it is well known that alcohol leads to myelination injury (De Bellis et al., 2008). Similarly, DWI studies have demonstrated that AUD is associated with deleterious effects on WM microstructure in recently detoxified individuals who reported, on average, two decades of alcohol use (Alhassoon et al., 2012, Konrad et al., 2012). While widespread deficits in WM tracts have been observed, damage has most consistently been demonstrated in the corpus callosum, frontal forceps, internal and external capsules, fornix, superior cingulate and longitudinal fasciculi (Pfefferbaum et al., 2009, Pfefferbaum et al., 2014, Bühler and Mann, 2011, Yeh et al., 2009). However, data on the consequences of alcohol misuse on WM integrity in college-age individuals (18-24 years of age) are extremely limited and equivocal. At a 2-year follow-up, 20-21 year-old binge drinkers had no changes in DTI-based metrics over time, and were not different from controls (Correas et al., 2016). In addition, while lower FA has been reported in binge drinkers ~17 years of age (Jacobus et al., 2009), higher FA has been observed in individuals with AUD of similar age (De

Bellis et al., 2008). Thus, additional work is needed to better understand the ramifications of hazardous drinking in college-age young adults.

Studies that employ DWI typically adopt a diffusion tensor model and quantify WM integrity utilizing fractional anisotropy (FA), which is a metric that represents the degree anisotropy of water diffusion. In the WM, lower FA values are indicative of less restriction in water movement, which suggests a disruption in the microstructural environment (Soares et al., 2013). In addition to FA, the full diffusion tensor shape can also be described with other scalar metrics such as mean, axial, and radial diffusivity (MD, AD, and RD, respectively; (Alexander et al., 2007)).

Chronic alcohol misuse has been associated with a reduction in DWI-based measures of WM integrity (Pfefferbaum et al., 2009, Zahr and Pfefferbaum, 2017), whereas, in adolescent populations, higher measurements of WM integrity are typically reported, which are thought to reflect a predisposition to development of alcohol use disorder (Silveri et al., 2016). Few studies have sought to investigate the effects of alcohol on WM microstructure in emerging adulthood (ages 18-24), when persistent hazardous drinking behaviors are typically established. Increased understanding of the neurobiological consequences of AUD in this critical development period could bridge the gap between findings from adolescent and adult AUD research. Additionally, most DWI studies have been conducted in detoxified/abstinent AUD subjects; therefore, the present study makes a further contribution to the limited body of knowledge on WM microstructural differences in currently drinking, non-treatment seeking AUD subjects.

While DWI is in widespread use in research and clinical examinations of WM microstructural defects, traditional metrics (e.g., FA) may not be sensitive enough to

detect structural differences in early AUD. However, network science-based connectomics methodology may offer a novel insight into microstructural deficits in early AUD. These methods are applied to data obtained from DWI tractography-modeled brain networks of nodes (regions) and edges (connections). One such network method is modularity, which represents the degree of segregation of a network into groups of interconnected nodes called communities (Newman, 2006, Sporns and Betzel, 2016). Putative differences in community structure between emerging adult AUD subjects and healthy individuals may represent a predisposition or an early consequence of AUD that has yet to be investigated.

The purpose of the present study was to investigate the WM integrity in young adults with or without AUD using both traditional metrics and a novel community detection approach. We hypothesized that, similar to older cohorts, younger AUD subjects would display significant differences in WM microstructure and altered connectivity due to the development of and/or consequences of AUD.

Materials and Methods

Subjects

All study procedures were approved by the Institutional Review Board at Indiana University. Informed consent was obtained from all subjects prior to study. Twenty-two subjects with alcohol use disorder (AUD) and eighteen healthy controls (CON) were recruited from the community as part of a larger study as described in (Finn et al., 2015). To qualify, participants had to be 18 – 30 years old, have at least 6th grade level of

English comprehension, had consumed alcohol previously, and had no history of psychiatric illness or head trauma. AUD subjects had a current lifetime diagnosis of AUD. Four AUD participants also had a past lifetime diagnosis of a Substance Use Disorder other than alcohol; one AUD participant met criteria for marijuana use disorder. Severity of lifetime alcohol problems was measured using the Semi-Structured Assessment for the Genetics of Alcoholism (SSAGA) (Bucholz et al., 1994), as the total count of all positive responses to all SSAGA questions in the Alcohol Diagnosis section (Cheng et al., 2018). The score range across all subjects was 0-99. Recent alcohol consumption was quantified as the total number of self-reported drinks in the last 2 weeks. Prior to study day, subjects were asked to abstain from alcohol for 12 hours. A breath alcohol test confirmed sobriety on scan day (Alco-Sensor IV, Intoximeters, St. Louis, MO).

Imaging

Data were acquired on a Siemens 3T Trio-Tim (Siemens, Erlangen, Germany). Diffusion weighted data were collected with a single-shell (b=1000 s/mm^2) 2D acquisition; 64 diffusion directions and 8 b = 0 volumes; A-P phase encoding; 128x128 matrix; 72 slices; 2 x 2 x 2 mm^3 voxels, iPAT factor = 2. A T1-weighted 3D anatomic sequence was also acquired (Field of view = 192x168 matrix, 160 sagittal slices, and 1.3 x 1.3 x 1.3 mm^3 voxels).

Image processing

An in-house Matlab-based pipeline that utilizes FSL (Version 5.0.9) (Jenkinson et al., 2012) and Camino (Cook et al., 2006) was applied for image processing. Each subjects' anatomic T1-weighted image was denoised (Coupé et al., 2008), skull stripped (*FSL bet*), and segmented according to tissue-type (*FSL FAST*). Diffusion weighted data were first denoised with local principal component analysis filter (Manjón et al., 2013), then the eight b0 volumes were registered to the first volume and averaged. The data were then corrected for motion, eddy currents, and registered to each subject's anatomic space. This image processing procedure has been previously published in detail elsewhere (Chumin et al., 2018). At each voxel, tensor estimation was done with multi-tensor fitting in Camino in which voxels were classified as isotropic, anisotropic Gaussian (single tensor), or nonGaussian (multi-tensor). Scalar metrics of diffusion including FA, MD, AD, and RD were derived from tensor data. Streamline tractography was carried out in Camino with Fiber Assignment by Continuous Tracking algorithm in each subject's anatomic space. Relevant tractography parameters were: 1 seed per voxel at the interface of gray matter (GM) and WM (obtained from the overlap of dilated GM and WM tissue masks), with an additional seed placed if a streamline encountered a multi-tensor voxel, whereupon each streamline followed one of the tensor directions; step size 1 voxel; maximum turning angle of 45 degrees over 5 steps. Streamlines terminated upon reaching another seed voxel at the GM/WM interface. After tracking, a length filter was applied to discard very short (<8mm) or extremely long (>180mm) streamlines. Throughout the processing, data were visually inspected for proper alignment and quality.

Tract-Based Spatial Statistics (TBSS)

FA maps for each subject were generated in subjects' anatomical space and analyzed via Tract-Based Spatial Statistics (TBSS) (Smith et al., 2006). These data were nonlinearly registered onto the FMRIB58 template FA image (FSL's FNIRT). The mean FA volume was created and thinned to generate a skeleton representation of core WM tracts. Each subject's FA data were then projected onto the skeleton and used for subsequent analysis.

Structural Network Assembly

For each subject, we generated a structural connectivity network matrix, where the cortical nodes were based on a previously published brain parcellation (Shen et al., 2013). For the subcortical nodes, we implemented regions defined by Mawlawi et al. (2001) for the striatum and by (Behrens et al., 2003) for the thalamus. The thalamic regions were further consolidated from 7 to 4 regions (pre-motor, primary motor, and sensory input regions were combined, and occipital and temporal regions were combined) per hemisphere to ensure sufficiently sized regions for tractography analysis. For all region pairs, number of streamlines and average seed surface area were extracted from the whole-brain tractogram with the Camino *conmat* function. The number of streamlines matrix was then thresholded to zero any values ≤ 2 to minimize the influence of false positive connections (Maier-Hein et al., 2017). Finally, network edges were quantified as fiber density (number of streamlines / average seed surface of connected regions; Hagmann et al. (2008)) between any pair of connected regions. Global metrics of

network connectivity were calculated from the fiber density matrices with the Brain Connectivity Toolbox (Rubinov and Sporns, 2010).

Community Structure (From Hierarchical Consensus Clustering)

For each subject's structural connectivity network matrix (see above), a set of 1000 modularity partitions was generated with methodology that is part of a novel Multiresolution Consensus Clustering procedure developed by Jeub et al. (2018). This method samples the full resolution range of resolution of modularity across a given number of partitions. A co-classification (CA) matrix was then generated, where edge weights are the frequency with which two nodes belong to the same module across the identified ensemble of partitions.

Statistical Analyses

Group subject demographics were assessed with independent-samples *t*-tests or chi-squared tests, and results at $p < 0.05$ were considered statistically significant. Group differences in FA images from TBSS were interrogated with permutation testing in FSL's *randomise.* Contrasts were generated after 10,000 permutations with Threshold-Free Cluster Enhancement (TFCE) for multiple comparisons correction across all skeleton voxels (Smith and Nichols, 2009). Significant clusters from all contrasts were ordered by size and thresholded at the largest 1% (corresponding to > 500 voxels in size) of clusters across all comparisons (8 contrasts with a total of 1469 clusters that range 1 to 12892 voxels in size). FSL's *cluster* tool was used to extract mean cluster FA. Comparisons of continuous measures of subject characteristics and global metrics of network connectivity

were conducted with independent samples *t*-tests. Chi-squared tests were used to test for differences in categorical variables. The Network Based Statistics (NBS; Zalesky et al. (2010)) Toolbox was used to compare the fiber density and CA network matrices between groups. False Discovery Rate (FDR) after 5,000 permutations was used to control for multiple comparisons.

Results

Subjects Characteristics

Subject characteristics are presented in Table 3. AUD and CON were well matched, with no significant differences in age, gender, education, or smoking status. In the AUD group, the mean age of AUD onset was 17.23 ± 1.4, and mean age at first drink was 14.82 ± 1.47, compared to 18 ± 1.91 in CON. Additionally, AUD reported significantly higher lifetime alcohol problem counts ($p < 1 \times 10^{-5}$) and total number of drinks in the two weeks prior to interview ($p < 1 \times 10^{-10}$) compared to CON.

TBSS: AUD vs. CON

Young individuals with AUD showed higher FA values compared to CON throughout the WM skeleton ($p_{TFCE} < 0.05$; Figure 5). This apparent difference in FA is likely a function of lower RD (Figure 6C; Figure 7A) in the AUD group. MD was also reduced in AUD ($p_{TFCE} < 0.05$; Figure 6A), predominantly in areas where FA differences are absent; these differences in MD were likely due to significantly reduced AD ($p_{TFCE} < 0.05$; Figure 6B). Concurrently, AUD subjects exhibited lower FA values in WM tracts

Table 3. Subject Characteristics. Data are mean ± standard deviation. CON: Controls; AUD: Alcohol Use Disorder; M: Male; F: Female. n/a: not applicable.

	CON (n = 18)	AUD (n = 22)	p-value
Age	22.39 ± 3.35	22.73 ± 2.73	0.73
Gender	9 F	8 F	0.36
Cigarette use (n)	4	8	0.33
Education (years)	14.17 ± 1.65	14.18 ± 1.22	0.97
Total Drinks (Last 2 Weeks)	6.22 ± 6.75	66.32 ± 49.49	9.68×10^{-6}
Lifetime Alcohol Problems	2.50 ± 3.19	48.10 ± 20.93	3.99×10^{-11}
Age at first drink	18 ± 1.91	14.82 ± 1.47	2.15×10^{-6}
Age of AUD onset	n/a	17.23 ± 1.41	

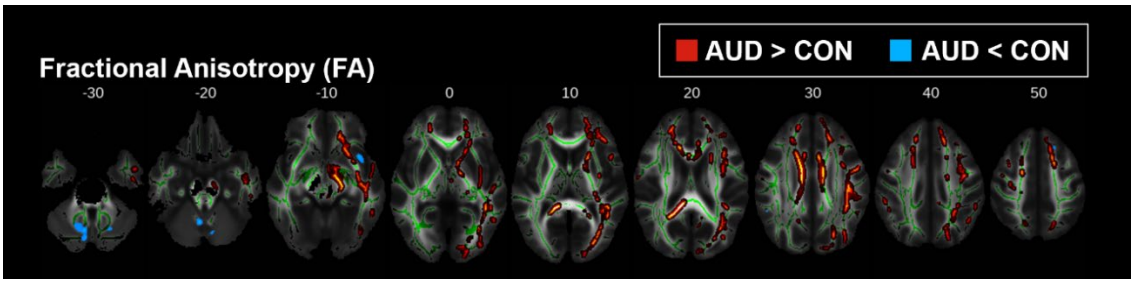

Figure 5. TBSS results for fractional anisotropy (FA). Areas where young adult alcohol use disorder (AUD) subjects had either higher (red-yellow) or lower (blue) FA compared to controls (CON) ($p_{TFCE} < 0.05$). Group differences are superimposed on the mean FA skeleton (green); the mean FA image of the sample is the underlay. For visualization purposes, significant voxels within the WM skeleton were thickened with *tbss_fill.*

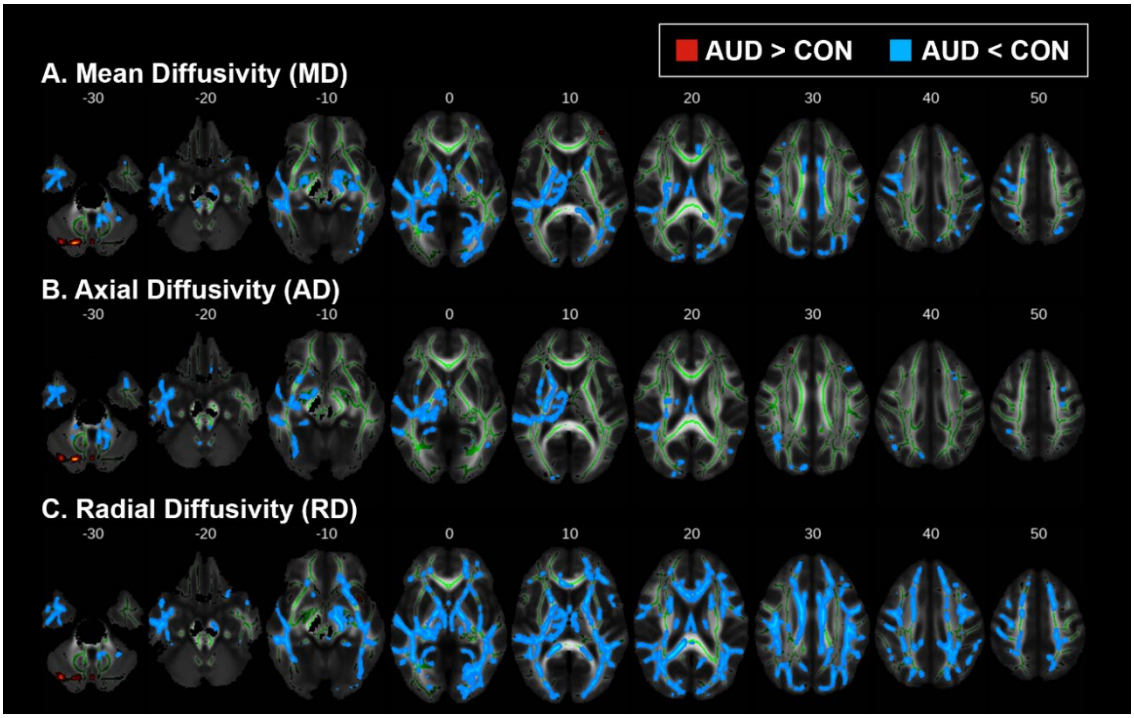

Figure 6. TBSS results for (A) mean diffusivity (MD), (B) axial diffusivity (AD), and (C) radial diffusivity (RD). Areas where alcohol use disorder (AUD) subjects had either higher (red-yellow) or lower (blue) scalar diffusion measures compared to controls (CON) ($p_{TFCE} < 0.05$). Group differences are superimposed on the mean FA skeleton (green); the mean FA image of the sample is the underlay. For visualization purposes, significant voxels within the WM skeleton were thickened with *tbss_fill*.

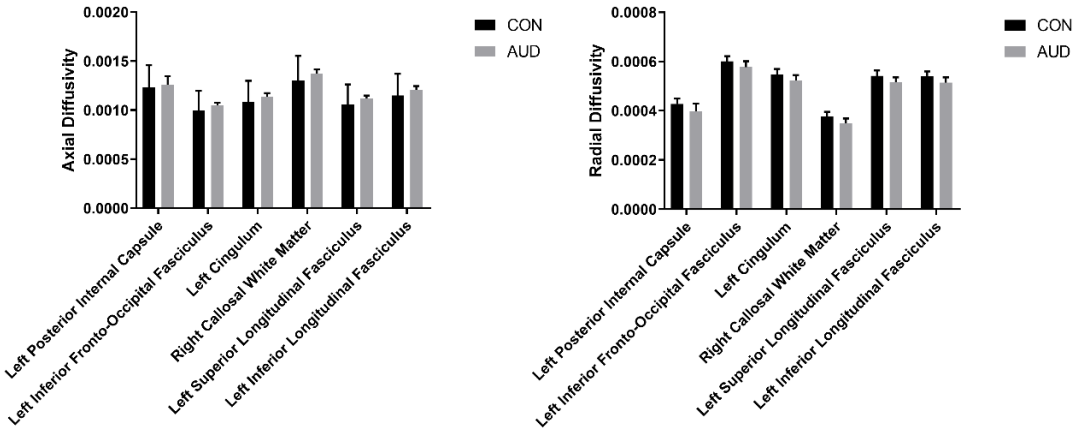

Figure 7. Mean axial (left) and radial (right) diffusivity values extracted from largest 1% clusters, which showed significant differences in fractional anisotropy. X-axis labels correspond to FA clusters shown in Figure 5. AUD-alcohol use disorder; CON-control. Diffusion data are presented as mean ± standard deviation in mm^2/s. For all clusters mean axial diffusivity did not differ, while mean radial diffusivity was statistically ($p < 0.05$) different between groups.

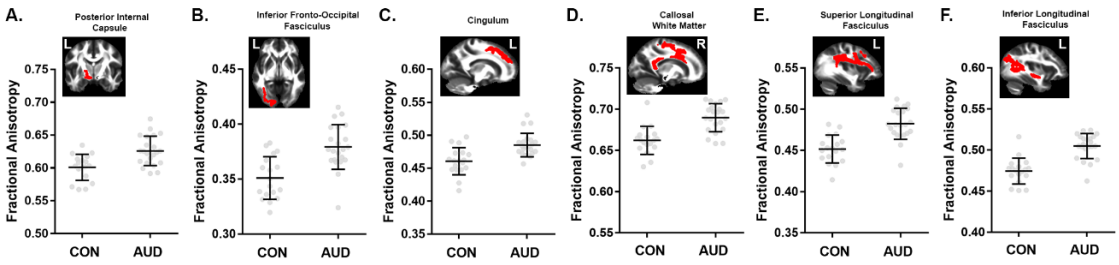

Figure 8. Comparisons of mean fractional anisotropy (FA) for largest 1% of clusters (> 500 voxels). TBSS results ($p_{TFCE} < 0.05$) showed higher FA in alcohol use disorder (AUD) subjects compared to controls (CON) in clusters encompassing the (A) posterior internal capsule, (B) inferior fronto-occipital, (C) cingulum, (D) callosal, (E) superior longitudinal, and (F) inferior longitudinal tracts. Mean FA images show the anatomic position of each cluster. Data are mean ± standard deviation (black), with individual data points in gray filled circles. Tract labels were obtained from the Johns Hopkins University white-matter tractography atlas available in FSL.

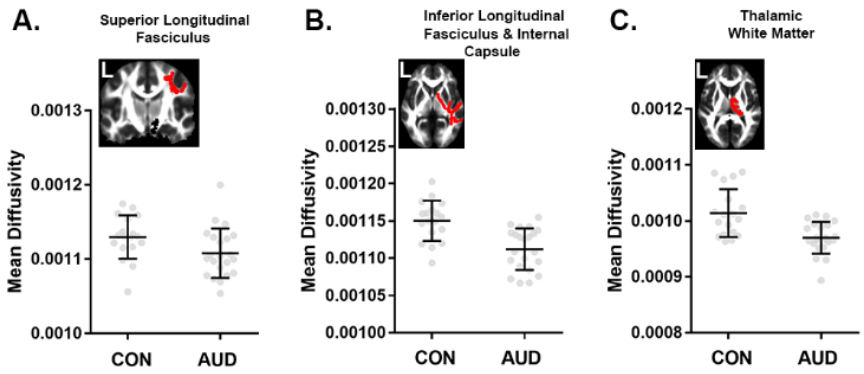

Figure 9. Comparisons of mean diffusivity (MD) for largest 1% of clusters (> 500 voxels). TBSS results ($p_{TFCE} < 0.05$) showed reduced MD in portions of the (A) superior longitudinal, (B) inferior longitudinal and internal capsule, as well as (C) thalamic white matter. Mean FA images from the sample show the anatomic position of each cluster in red. Data are mean ± standard deviation (black), with individual data points in gray filled circles. Tract labels were obtained from the Johns Hopkins University white-matter tractography atlas in FSL.

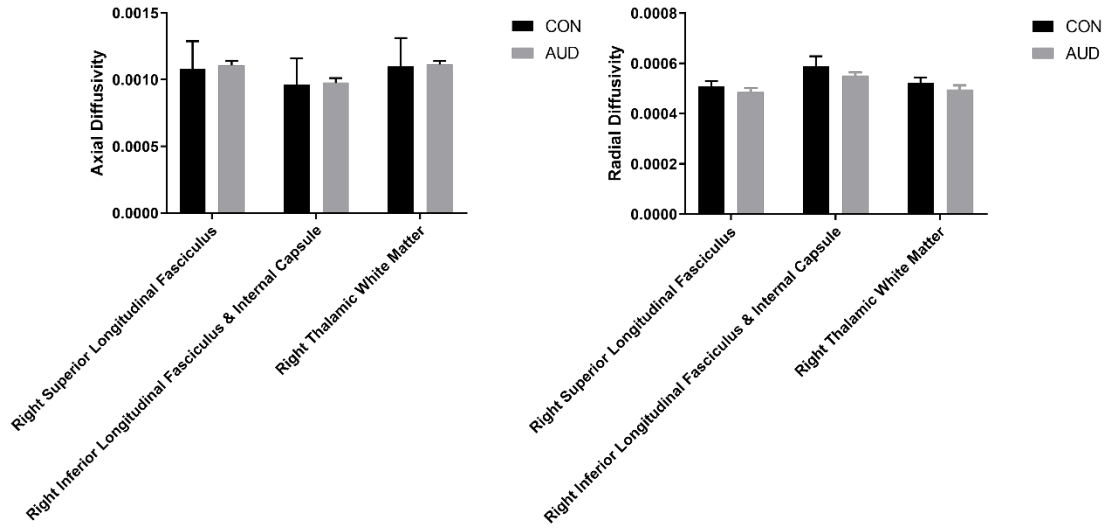

Figure 10. Mean axial (left) and radial (right) diffusivity values extracted from largest 1% clusters, which showed significant differences in mean diffusivity. X-axis labels correspond to MD clusters in Figure 6A. AUD-alcohol use disorder; CON-control. Diffusion data are presented as mean ± standard deviation in mm^2/s. For all clusters mean axial diffusivity did not differ, while mean radial diffusivity was statistically ($p < 0.05$) different between groups.

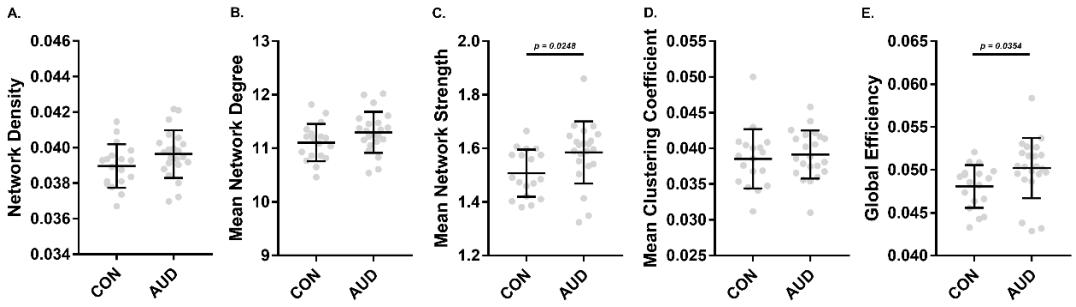

Figure 11. Characterization of networks from tractography-based structural connectomes (A, B, C) and comparisons of measures of network segregation and integration (D,E). Structural networks of CON and AUD groups were similar in density (A) and mean degree (B), while mean strength of edges was significantly (*p = 0.0248)* higher in the AUD group. Clustering coefficient, a measure of network segregation did not differ between groups, while global efficiency, a network integration metric, was significantly (*p = 0.0354*) higher in the AUD group. *P-values* for independent-samples *t*-test are indicated when significant.

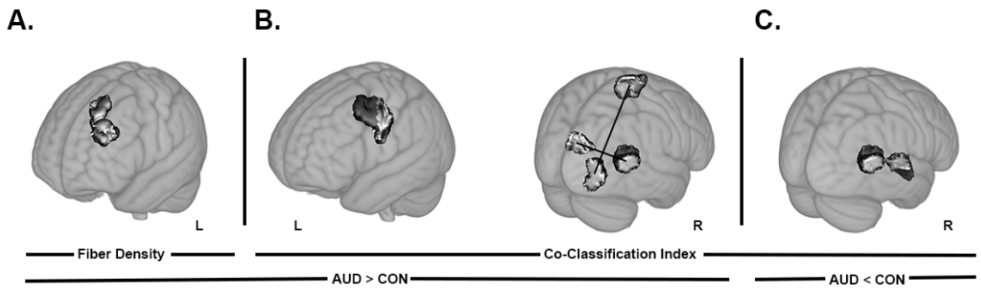

Figure 12. Results from the network based statistics comparison of fiber density and co-classification ($p_{FDR} < 0.05$). (A) Higher fiber density in alcohol use disorder (AUD) subjects compared to controls (CON) was found between nodes located in the middle frontal and superior frontal gyri. (B) Co-classification index (measure of strength of association of a pair of nodes in an ensemble of community structure partitions obtained from modularity), was higher in AUD compared to CON in edges that connect middle frontal gyrus and pre/postcentral gyrus (left) node pairs, cuneus and middle temporal gyrus (right), and supplementary motor area and middle occipital gyrus (right). (C) One edge that connected nodes in the cuneus and inferior insula showed lower co-classification in AUD compared to CON. Renders are on a Montreal Neurological Institute 1mm template included in FSL, visualized with MRIcroGL software. Node pairs with edges that differed between groups are overlaid in shaded gray. A black line was used to specify the connected pair, when multiple pairs are presented on a single underlay. R and L represent right and left hemisphere, respectively.

associated with the right insular cortex and in cerebellar WM ($p_{TFCE} < 0.05$; Figure 5). Mean FA and MD values and anatomical position for clusters > 500 voxels are shown in Figures 8 and 9, respectively. Mean AD and RD values from clusters with significant differences in FA or MD are shown in Figures 7 and 10, respectively.

Network Metrics of AUD vs. CON Structural Connectivity

Comparisons of global measures of structural connectivity showed increased network strength ($p_{FDR} < 0.02$) and global efficiency ($p_{FDR} < 0.04$) in AUD, while network density, degree, and clustering coefficient did not differ (Figure 11). AUD had higher fiber density in a single connection between a node in the middle frontal gyrus and a node in the superior frontal gyrus (Figure 12A). In AUD, co-classification (CA) was greater between nodes in middle frontal and pre/postcentral gyri (Figure 12B, left), between nodes in the cuneus and the middle temporal gyrus, and between supplementary motor and middle occipital areas (Figure 12B, right). AUD also had lower CA between nodes in the middle temporal gyrus and inferior insula (Figure 12C).

Discussion

Studies employing DWI frequently focus on alcoholism in detoxified/abstinent older adults, but few DWI studies have investigated the WM differences in currently-drinking young adults with AUD. Emerging adulthood is a critical period for alcohol use as it represents the time period when one reaches the legal drinking age with greater access to alcohol use. This, coupled with increasing social acceptance of heavy drinking

at this age, means that emerging adulthood is likely an important stage for the development and/or maintenance of AUD (Jennison, 2004). The present study demonstrates that there are alterations in WM microstructure in young adults with AUD. Additionally, our investigation of structural network modularity utilizing a novel connectomics based approach yielded differences in community structure in the brains of young AUD subjects. This study represents one of the first investigations of WM differences in an emerging adulthood AUD sample using a network science based analysis in addition to traditional DWI metrics.

Alterations in FA, MD, AD, and RD values reflect differences in axonal diameters, density, and myelination (Alexander et al., 2011, Alexander et al., 2007, Feldman et al., 2010). Consistently, the literature has reported that decrements in WM integrity are associated with alcohol use (for review see Zahr and Pfefferbaum (2017)) and higher WM integrity is associated with better cognitive functioning (Elofson et al., 2013). However, our results show that young AUD subjects have elevated FA, with lower MD, RD, and AD throughout major WM tracts of the TBSS FA-skeleton. This suggests that young AUD may have differential axonal diameters, density, and/or myelination compared to CON subjects. The present findings are consistent with several reports that observed higher FA in at-risk adolescent populations and adolescent-onset AUD (De Bellis et al., 2008, Tapert and Schweinsburg, 2005, Bava et al., 2009). There are several potential explanations for these unexpected results. It is possible that accelerated myelination of callosal tracts may present a vulnerability for adolescent AUD (De Bellis et al., 2008). Alternatively, such WM changes might reflect compensatory responses that occur during the early progression of AUD (Bava et al., 2009). Indeed, fMRI studies have

shown that subtle reorganization of functional activation may occur during the progression of AUD with increasing use (Tapert et al., 2004). Taken together, these findings could suggest that the early stages of AUD may be associated with higher FA in many regions, either as a function of predisposition to AUD (Cardenas et al., 2013) or as a result of the effects of extensive alcohol exposure during the early stages of AUD. Further work is needed to understand whether or not these neurophysiological signatures are related to behavioral and cognitive endophenotypes in early-stage AUD, and whether they are predictive of sustained alcohol use disorders throughout adulthood.

The lower FA values in WM tracts near the insula indicate potential demyelination or damage in insular tracts. The insula is an important neural substrate for reward and addiction, and is critical for mediating cue-induced craving that can drive drug use (Naqvi et al., 2014, Droutman et al., 2015). This is supported by rodent models of alcohol addiction, which have shown that disrupting excitatory insular-striatal circuitry decreases alcohol self-administration and increases sensitivity to alcohol (Jaramillo et al., 2018a, Jaramillo et al., 2018b). Decrements in FA in the vicinity of the insula in our young adult AUD sample may lead to impaired ability to detect changes in internal states such as alcohol intoxication (Berk et al., 2015, Migliorini et al., 2013). Additionally, the key role of the insula in salience attribution (Seeley et al., 2007) to the effects of alcohol intoxication could also be altered with deficits of WM adjacent to the insula. In support of this, a recent resting state fMRI study demonstrated that alcohol disrupted the connectivity between the anterior insular cortex and dorsal cingulate cortex (key nodes in the salience network), and that this disrupted connectivity was associated with greater "relaxing" effects of alcohol (Gorka et al., 2018).

To our knowledge, only one other structural connectivity study used graph theory analyses in AUD and demonstrated that the AUD group had significantly weaker connectivity, primarily in the right hemisphere (Zorlu et al., 2017). The edges or tracts of significance included connections of the putamen and hippocampus with other brain regions (Zorlu et al., 2017). We add to these findings by reporting AUD had lower co-classification of nodes between ventral attention (supplementary motor and inferior insula/superior temporal areas) and default mode (superior middle temporal gyrus) networks and higher co-classification between nodes of visual (middle occipital/temporal areas) and somatomotor (supplementary motor area) networks. Additionally, AUD had higher fiber density between a pair of nodes within the default mode (middle frontal and superior frontal areas) network and a pair of nodes between the dorsal attention (precentral/middle frontal area) and somatomotor (precentral/postcentral area) networks.

We recently reported structural connectivity differences in the ventral and dorsal attention networks, frontoparietal network, and default mode network in adult nontreatment-seeking AUD subjects (Chumin et al., 2018). In agreement with our previous findings, here we demonstrate that younger AUD subjects have altered connectivity in the ventral and dorsal attention networks and default mode network in addition to differences in the visual and somatomotor networks. Structural networks generally correspond to functional networks (Bullmore and Sporns, 2009); therefore, alterations to structural networks likely result in disrupted function. Respectively, the dorsal and ventral attention networks mediate voluntary shifts in attention, and detect unexpected, behaviorally-relevant stimuli (Vossel et al., 2014). The default mode network is a set of nodes broadly thought to be active during rest and silent during

cognitive activities (Greicius et al., 2003). Importantly, the functions of the dorsal and ventral attention network and default mode network are relevant to alcohol abuse and dependence. Disrupted functional connectivity in the default mode has been reported in heavy drinking populations (Chanraud et al., 2011, Shokri-Kojori et al., 2016). Attentional bias and deficits are also frequently observed in AUD patients (Field and Cox, 2008, Fryer et al., 2013). Disruptions in the somatomotor and visual networks are less frequently associated with AUD; however, altered functional connectivity has been observed in the somatomotor and visual networks during alcohol intoxication (Esposito et al., 2010, Khalili-Mahani et al., 2012). Thus, the functional findings in the literature are consistent with our present structural connectivity data in young adult AUD.

Nodes within the networks referred to above, including the superior frontal cortex, insular cortex, temporal cortex and lateral parietal cortex, have been shown to be highly connected regions with a central position in the overall network (van den Heuvel and Sporns, 2013). These densely connected "hubs" or "rich clubs" play key roles in integrating information between segregated parts of the brain. It has been suggested that alterations in these hubs or interconnections could likely lead to severe impairments because of their roles in whole-brain integrative processes (van den Heuvel and Sporns, 2013, van den Heuvel et al., 2013). For instance, abnormal rich club organization has been reported in structural connectivity analysis of patients with AUD (Zorlu et al., 2017). The differences seen here may represent a network phenotype associated with a predisposition to develop AUD. However, it should be noted that the neurophysiological and cognitive/behavioral relevance of alterations in hubs and their interconnectedness are not fully understood.

The present study contains some limitations that should be considered. Not all individuals with hazardous drinking behavior in emerging adulthood will continue on to AUD as they age (for review see O'Malley (2004)). It is possible that subjects meeting the criteria for AUD in our study may "grow out" or "age out" of the AUD status as they progress through adulthood. Nonetheless, identifying differences in WM integrity and structural connectivity in young adult subjects currently meeting AUD criteria and experiencing the burden of heavy alcohol use is necessary, as these differences could represent areas of lasting neuroanatomical changes that continue regardless of the retention of AUD status. In addition, information on family history of AUD, which is a strong predictor for eventual development of AUD, was not available for this sample, and may be a contributing predisposing factor toward alterations of DWI scalar metrics (for review see Cservenka (2016)). Finally, this study utilized a relatively small, retrospective sample; longitudinal research with larger sample sizes is necessary to determine whether differences in scalar DWI metrics, fiber densities, and node associations contribute to the development of AUD, or are a consequence of the early stages of AUD.

In summary, we utilized traditional DWI metrics and a novel connectomics-based approach to examine WM differences in young adult AUD subjects. We demonstrated that young AUD subjects had distinct differences in microstructure with both higher WM integrity in many tracts and lower WM integrity in others. The connectomics analysis also revealed altered structural connectivity in this young adult AUD sample. The presence of these differences indicates that alterations in WM may not only appear after years of chronic alcohol abuse, but may in fact emerge during the early stages of AUD. The connectomics approach also detected structural connectivity differences in regional

and global network connectivity measures in these emerging adulthood AUD subjects, and suggests that DWI studies investigating WM microstructure in AUD populations may benefit from utilizing this complementary, network science-based approaches. The present findings demonstrate WM microstructural structural connectome patterns that may be important for further understanding the early stages of AUD. This is clinically relevant, as young adult AUD represents a crucial time period for intervention to prevent maintenance of AUD throughout adulthood and subsequent potentially damaging changes to brain tissue.

Chapter 3: Differences in Consensus Community Structure in Cigarette Smokers with and without Alcohol Use Disorder

This chapter utilizes graph theory methodology to investigate the relationships between alcohol and/or cigarette use and structural brain connectivity as indexed by diffusion weighted imaging (DWI). Structural connectomes (N x N matrix, where N is number of brain regions) were estimated for healthy controls (CON), otherwise healthy cigarette users (SMK), and cigarette smoking nontreatment-seeking alcoholics (SNTS). Each group consisted of 19 demographically matched participants. Global measures of network connectivity (density, degree, and strength) as well as measures of network segregation (transitivity) and integration (global efficiency) were compared between groups. Additionally, community detection was utilized to identify a consensus brain partition for each group.

Results from this analysis revealed that consensus community organization was similar between groups. However, SMK and SNTS showed a reduction in longer inter-community structural connections, compared to CON. These results suggest that cigarette smoking may be the dominant contributor to observed differences in DWI tractography-derived structural brain connectivity, possibly through disruption of the microstructural environment of longer inter-community white matter connections.

Introduction

Cigarette smoking is one of the leading causes of mortality in the world, with 7 million deaths per year attributed to tobacco use (WHO, 2017). Chronic cigarette use also increases the risk of multiple forms of cancer (Onor et al., 2017), as well as respiratory and cardiac diseases (D'Alessandro et al., 2011, Rab et al., 2013). In certain populations, cigarette use rates are greatly increased. In particular, approximately 60-90% of individuals with alcohol use disorders (AUD) are chronic smokers (Falk et al., 2006, Kalman et al., 2005, Romberger and Grant, 2004), compared to ~15% of the general population of the United Sates (WHO, 2017). Adverse effects of cigarette smoking on the brain have been demonstrated by magnetic resonance imaging (MRI) studies. For example, structural MRI of brain morphology in smokers showed reduced cortical and subcortical gray matter volumes (Durazzo et al., 2017, Sutherland et al., 2016, Yu et al., 2018, Zhong et al., 2016). Diffusion weighted imaging (DWI) studies have shown both increased (Hudkins et al., 2012, Liao et al., 2011) and decreased white matter (WM) integrity in smokers (Baeza-Loya et al., 2016, Lin et al., 2013). Similar to chronic smoking, AUD is also associated with widespread brain abnormalities (Bühler and Mann, 2011). Reductions in gray and callosal WM volumes (Gazdzinski et al., 2005, Pfefferbaum et al., 1996) as well as WM integrity have been found in detoxified alcoholics (Pfefferbaum et al., 2006b, Pfefferbaum et al., 2000, Rosenbloom et al., 2008, Yeh et al., 2009, Zorlu et al., 2013). In addition, community-dwelling, actively drinking AUD individuals (who represent a distinct population of AUD), also have decrements in WM integrity (Cardenas et al., 2005, Chumin et al., 2018, Fortier et al., 2014).

Recently, novel methodologies have offered valuable insight into disruptions of brain structure and function in substance abuse. For example, brain connectomics applies network science to the study of biological networks and combines information from multiple MRI modalities to represent and study the brain as a network of interconnected regions (Fornito et al., 2015). This network, referred to as a "connectome", is comprised of gray matter nodes and edges that represent pairwise structural connections or functional associations (Rubinov and Sporns, 2010). In structural connectomes, an edge indicates the existence and possibly strength of a connection obtained from DWI and streamline tractography metrics. For functional connectomes, an edge is typically represented by a correlation coefficient between functional MRI (fMRI) time series of two nodes (Rubinov and Sporns, 2010) and estimates the level of functional coupling. Findings based on connectomics of human neuroimaging data have shown alterations of network structure in clinical populations, including psychiatric disorders (Fornito et al., 2015, Tomasi and Volkow, 2014, Zalesky et al., 2015), neurodegenerative diseases and aging (Gallen et al., 2016, Hojjati et al., 2017, Tinaz et al., 2017), and addiction/reward disorders (Kim et al., 2011, Verdejo-Román et al., 2016, Wang et al., 2015).

Quantitative metrics of the brain connectomics can be classified as either indicators of network integration (the combination of information from distributed nodes), or segregation (specialized processing within interconnected regions) (Rubinov and Sporns, 2010). One approach to study network segregation is community detection, which divides a network into groups of (highly) interconnected regions (communities). The quality of the partition into communities can then be assessed by modularity (for review see Sporns and Betzel (2016)). A widely used maximization function for

modularity is Newman's Q, which quantifies the quality of a network partition into communities compared to a random network (Newman, 2006). Functional networks in subjects with alcohol use disorder and cigarette smokers have been generally characterized by lower measures of segregation and integration compared to controls (Cao et al., 2014, Holla et al., 2017, Lin et al., 2014, Sjoerds et al., 2017, Wozniak et al., 2012), although the evidence is less clear in cigarette smokers (Breckel et al., 2013). In structural networks of heroin-dependent individuals, global measures of network integration were either greater than (Zhang et al., 2015) or did not differ from controls (Sun et al., 2015).

We are unaware of any applications of whole-brain structural network studies or community detection methodology to brain networks in either cigarette smokers or in AUD subjects. Whole-brain structural connectomics approaches are especially advantageous because the negative physiological consequences of cigarette and alcohol use are likely to be distributed throughout the brain (Laviolette and van der Kooy, 2004, Ron and Barak, 2016). Taken together, the goal of this retrospective analysis was to compare global network measures and community organization of structural brain networks in cigarette smokers, nontreatment-seeking AUD subjects who smoke, and nonsmoking controls.

Materials and methods

Subjects

Participants were recruited through local advertisements and social media from the greater Indianapolis area. Informed consent was obtained from all participants after confirmation that breath alcohol concentration was zero and all study procedures were explained. The study was approved by the Indiana University Institutional Review Board in accordance with the Belmont Report. Participants were between the ages of 21 and 55, right-hand dominant, and were able to read, understand, and compete all procedures in English. Magnetic Resonance Imaging (MRI) data were collected as part of positron emission tomography (PET) studies designed to investigate the dopamine system; PET data from these subjects have been previously published (Albrecht et al., 2013, Oberlin et al., 2015a, Yoder et al., 2016, Yoder et al., 2011b, Yoder et al., 2011a). Tract-Based Spatial Statistics (Smith et al., 2006) analysis of diffusion-weighted imaging (DWI) in cigarette-smoking participants herein has also been published (Chumin et al., 2018). The present study focuses on a retrospective analysis of DWI data using graph theory measures of structural brain network connectivity in a sample of smoking, nontreatment-seeking alcohol-dependent participants (SNTS), otherwise healthy cigarette smokers (SMK), and nonsmoking controls (CON). Exclusion criteria were: any contraindications for MRI, positive urine pregnancy screen, positive urine toxicology screen for illicit substances, current use of any psychotropic medication, and history or presence of any psychiatric, neurological, or other medical disorders. At the time of study, all SNTS participants met DSM-IV criteria for alcohol dependence, had not sought treatment for

alcohol use disorder (AUD) in the past year, and were not actively seeking treatment at time of study. In all participants, presence or absence of AUD was confirmed by the Semi-Structured Assessment for the Genetics of Alcoholism (SSAGA). Other administered questionnaires included the medical history and demographics questionnaire, the 90-day Timeline Follow-Back for alcohol use, Edinburgh Handedness Inventory, Fagerstrom Test for Nicotine Dependence (Pomerleau et al., 1994), Alcohol Dependence Scale (Horn et al., 1984), and an internally-developed substance use questionnaire.

Image acquisition and processing

MRI data were acquired on a 3T Siemens Magnetom Trio with a 12-channel coil array (Siemens, Erlangen, Germany). Whole brain DWI data were collected with a 2mm isotropic voxel resolution and 48 distinct diffusion directions at $b = 1000$ s/mm^2 after initial 8 $b = 0$ (b0) volumes. A small subset of data ($n = 4$) were collected with a single $b0$ volume. A high-resolution T1-weighted volume (3D MP-RAGE; 1.05x1.05x1.2 mm^3 voxels) was acquired with the parameters optimized for the Alzheimer's Disease Neuroimaging Initiative (ADNI-1; http://adni.loni.usc.edu). A full description of the MRI acquisition and processing steps is provided in Chumin et al. (2018).

Each participants' T1-weighted image was preprocessed to facilitate parcellation of gray matter into network nodes (see below). T1-weighted images were denoised with an optimized nonlocal means filter (Coupé et al., 2008). The FMRIB Software Library (FSL) version 5.0.9 (Jenkinson et al., 2012) was then used to crop and bias-field correct (Zhang et al., 2011), skull-strip (Smith, 2002), and segment tissue types and subcortical

structures (Patenaude et al., 2011). All diffusion volumes were visually inspected for signal dropout and head motion artifacts. DWI data were denoised with a local principal component analysis filter (Manjón et al., 2013). For each participant, the diffusion-weighted volumes were spatially registered (rigid-body) to a reference (mean) *b*0 volume and corrected for head motion during acquisition (Jenkinson et al., 2002). Eddy current correction was performed with FSL *eddy_correct* (Jenkinson and Smith, 2001). Finally, the mean *b*0 volume was coregistered to the T1-weighted image and the resultant spatial transformation was applied to the remaining diffusion data volumes. White matter tractography was carried out in each subjects' T1 space. Visual quality control was done at all processing steps.

Tractography and network construction

Tensor modeling with multi-tensor fitting and calculation of voxelwise fractional anisotropy (FA) values from the DWI data were implemented in the Camino software suite (Cook et al., 2006). At each voxel, the tensor was classified as either isotropic, single-tensor (anisotropic, Gaussian), or crossing fiber (anisotropic, non-Gaussian). Deterministic streamline tractography was implemented in Camino with the Fiber Assignment by Continuous Tracking (Mori et al., 1999) algorithm using seed voxels at the gray-white matter interface. Other pertinent tractography parameters were: 1 seed/voxel, 1 mm step size, maximum turning angle of 45 degrees over 5 steps, fractional anisotropy (FA) > 0.1, and an inclusion mask that was the result of addition of the seed voxels and the white matter mask obtained from the FSL segmentation. If a streamline (a line connecting image voxels based on their principal orientation) encountered a crossing

fiber voxel, a seed was placed into that voxel with one streamline following each direction. Streamlines were terminated upon reaching a seed voxel at the gray-white matter interface. Very short (< 8 mm) streamlines were discarded, whereas very long (> 180 mm) streamlines were truncated at maximum allowable length of 180 mm.

The 278-region brain parcellation described by Shen et al. (2013) was used to subdivide each participants' gray matter into network nodes using the Camino *conmat* function. All nodes in this parcellation are similar in size, thus reducing the influence of seeded surface on connectivity measures. We used streamline density (e.g., number of streamlines connecting any pair of nodes, divided by the average seed surface of that node pair) to define network edges. Therefore, the brain structural network of each participant was represented as a 2-dimensional 278x278 adjacency matrix, in which streamline density values were edge weights. To reduce influence of false-positives, any edges with less than two streamlines (<2) were discarded and set to zero.

Network measures and modularity

Mean network density, strength, and degree, as well as global efficiency and transitivity of the networks were calculated using the Brain Connectivity Toolbox (brain-connectivity-toolbox.net) (Rubinov and Sporns, 2010). Modularity quantification and community detection were performed with a generalized Louvain method as described in Mucha et al. (2010). This method identifies a common (consensus) partition in a group of networks. All of the participant networks within each group were stacked to form a categorical multi-slice network (i.e., each slice representing a network of a single participant). Community detection within the multi-slice networks of each group were

done at six different modularity resolution parameters (γ = 1, 2, 3, 4, 5, 6). At each resolution, the coupling parameter omega (ω) was incrementally increased in steps of 0.005 with 100 iterations per step, until 17 out of 19 participants (~90% of group) had a consensus partition across 90% of iterations. Due to the nature of the algorithm, the consensus partitions obtained at each iteration could differ. To obtain a single representative partition per group at each γ parameter value, all partitions from the 100 iteration run that met the above described criteria underwent consensus clustering as described by Lancichinetti and Fortunato (2012). Briefly, the partitions were used to create a co-assignment matrix (number of times any node pair was assigned to the same partition) that was thresholded to zero values below a predetermined parameter to facilitate convergence. Here, this parameter was set to zero, as the 100 partitions were similar enough to converge without the need for a threshold. The co-assignment matrix was then entered into the generalized Louvain modularity to obtain another set of 100 partitions. This was repeated until all 100 partitions were identical. This partition was then used as the representative community structure for the group. Visualization of group consensus partitions was done with MRIcroGL (http://www.mccauslandcenter.sc.edu/mricrogl), in which partitions that shared highest number of nodes in common both between groups and across resolutions within group were assigned the same color label. For any particular community partition, network edges were classified as either within- or between-community if they connected nodes of the same or different communities, respectively.

Statistical analyses

Group differences in sample characteristics were assessed with a one-way analysis of variance (ANOVA) or χ^2 test when appropriate. Differences in tissue, seed, and streamline inclusion volumes were evaluated with a one-way ANOVA. Because global connectivity measures were not normally distributed, they were log transformed prior to group comparisons with an ANOVA, with Bonferroni-corrected post-hoc comparisons. Normalized (adjusted for number of elements) area under the curve of streamline length distributions obtained from the modularity partitions were compared with a mixed effects ANOVA, with Bonferroni corrected post-hoc *t*-tests. Associations between years of education and connectivity measures were investigated with linear regression. All statistical tests were performed in SPSS version 24 (IBM, Armonk, NY USA).

Results

Sample Characteristics

The groups were matched for age and sex. Scores on the Fagerstrom test for nicotine dependence did not differ between the two smoking groups. All three groups were similar with respect to total intracranial and white matter volumes (Table 4). Years of education differed between groups (one-way ANOVA, $F(2,53)=7.81$, $p < 0.001$), however, there were no significant correlations between years of education and global network measures (degree, strength, density, transitivity, or global efficiency; Figure 13).

Table 4. Sample Characteristics. Data are presented as mean ± standard deviation. CON: Controls; SMK: Cigarette smokers; SNTS: smoking nontreatment-seeking alcohol use disorder. M: Male; F: Female; ANOVA: analysis of variance; n.s.: not significant; n/a: not applicable.

*Education was not available for one nonsmoking control.

^Fagerstrom Test for Nicotine Dependence data were not available for two smoking controls.

	CON	SMK	SNTS	*p-value*
Demongraphics				
Group n	19	19	19	
Age	34.7 ± 7.3	37.8 ± 8.6	35.8 ± 6.0	n.s.
Education*	15.4 ± 2.5	12.8 ± 2.3	13.4 ± 1.4	<0.001
Sex	12M, 7F	16M, 3F	15M, 4F	n.s.
Substance Use				
Drinks per week	3.2 ± 3.2	6.4 ± 7.5	38.3 ± 16.4	<0.0005
Alcohol Dependence Scale	2.7 ± 2.9	3.9 ± 2.8	13.7 ± 5.8	<0.0005
Fagerstrom score^	n/a	4.4 ± 1.4	4.1 ± 1.9	n.s.
Tissue Properties				
Intracranial volume (voxels)	1434170.05 ± 166198.82	1454557.21 ± 181615.35	1405396.95 ± 149484.47	n.s
White matter volume (voxels)	408221.26 ± 38669.82	426398.32 ± 55673.40	391277.79 ± 34582.97	n.s.

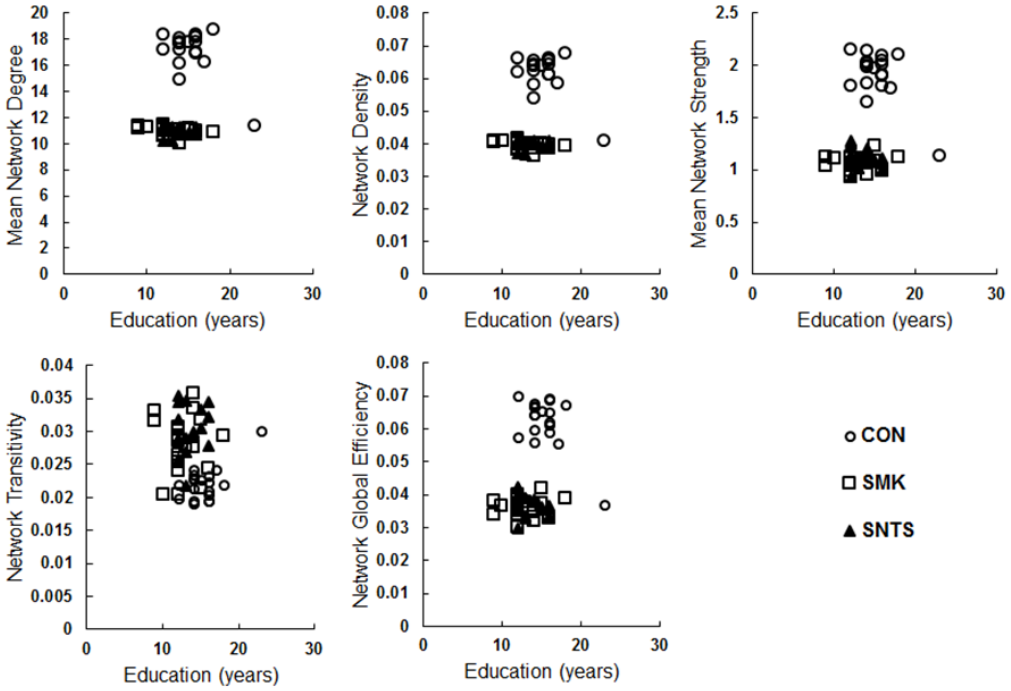

Figure 13. Global characteristics and measures of structural network connectivity were not related to years of education. CON: nonsmoking controls; SMK: otherwise healthy smokers; NTS: smoking nontreatment-seeking alcoholics.

SNTS reported greater alcohol consumption in standard drinks per week on the 90-day timeline follow-back and scored significantly higher on the Alcohol Dependence Scale.

Global Network Characteristics

In this sample, ANOVA revealed significant differences in means between groups on all investigated connectivity measures. Post-hoc tests showed that compared to CON, both SMK and SNTS had lower network density ($F(2,54) = 247.72$, $p < 0.0005$; Figure 14a), mean degree ($F(2,54) = 247.72$, $p < 0.0005$; Figure 14b), and mean strength ($F(2,54) = 197.32$, $p < 0.0005$; Figure 14c). Relative to CON, SMK and SNTS also had significantly higher network transitivity ($F(2,54) = 24.8$, $p < 0.0005$; Figure 14d) and lower global efficiency ($F(2,54) = 154.94$, $p < 0.0005$; Figure 14e).

We also assessed whether differences in network density (Figure 14a) are influenced by the relative surface areas available for tractography, or intracranial and WM tissue volumes. The three groups did not differ on number of voxels within either the intracranial (ANOVA, $F(2,54)=0.42$, $p > 0.05$) or the WM volume (ANOVA, $F(2,54) = 3.04$, $p > 0.05$) masks (Table 4). Figures 15a-c show overlaid, semi-transparent histograms of mean streamline length in millimeters for all subjects within each group. Within each group, distributions were consistent across subjects. To assess group differences in distributions of streamline length, we compared the areas under the curve (AUC; Figure 16). Distributions between groups were significantly different (one-way ANOVA, $F(2,54)=236.16$, $p < 0.0001$). Tukey's multiple comparison-adjusted post-hoc tests showed that both smoking groups had lower AUC of distributions compared to CON ($p < 0.0001$).

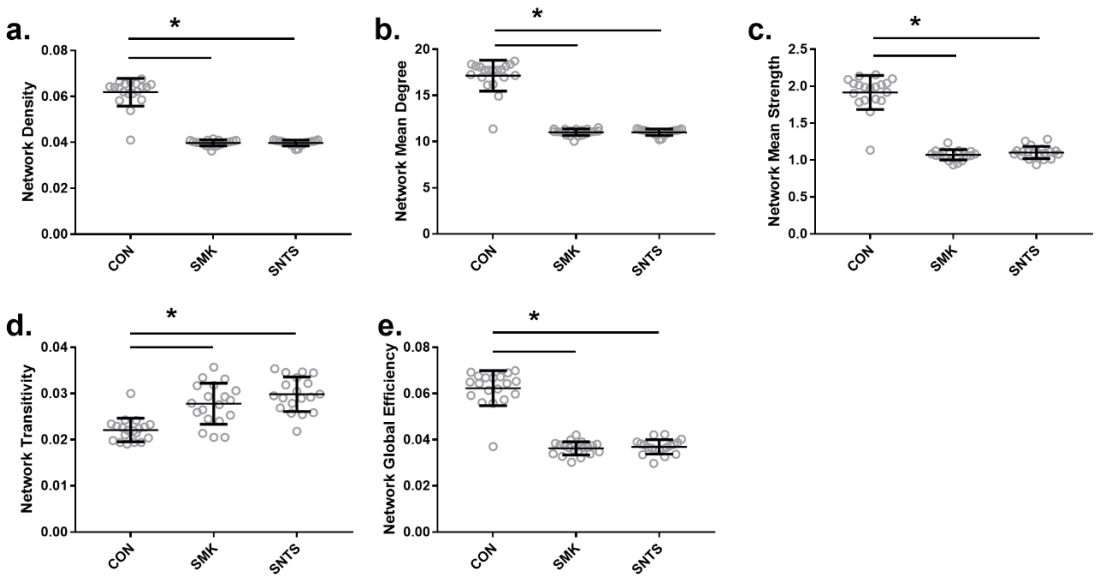

Figure 14. Global network characteristics and connectivity measures by group. Both otherwise healthy cigarette smokers (SMK) and smoking nontreatment-seeking alcoholics (SNTS) had significantly lower (a) network density (number of edges in a network), (b) mean degree (average number of edges of all nodes in a network), and (c) network strength (average of all weights in a network). Compared to controls (CON), SMK and SNTS had higher network segregation as measured by (d) transitivity (ratio of triangles to triplets in a network; a measure of clustering) and lower integration, as measured by (e) global efficiency (inverse of average shortest path between all node pairs in a network). *Comparisons were carried out on log-transformed data with a one-way analysis of variance and Bonferroni corrected post-hoc comparisons ($p < 0.0005$). Data are shown as untransformed mean ± standard deviation.

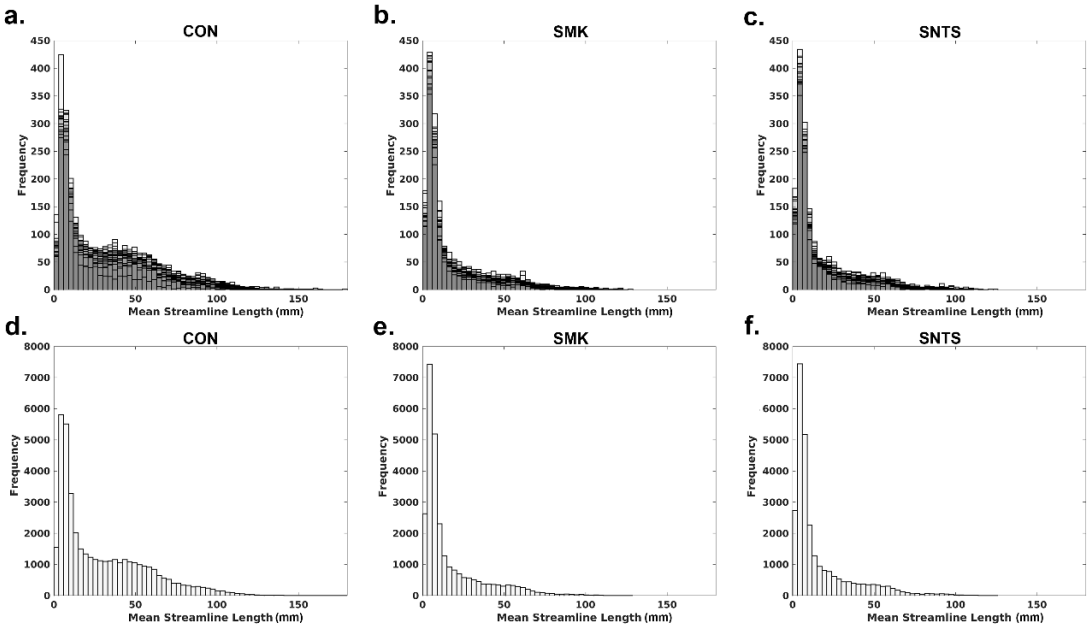

Figure 15. Distributions of streamline lengths (mm). Top: semi-transparent distributions of streamline lengths for each subject were overlaid on each other for (a) controls (CON), (b) otherwise healthy smokers (SMK), and (c) smoking nontreatment-seeking (SNTS) alcoholic groups. Bottom: frequency distributions of streamline lengths of CON (d), SMK (e), and SNTS (f) groups.

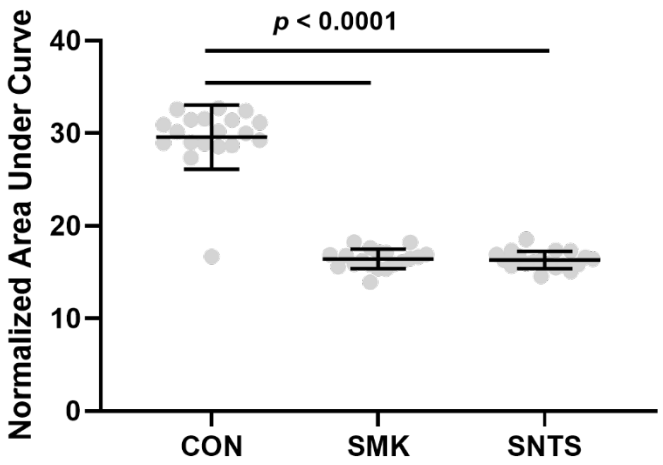

Figure 16. Area under curve differences between groups. Controls (CON) had significantly higher area under curve of mean streamline length distributions compared to both otherwise healthy smokers (SMK) and smoking nontreatment-seeking (SNTS) alcoholics (one-way analysis of variance with Tukey's multiple comparisons corrected post-hoc tests). SMK and SNTS did not significantly differ from one another.

Network Community Structure

Consensus partitions of each group were highly similar to one another in the number of identified communities at each of the six resolution parameter γ values (Figure 17a). Figure 18 shows volume renders of group consensus partitions at $\gamma = 2$ (partitions for other values are presented in Figure 19), which illustrates the overall similarity among the groups (although note that the CON group has a partition in the left parietal lobe that is not present in SMK or SNTS). High pairwise normalized mutual information (NMI) among the group partitions (Figure 17b) provided further evidence that the consensus community structure of the three groups was similar for different spatial resolutions. To better understand the observed community structure, the edges of group frequency distributions in Figures 15d-f were stratified based on whether the nodes they connect belonged to the same or different communities from the group consensus partitions at $\gamma = 2$ (Figure 20). Comparison of these distributions with a three factor mixed effects ANOVA, showed a significant main effect of group ($F(2,54)=237.14$, $p <0.0005$) and a significant interaction of group*connection type (within, between community; Greenhouse-Geisser $F(2)=86.48$, $p < 0.0005$). As compared by post-hoc t-tests with Bonferroni correction for multiple comparisons ($p < 0.05/18$), SMK and SNTS had lower AUC of between community mean streamline length compared to CON across all γ resolution parameters (all $ps < 1x10^{-10}$). SMK had significantly lower AUC compared to SNTS at γ values of 1 and 2 only (i.e., at coarse spatial resolutions; all $ps < 1x10^{-6}$), while at remaining γ values, corrected significance threshold was not met (all $p > 0.0028$).

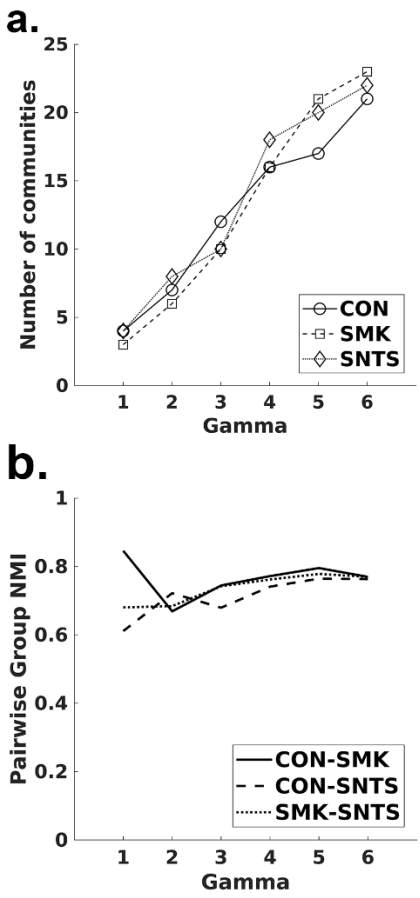

Figure 17. Obtained consensus partitions of all three groups were similar at each γ resolution value. (a) Number of communities in the consensus partition of controls (CON), otherwise healthy smokers (SMK), and smoking nontreatment-seeking (SNTS) alcoholics for different γ resolution values. (b) Pairwise normalized mutual information (NMI) between groups.

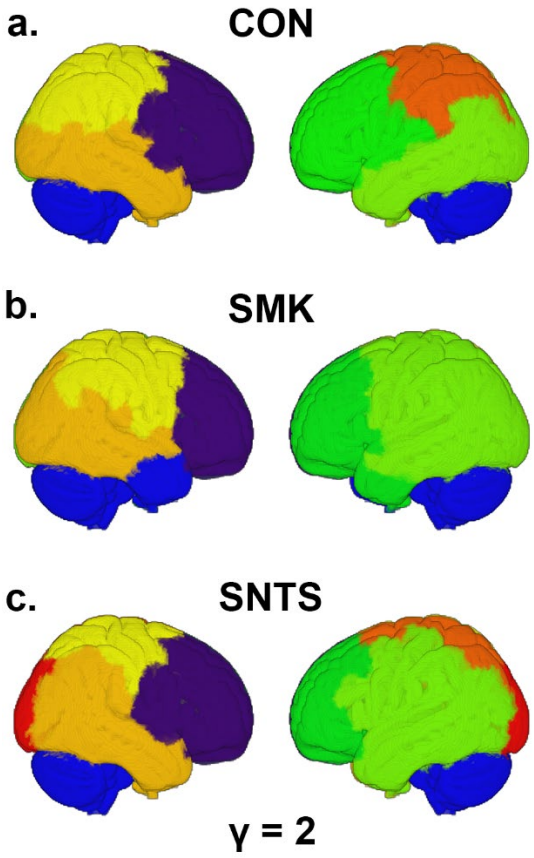

Figure 18. Group consensus community partitions for resolution parameter $\gamma = 2$. Integer community indices for consensus group partitions of (a) controls (CON), (b) otherwise healthy smokers (SMK), and (c) smoking nontreatment-seeking (SNTS) alcoholics allowed us to visualize the community structure by assignment of a random color to each integer index value. Volume renders were generated in MRIcroGL software package.

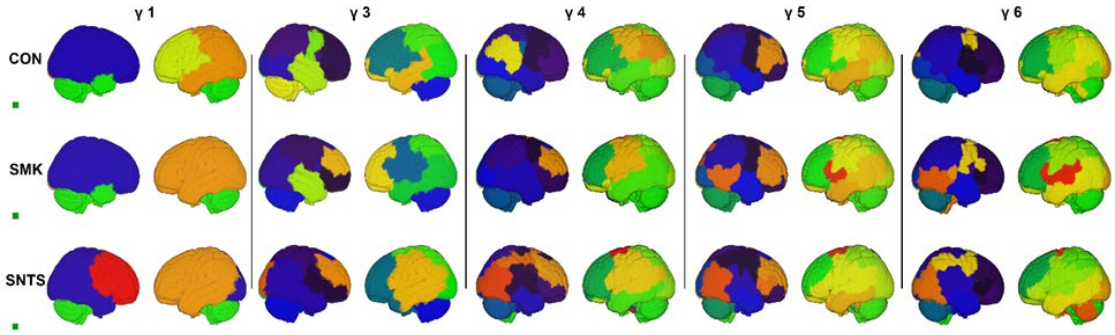

Figure 19. Group consensus community partitions at $\gamma = 1, 3 - 6$ resolution values for controls (CON; top), otherwise healthy smokers (SMK; middle), and smoking nontreatment-seeking (SNTS) alcoholics (bottom). Colors were assigned randomly to each community integer index value. Volume renders were generated in MRIcroGL software package.

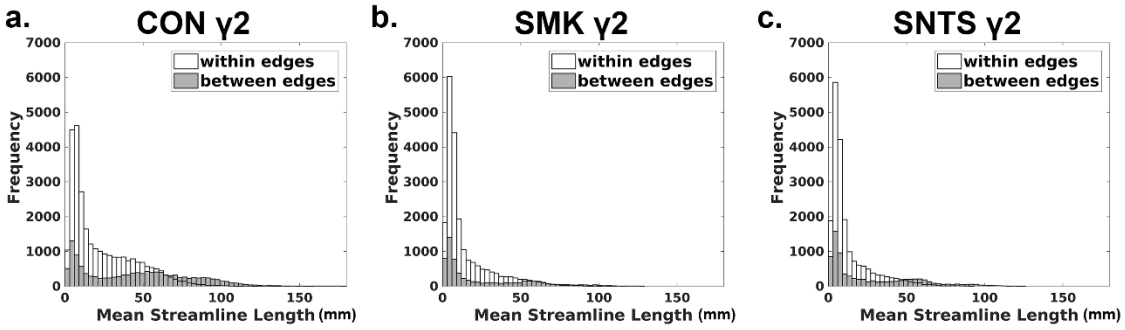

Figure 20. Frequency distributions (data taken from Figure 15) at $\gamma = 2$ for each group were further subdivided based on classification of edges as "within" or "between" (i.e., connecting nodes within- or between- communities).

Discussion

In this retrospective analysis, we investigated the structural connectivity and community organization of otherwise healthy cigarette smokers, AUD subjects who smoke, and a reference sample of nonsmoking controls. Both smoking groups had significantly lower mean network density, strength, and degree compared to controls. They also displayed higher network segregation and lower integration of their structural connectomes. Community structure analysis revealed qualitatively similar group consensus structure, however, the spatial boundaries of communities varied between groups. Comparison of frequency distributions of streamline length revealed that modeled streamline distributions in both smoking groups were altered as compared to controls. Based on comparisons of group frequency distributions, both otherwise healthy smokers and AUD smokers showed a lower number of modeled streamlines of intermediate/long length (those exceeding ~30 mm). These longer connections may play a functional role in integration of information from spatially distributed brain regions. In support of the foregoing, we showed that when stratified by community structure as connecting either within- or between-module regions, the distributions of inter-modular connections differed, showing reduced inter-modular connectivity in the smoking groups.

To our knowledge, this work is the first to apply graph theory analysis to structural brain networks in smoking AUD subjects and/or cigarette smokers without an AUD or substance use disorder. There have been some investigations of resting-state functional MRI networks, but those findings have been inconsistent. One study showed differences in local efficiency of nodes in the cingulate cortex and cerebellum (Chanraud

et al., 2011), while another found no group differences in global efficiency of functional networks in abstinent, in-treatment individuals with AUD (Sjoerds et al., 2017); however, these studies did not assess for the potential effects of smoking in the AUD participants. Similarly, in a sample of cigarette smokers there was reduced global efficiency in functional networks (Lin et al., 2014), while another study did not find any group differences in graph theory measures of efficiency or clustering (Breckel et al., 2013). However, interpretations of functional networks are difficult, because an edge weight in such a network reflects an association of information, rather than a physical connection (Bassett et al., 2018). Alternatively, structural tractography-based networks probe direct connections between regions, in which each edge weight can viewed as the strength of connectivity, indexed by either the number of streamlines and/or streamline density.

In this work, we showed that the structural networks of both otherwise healthy cigarette smokers and smokers with AUD have fewer modeled streamlines, lower global efficiency, and higher transitivity compared to controls. Global network connectivity measures did not differ between the two smoking groups. The overall deficiency in connectivity is likely due to disrupted microstructural environment of white matter in cigarette smokers. Extensive research has shown microstructural deficits within white matter in AUD (Pfefferbaum et al., 2006a, Pfefferbaum et al., 2000, Pfefferbaum et al., 2014, Segobin et al., 2015, Yeh et al., 2009), and cigarette use (Baeza-Loya et al., 2016, Savjani et al., 2014, Zou et al., 2017). Interestingly, results from AUD and cigarette smoking samples may not generalizable to other substance use disorders, as structural networks of heroin-dependent individuals have been shown to have greater efficiency compared to controls (Zhang et al., 2001); although see Sun et al. (2015).

Similarly, this is likely the first application of analysis of community structure (modularity) in AUD and cigarette smoking samples. Group consensus community structure did not appreciably differ between groups; however, there was a difference in distributions of between-community connections between groups. This suggests that long-distance WM connections may be more susceptible to disruptions in the microstructural environment due to chronic cigarette and possibly alcohol misuse. With exception of coarse modular resolution, there were no other observed differences in structural connectivity of otherwise healthy smokers and smoking AUD participants. This could be because the SNTS in this study were actively drinking, and may have less severe AUD-related brain pathology compared to the more-often studied detoxified and/or in-treatment AUD individuals.

The reported findings should be considered within the framework of methodological limitations related to the selection of tractography algorithm as well as the brain parcellation scheme. Recently, it has been shown that tractography algorithms are prone to both false positives and false negatives (Maier-Hein et al., 2017). In simulated datasets, deterministic approaches were unable to reconstruct all tracts, while probabilistic approaches reconstructed tracts with greater accuracy at the expense of higher false positive rates. In this work, we employed a deterministic tractography algorithm that accounted for crossing fibers at the voxel-wise level. As such, this approach may not capture data from more complex white matter architecture and/or high curvature tracts. However, we believe it is an accurate estimation of connectivity of major white matter bundles of the brain. Finally, due to the retrospective nature of this analysis, we were unable to include a nonsmoking AUD sample. Thus, we could not fully

disassociate the effect of chronic alcohol consumption from that of cigarette use. Future studies that utilize graph theory with structural networks in AUD and cigarette smoking are necessary to better understand the impact of chronic consumption of these substances on network structure of the human brain.

In conclusion, this retrospective analysis study applied a network science approach to structural brain networks of otherwise healthy cigarette smokers and smoking AUD individuals. The results revealed that chronic cigarette as well as cigarette and alcohol use are associated with lower regional connectivity and community structure compared to nonsmoking control subjects. These apparent deficits are likely the result of a disrupted white matter microstructural environment that negatively impacts structural connectivity as evaluated by diffusion imaging. This combination of advanced diffusion imaging and graph theoretical analyses offered unique insights into the potential impact of substance use disorders on the brain. Further studies applying these novel analytical approaches are needed to better elucidate structural and functional substrates of substance use disorders.

Chapter 4: Differential Relationship of White Matter Integrity and Striatal Dopamine in Alcohol Use Disorder and Social Drinking Individuals

This chapter describes preliminary multimodal analysis of diffusion weighted imaging (DWI) and [^{11}C]raclopride (RAC) positron emission tomography (PET) data in a sample of seventeen Alcohol Use Disorder (AUD) individuals and twenty-four social drinking controls. Subjects underwent magnetic resonance imaging (MRI) to obtain a high-resolution anatomical T1-weigted scan as well as a DWI scan with either 48 or 60 diffusion directions. Additionally, PET imaging was done with the dopamine (DA) D_2/D_3 receptor antagonist tracer [^{11}C]raclopride. DWI were preprocessed and transformed into standard space via the Tract-Based Spatial Statistics (TBSS) framework. After preprocessing, PET data were input into the Multilinear Reference Tissue Model (MRTM) to obtain regional estimates of striatal dopamine tone.

Results from multiple regression models in the Statistical Parametric Mapping (SPM) software package revealed a significant group interaction of bilateral anterior corona radiata fractional anisotropy (FA; a measure of white matter (WM) integrity) and right ventral striatum nondisplaceable binding potential (BP_{ND}; a measure of DA tone). In the AUD group, higher WM integrity was associated with lower BP_{ND} (higher DA tone), while in controls, higher FA was associated with higher BP_{ND}. These findings suggest a disruption in the relationship between frontostriatal WM integrity and striatal DA tone in AUD.

Introduction

In 2015, an estimated 15 million people had an alcohol use disorder (AUD) (Department of Health and Human Services, 2015b), with ~88,000 alcohol related deaths annually (CDC, 2013). Chronic alcohol misuse has been linked to detrimental structural and functional changes in the brain. Diffusion weighted imaging (DWI) studies in detoxified and in-treatment AUD samples have shown reductions in diffusion tensor metrics, suggestive of demyelination of white matter (WM) (Pfefferbaum et al., 2009, Pfefferbaum and Sullivan, 2002, Zahr and Pfefferbaum, 2017). Additionally, positon emission tomography (PET) has been employed to show altered function of dopaminergic (DAergic) (Martinez et al., 2005), glutamatergic (GLUergic) (Akkus et al., 2018), and other neurotransmitter systems (Weerts et al., 2011, Hillmer et al., 2014, Ceccarini et al., 2014). Yet while these methodological lines of research have independently demonstrated negative consequences of AUD, no multimodal investigations that relate them have been carried out in AUD samples.

In healthy individuals, Tziortzi et al. (2014) have shown that a connectivity-based parcellation of the striatum is more representative of patterns of striatal dopamine (DA) release compared to anatomical subdivisions. WM tractography was performed with seeds placed in the cortex and their streamline terminations were mapped onto the striatum. Frontal lobe input mapped onto the majority of striatal volume, with limbic frontal region (orbitofrontal cortex and anterior cingulate cortex) connections terminating within the ventral striatum (VST). Homogeneity of DA release in [^{11}C]raclopride (RAC) PET post d-amphetamine challenge then showed the greatest change in limbic striatum,

with higher homogeneity of DA release in connectivity-based subdivision, compared to anatomical subdivision of the striatum (Tziortzi et al., 2014). We therefore hypothesized that a relationship may exist between metrics of WM integrity of frontostriatal tracts and DA tone in the striatum and that this relationship is disrupted in chronic AUD. To test this hypothesis multiple regression models were used to probe for relationships between voxelwise fractional anisotropy (FA) in frontal WM and RAC PET baseline binding potential (BP_{ND}; a ratio of specific binding relative nondisplaceable binding in the tissue).

Materials and Methods

Subjects

Written informed consent was obtained from all participants and all study procedures were approved by the Indiana University Institutional Review Board in accordance with the Belmont Report. Subjects were recruited via advertisement in the local paper, were 21-55 years old, and were able to read, understand, and complete all study procedures in English. Exclusion criteria were: history or presence of any psychiatric, neurological, or other medical disorder, current use of any psychotropic medication, positive urine pregnancy test, positive urine toxicology screen for illicit substances, and contraindications for safety in the magnetic resonance imaging (MRI) scanner. The Semi-Structured Assessment for the Genetics of Alcoholism was administered to confirm presence or absence of AUD. The following questionnaires were also administered: a medical history and demographics questionnaire, the 90-day Timeline Follow-Back for alcohol use (TLFB), Alcohol Dependence Scale (ADS),

Fagerstrom Test for Nicotine Dependence (Pomerleau et al., 1994), Edinburgh Handedness Inventory, and an internally-developed substance use questionnaire.

Imaging

Imaging was performed across two MRI scanners, a Siemens 3T SKYRA (10 controls and 8 AUD) and a Siemens 3T PRISMA (14 controls and 9 AUD). A high resolution T1-weighted anatomical image first was acquired, followed by DWI acquisition. For the PRISMA scanner, T1-weighted data were obtained with a whole-brain magnetization prepared rapid gradient echo (MP-RAGE) sequence at a 1.05 x 1.05 x 1.2 mm voxel resolution and 176 sagittal slices. DWI data were acquired using monopolar Stejskal-Tanner diffusion weighting, single shell (b-value = 1000 s/mm^2), and 60 distinct diffusion gradients (three b = 0 images acquired first). Other parameters were 64.8 ms echo time (TE), multiband factor of 3, scan duration 2:56min, anterior to posterior phase-encoding, 69 axial slices, and 2 x 2 x 2 mm isotropic voxels. Data acquisition on the SKYRA was similar to that of PRISMA with the exception that DWI data were collected with 48 diffusion gradients and one b = 0 image, 68 axial slices, but using a product sequence (GRAPPA acceleration = 2), with a longer (7:43min) duration.

RAC PET data were acquired on a Siemens Biograph mCT scanner. PET scans were initiated with a single bolus injection of 14.37±0.9 mCi of the D_2/D_3 antagonist [^{11}C]raclopride. Dynamic acquisitions were 50 minutes (10 x 30 s, 45 x 60 s frames). Data were reconstructed with Siemens software using the filtered backprojection algorithm (5 mm Hanning filter) with corrections for random coincidences, attenuation, and scattering.

Image Processing

For T1-anatomical and DWI data preprocessing refer to the *Materials and Methods* section in Chapter 1.

PET preprocessing

RAC PET data preprocessing was done in the Statistical Parametric Mapping software version 12 (SPM12; https://www.fil.ion.ucl.ac.uk/spm/software/spm12/). For each subject, dynamic data were first coregistered to an early mean PET image to correct for motion, then coregistered to the anatomical MRI. Regions of interest (ROI; left and right precommissural caudate, precommissural putamen, and ventral striatum (VST) (Mawlawi et al., 2001)) were delineated on a Montreal Neurological Institute (MNI) standard space template, then spatially transformed into each subjects' T1-space with a combination of nonlinear (FNIRT) and linear (FLIRT) transformations, part of the FSL software package (Jenkinson et al., 2012). An additional cerebellar gray matter (with the vermis excluded) reference region (a region with little or no D_2/D_3 binding) was defined in each subject's T1 space. Time activity curves for each region were generated in Matlab (R2018b), and for each striatal ROI, DA tone was defined as D_2/D_3 receptor availability (binding potential (BP_{ND}); ratio of specific to nondisplaceable bindning) of RAC (Innis et al., 2007). Regional BP_{ND} was estimated with the Multilinear Reference Tissue Model (MRTM; Ichise et al. (2003)).

Statistical Analyses

Demographic comparisons were carried out in SPSS (version 24) with independent samples *t*-test or χ^2-test where appropriate. Relationships of fractional anisotropy (FA; index of white matter integrity) and regional BP_{ND} were investigated with a multilinear regression model in SPM12, with scanner, years of education, sex, and cigarette use as nuisance covariates.

Results

Subjects

Subject characteristics and PET tracer dose information are presented in Table 5. AUD and controls were matched on age, but did differ with respect to years of education, sex, and cigarette use. AUD participants reported higher quantities of alcohol consumption as well as scored higher on the ADS scale. PET injected dose, mass, and activity did not differ between groups. There were no voxelwise group differences in FA. Of the six striatal regions, only the left precommissural caudate showed a difference in BP_{ND} between groups ($p = 0.049$).

SPM12: Multilinear Regression

Of the six statistical models for voxelwise FA (one for each striatal regions of interest) only the right VST BP_{ND} was found to have a significant group interaction with FA in the left (peak $p_{FWE} = 0.006$, k = 1074 voxels) and right (peak $p_{FWE} = 0.02$, k = 316 voxels) anterior corona radiata (Figure 21).

Table 5. Subject Characteristics. Data are mean (standard deviation). CON: controls. AUD: Alcohol Use Disorder. S: SKYRA. P: PRISMA. M: Male. F: Female. R: right. L: left. CC: Caucasian. AA: African American. AS: Asian. Mx: Mixed. HL: Hispanic-Latino. ADS: Alcohol Dependence Scale. cm: centimeters. kg: kilograms. mCi: millicuries. nmol: nanomolar. n.s.: not significant.

	CON	AUD	*p*-value
n	24	17	
Scanner (S/P)	10/14	8/9	n.s.
Age mean(std)	40.7(10.7)	43.0(10.1)	n.s.
Education mean(std)	15.5(2.0)	13.5(2.2)	.003
Sex (M/F)	12/12	14/3	.03
Handedness (R/L/RL)	20/4/0	15/1/1	n.s.
Race (CC/AA/AS/Mx)	13/9/1/1	10/7/0/0	n.s.
Ethnicity (#HL)	2	0	n.s.
Cigarette Use (#)	4	10	.005
Drinks/week mean(std)	9.0(5.7)	30.3(23.7)	.006
ADS mean(std)	3.8(3.2)	9.6(5.8)	.007
Height cm mean(std)	171.5(9.2)	174.4(15.4)	n.s.
Weight kg mean(std)	87.3(22.2)	93.0(21.8)	n.s.
mCi_injected	14.1(1)	14.7(.7)	n.s.
Mass does nmol/kg	.144(.084)	.125(.058)	n.s.
Dose volume mL	6.6(1.6)	7.3(1.2)	n.s.
Specific Activity (mCi)	18.2(7.4)	17.0(6.5)	n.s.

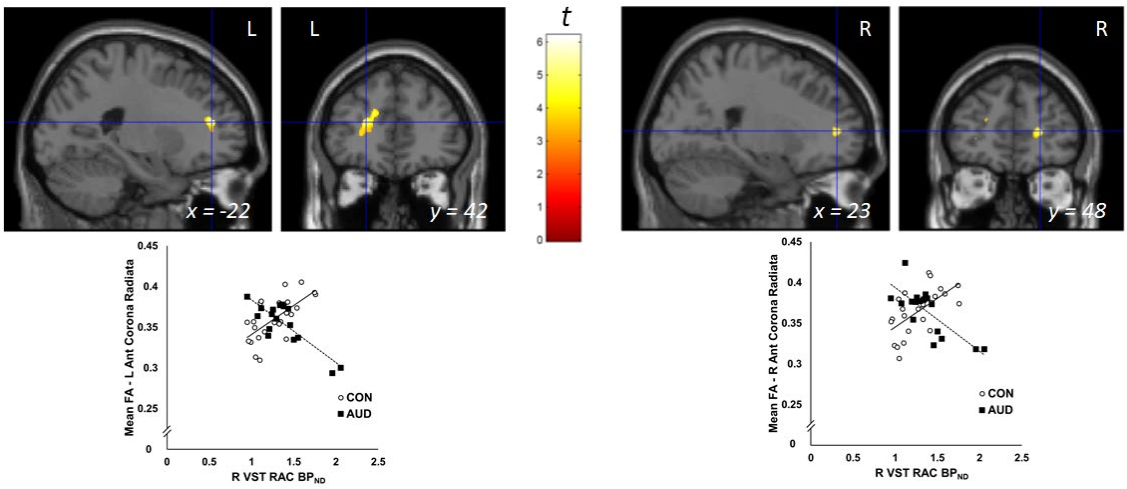

Figure 21. Interaction of right ventral striatum binding potential (BP_{ND}) with fractional anisotropy (FA) in the left and right anterior corona radiata between alcohol use disorder (AUD) and control (CON) groups. Images are Montreal Neurological Institute (MNI) standard space T1 templates, with *t*-statistic results overlaid on top with red-yellow colormap. Data were visualized at $p < 0.001$, k > 300 voxels). Bottom are mean FA values extracted from significant clusters and plotted against right ventral striatum BP_{ND} by group.

Discussion

In this chapter, a multimodal analysis was carried out that combined structural information about WM integrity and molecular information of striatal DA tone in order to investigate possible relationships between frontostriatal connectivity and striatal DA function in alcoholism. The results showed that right VST BP_{ND}, an index of DA tone, was related to WM integrity (FA) in clusters located bilaterally in the anterior corona radiata. Additionally, this relationship differed as a function of group, such that a positive association was observed in controls, while a negative relationship was found in AUD.

BP_{ND} is an outcome metric that captures the state of the DAergic system at a particular window in time. It combined information about quantity of unoccupied receptors and levels of synaptic and extrasynaptic DA. Higher BP_{ND} values correspond to lower DAergic tone, as a result of higher retention of tracer in the tissue due to less extracellular DA and/or higher receptor availability. Likewise, lower BP_{ND} values mean the tracer is less likely to bind (higher DAergic tone) and is being cleared from the area via venous blood. In this analysis we observed a positive relationship of BP_{ND} and anterior corona radiata FA in our social drinking controls, which suggests that higher frontal WM integrity is associated with lower VST DA tone. Both cortical GLUergic and midbrain DAergic inputs terminate onto medium spiny neurons in the striatum, however, they do not make direct synaptic connections to each other (Gonzales et al., 2004). Therefore, the observed relationship may be due to one or several feedback loop mechanisms within the cortico-basal ganglia circuitry (Haber (2014); also see below). Additionally, FA is a metric of WM integrity that is sensitive to disruption in myelination

and is not a direct metric of neurotransmitter function. It is likely that FA provides indirect information in regard to action potential propagation and/or neurotransmission speed (Barron et al., 2018, Waxman, 1980), which in turn, mat alter DA release via feedback loops.

As hypothesized, the opposite relationship was observed in AUD compared to controls, in which higher FA was associated with lower BP_{ND} (higher DA tone). Transition to habitual/dependent alcohol use patterns in marked by the adaptation of the GLUergic system to maintain excitatory/inhibitory neurotransmission balance in the brain. The mesolimbic circuitry contains GLUergic projections from the prefrontal cortex to the ventral tegmental area DAergic neurons (Alasmari et al., 2018) and increasing GLUergic action through that pathway may alter the relationship to that seen in the AUD group compared to controls. Chronic alcohol use is also suggested to show increased involvement of amygdala, hippocampal, and thalamic circuity, which may alter the frontostriatal structure/VST DA function in AUD (Alasmari et al., 2018, Haber, 2014, Haber and Behrens, 2014, Goldstein and Volkow, 2002). It is possible measures of myelination such as FA, are related to neurotransmitter action by capturing the efficiency with which neurotransmission occurs. As such, higher WM integrity in tracts that contain GLUergic projections may be indirectly related to DA tone through its relationship to efficiency of neurotransmission.

This analysis was a novel and preliminary investigation of relationships between frontostriatal WM integrity and striatal DAergic function. We found that right VST DA tone was related to WM integrity in the bilateral anterior corona radiata and that this relationship differed between social drinking controls and AUD individuals. Future work

that employs tractography-based structural connectivity is needed to better characterize tract-dependent relationships among frontal, striatal, midbrain, and other region of the cortico-basal ganglia circuitry that have been implicated in addiction and habitual/dependent alcohol use.

Summary

Here, microstructural alterations were reported in relatively understudied alcohol dependent samples of actively drinking nontreatment-seeking alcoholics and college-age early onset alcohol use disorder (AUD) individuals. Additionally, network science methodology was utilized to better understand the relationship between alcohol misuse and structural connectivity of the brain. Chapter one compared fractional anisotropy (FA), a measure of white matter (WM) integrity, between active AUD community dwelling individuals and social drinking controls. All participants were cigarette users, which addressed a possible confound of high cigarette use comorbidity of AUD samples in neuroimaging literature. The results are in agreement with the body of work in detoxified/in-treatment AUD samples, showing a reduction in WM integrity in alcoholics compared to controls. There was also a negative relationship between self-reported number of drinks per week in the 90-days prior enrollment and average FA from core cerebral WM across the full sample. Finally, a novel WM tractography method was utilized in order to approximate the GM termination areas of WM projections through regions of group difference. The results from Chapter 1 show that community dwelling active AUD individuals, which may represent a distinct and less severe population compared to treatment-seeking AUD, display similar WM integrity disruptions, although the differences reported here were observed primarily in the left hemisphere. These differences could be interpreted as demyelination of axons or axonal loss as a consequence of chronic alcohol misuse. It is likely demyelination is the primary contributor, as follow-up studies in individuals who cease alcohol use and remain

abstinent have reported a recovery in their WM integrity (Durazzo et al., 2014b), suggesting remyelination. However, additional research is necessary to disentangle demyelination and neuronal loss contributions to observed differences in FA in alcoholism.

Chapter 2 of this report was a retrospective analysis of diffusion weighted imaging (DWI) data in a sample of emerging adulthood AUD individuals and social drinking controls. Alcohol dependent individuals met criteria for lifetime AUD diagnosis, with an approximate age of onset of ~18 years. Voxelwise comparisons of diffusivity metrics showed a spatially extensive increase in FA and reductions in mean, axial, and radial diffusivity (MD, AD, and RD, respectively). The increased FA has been reported previously in younger samples (Bava et al., 2009, Tapert and Schweinsburg, 2005); however, this finding is inconsistent with the DTI literature in chronic AUD. It is possible that hyper-connectivity of certain brain regions is a predisposing factor to substance abuse. In this sample, the increased FA seems to be driven by reductions in RD. As increases in myelination as a result of alcohol use are unlikely, it is possible this represents disruptions in crossing fibers in the WM (Winston, 2012). Such alterations in connectivity may be captured via application of network science. When the brain is represented as a network, one of its properties is the interconnectivity of groups of brain regions to achieve a specialized function. This property can be estimated via modularity to obtain a community structure partition of the brain. Here, we employed a novel modularity procedure in order to obtain a connectivity matrix that quantifies the probability that any two brain regions will be classified to the same community across the full range of modularity resolution spectrum. These co-classification matrices were then

compared between groups to assess for differences in association strength. The results found alterations in association strength among brain regions that are related to attention and default mode function. This altered attention and default mode modularity association could be indicative of a predisposition to substance use in the AUD group via the function of attentional networks orienting to salient stimuli. Further work is necessary to validate these findings in larger samples as well as in other populations where predisposition to substance abuse if of interest, such as those with positive family history for AUD.

The third chapter of this report describes a secondary analysis of a subsample obtained from the subjects in Chapter 1, with an addition of a third group of nonsmoking social drinking controls. Three groups of nineteen participants (nonsmoking controls (CON), cigarette smoking controls (SMK), and smoking nontreatment-seeking AUD (NTS) individuals) underwent DWI. Structural connectomes were generated for all subjects and data were tested for differences in group consensus community structure. Group consensus community structure partitions were highly similar among the three groups, yet they differed in their underlying distributions of mean streamline length, when the network edges were stratified as either within- or between-communities. Cigarette use, with or without comorbid AUD, was shown to be associated with altered graph theory global network metrics and reduced between-community mean streamline length, as assessed by area under the curve. Qualitatively, this difference was due to a reduction of intermediate/long streamline length edges in the networks of smoking groups. Due to methodological concerns (i.e. tractography algorithm and parameter selection variation) and their effects on the connectivity metrics, these findings should be

interpreted carefully. It is likely that cigarette use negatively affects WM microstructure, thus leading to observed reduction in connectivity. The absence of differences between the smoking controls and smoking NTS should not be interpreted as the absence of effects of alcohol. In order to fully understand the impact of AUD, further work with larger samples and nonsmoking AUD groups is necessary. Unfortunately, due to the high comorbidity of AUD and cigarette use, recruitment of such individuals is difficult.

The final chapter described a novel preliminary analysis that combines structural WM integrity information from DWI data with a PET-derived index of DA tone (BP_{ND}) from. Seventeen active alcohol-dependent individuals and twenty-four age matched controls were included in the analysis. DWI data were preprocessed as described in Chapter 1 to obtain voxelwise FA images, and motion-corrected PET data were analyzed with the Multilinear Reference Tissue Model (MRTM) to obtain regional BP_{ND} estimates for precommissural caudate and putamen and ventral striatum (VST). Multiple regression models revealed a group interaction of bilateral anterior corona radiata FA and BP_{ND} from the right VST, after accounting for scanner, education, sex, and cigarette use. Higher WM integrity was associated with lower DA tone in controls, but higher tone in AUD participants. The altered relationship observed in AUD may be an indirect indicator (via degree of myelination) of altered neurotransmission of frontostriatal connections. This neurotransmitter action is likely excitatory in nature, as glutamatergic adaptation has been suggested as one of the contributors to habitual/dependent alcohol use in AUD.

In summary, this document detailed investigations into the structural connectivity of understudied populations of AUD individuals. This report also showed that comorbid cigarette use is a serious confound in AUD research. In the first two chapters, we used

DWI to report microstructural and structural connectivity disruptions in active NTS AUD and in early onset college-age AUD populations. NTS represent a less severe phenotype of AUD; however, they still meet several of the disorder criteria and clearly show signs of dependence. Chapter 1 results show that that NTS, similar to detoxified alcoholics, show a reduction in cortical WM integrity that is correlated with self-reported alcohol use. However, contrary to adult AUD, in a college-age sample of individuals with early onset AUD, WM integrity increased. This may serve as a predisposition to alcohol or substance abuse in general. Further work in larger sample with follow-up visit is needed to validate these findings and to determine whether those that continue on to chronic AUD post-college demonstrate the reduction in WM integrity that has been so widely reported. Results from Chapter 3 emphasize the need for proper control of cigarette use status as well as severity/frequency. Our results show that graph theory-based measures of structural connectivity as well as tractography-dependent community structure are greatly influenced by cigarette use status. Finally, Chapter 4 examined structure/function relationships in AUD with a multimodal neuroimaging analysis. The methodology utilized in this report to investigate connectivity alteration in structural connectomes can be applied to other AUD and substance use populations. Consensus in methodological application is an essential and arguably necessary condition for reproducibility and generalizability of findings across studies and will lead to significant leaps forward in our understanding of the neurobiology of alcoholism and addiction.

References

AALTO, S., INGMAN, K., ALAKURTTI, K., KAASINEN, V., VIRKKALA, J., NÅGREN, K., RINNE, J. O. & SCHEININ, H. 2015. Intravenous Ethanol Increases Dopamine Release in the Ventral Striatum in Humans: PET Study Using Bolus-Plus-Infusion Administration of [11C]raclopride. *Journal of Cerebral Blood Flow & Metabolism,* 35**,** 424-431.

AKKUS, F., MIHOV, Y., TREYER, V., AMETAMEY, S. M., JOHAYEM, A., SENN, S., RÖSNER, S., BUCK, A. & HASLER, G. 2018. Metabotropic glutamate receptor 5 binding in male patients with alcohol use disorder. *Translational Psychiatry,* 8**,** 17.

ALASMARI, F., GOODWANI, S., MCCULLUMSMITH, R. E. & SARI, Y. 2018. Role of glutamatergic system and mesocorticolimbic circuits in alcohol dependence. *Progress in Neurobiology,* 171**,** 32-49.

ALBRECHT, D. S., KAREKEN, D. A. & YODER, K. K. 2013. Effects of smoking on D(2)/D(3) striatal receptor availability in alcoholics and social drinkers. *Brain Imaging Behav,* 7**,** 326-34.

ALEXANDER, A. L., HURLEY, S. A., SAMSONOV, A. A., ADLURU, N., HOSSEINBOR, A. P., MOSSAHEBI, P., TROMP, D. P. M., ZAKSZEWSKI, E. & FIELD, A. S. 2011. Characterization of Cerebral White Matter Properties Using Quantitative Magnetic Resonance Imaging Stains. *Brain Connect,* 1**,** 423-46.

ALEXANDER, A. L., LEE, J. E., LAZAR, M. & FIELD, A. S. 2007. Diffusion Tensor Imaging of the Brain. *Neurotherapeutics : the journal of the American Society for Experimental NeuroTherapeutics,* 4**,** 316-329.

ALHASSOON, O. M., SORG, S. F., TAYLOR, M. J., STEPHAN, R. A., SCHWEINSBURG, B. C., STRICKER, N. H., GONGVATANA, A. & GRANT, I. 2012. Callosal white matter microstructural recovery in abstinent alcoholics: a longitudinal diffusion tensor imaging study. *Alcohol Clin Exp Res,* 36**,** 1922-31.

ALVANZO, A. A. H., WAND, G. S., KUWABARA, H., WONG, D. F., XU, X. & MCCAUL, M. E. 2017. Family history of alcoholism is related to increased D2/D3 receptor binding potential: a marker of resilience or risk? *Addiction Biology,* 22**,** 218-228.

ANDREWS-HANNA, J. R., REIDLER, J. S., SEPULCRE, J., POULIN, R. & BUCKNER, R. L. 2010. Functional-Anatomic Fractionation of the Brain's Default Network. *Neuron,* 65**,** 550-562.

APA 2013. Diagnostic and statistical manual of mental disorders 5th Ed. *Americal Psychiatric Association*.

BAEZA-LOYA, S., VELASQUEZ, K. M., MOLFESE, D. L., VISWANATH, H., CURTIS, K. N., THOMPSON-LAKE, D. G. Y., BALDWIN, P. R., ELLMORE, T. M., DE LA GARZA, R. & SALAS, R. 2016. Anterior cingulum white matter is altered in tobacco smokers. *The American Journal on Addictions,* 25**,** 210-214.

BAGGA, D., SHARMA, A., KUMARI, A., KAUR, P., BHATTACHARYA, D., GARG, M. L., KHUSHU, S. & SINGH, N. 2014. Decreased white matter integrity in fronto-occipital fasciculus bundles: relation to visual information processing in alcohol-dependent subjects. *Alcohol,* 48**,** 43-53.

BARRON, T., SAIFETIAROVA, J., BHAT, M. A. & KIM, J. H. 2018. Myelination of Purkinje axons is critical for resilient synaptic transmission in the deep cerebellar nucleus. *Scientific Reports,* 8**,** 1022.
BASSETT, D. S., ZURN, P. & GOLD, J. I. 2018. On the nature and use of models in network neuroscience. *Nature Reviews Neuroscience*.
BAVA, S., FRANK, L. R., MCQUEENY, T., SCHWEINSBURG, B. C., SCHWEINSBURG, A. D. & TAPERT, S. F. 2009. Altered white matter microstructure in adolescent substance users. *Psychiatry Research: Neuroimaging,* 173**,** 228-237.
BAVA, S. & TAPERT, S. F. 2010. Adolescent Brain Development and the Risk for Alcohol and Other Drug Problems. *Neuropsychology Review,* 20**,** 398-413.
BEHRENS, T. E. J., JOHANSEN-BERG, H., WOOLRICH, M. W., SMITH, S. M., WHEELER-KINGSHOTT, C. A. M., BULBY, P. A., BARKER, G. J., SILLERY, E. L., SHEEHAN, K., CICCARELLI, O., THOMPSON, A. J., BRADY, J. M. & MATTHEWS, P. M. 2003. Non-invasive mapping of connections between human thalamus and cortex using diffusion imaging. *Nature Neuroscience,* 6**,** 750-757.
BERK, L., STEWART, J. L., MAY, A. C., WIERS, R. W., DAVENPORT, P. W., PAULUS, M. P. & TAPERT, S. F. 2015. Under pressure: adolescent substance users show exaggerated neural processing of aversive interoceptive stimuli. *Addiction,* 110**,** 2025-2036.
BERRIDGE, K. C. 2006. The debate over dopamine's role in reward: the case for incentive salience. *Psychopharmacology,* 191**,** 391-431.
BERRIDGE, K. C. & ROBINSON, T. E. 2016. Liking, wanting, and the incentive-sensitization theory of addiction. *The American psychologist,* 71**,** 670-679.
BIRN, R. M., CONVERSE, A. K., RAJALA, A. Z., ALEXANDER, A. L., BLOCK, W. F., MCMILLAN, A. B., CHRISTIAN, B. T., FILLA, C. N., MURALI, D., HURLEY, S. A., JENISON, R. L. & POPULIN, L. C. 2019. Changes in Endogenous Dopamine Induced by Methylphenidate Predict Functional Connectivity in Nonhuman Primates. *The Journal of Neuroscience,* 39**,** 1436.
BLANCO, C., OKUDA, M., WRIGHT, C., HASIN, D. S., GRANT, B. F., LIU, S. M. & OLFSON, M. 2008. Mental Health of College Students and Their Non-college-attending Peers: Results from the National Epidemiologic Study on Alcohol and Related Conditions. *Arch Gen Psychiatry,* 65**,** 1429-37.
BOILEAU, I., ASSAAD, J. M., PIHL, R. O., BENKELFAT, C., LEYTON, M., DIKSIC, M., TREMBLAY, R. E. & DAGHER, A. 2003. Alcohol promotes dopamine release in the human nucleus accumbens. *Synapse,* 49**,** 226-231.
BOLAM, J. P. & IZZO, P. N. 1988. The postsynaptic targets of substance P-immunoreactive terminals in the rat neostriatum with particular reference to identified spiny striatonigral neurons. *Experimental Brain Research,* 70**,** 361-377.
BRECKEL, T. P. K., THIEL, C. M. & GIESSING, C. 2013. The efficiency of functional brain networks does not differ between smokers and non-smokers. *Psychiatry Research: Neuroimaging,* 214**,** 349-356.
BUCHOLZ, K. K., CADORET, R., CLONINGER, C. R., DINWIDDIE, S. H., HESSELBROCK, V. M., NURNBERGER, J. I., REICH, T., SCHMIDT, I. & SCHUCKIT, M. A. 1994. A new, semi-structured psychiatric interview for use in

genetic linkage studies: a report on the reliability of the SSAGA. *Journal of Studies on Alcohol,* 55**,** 149-158.
BÜHLER, M. & MANN, K. 2011. Alcohol and the Human Brain: A Systematic Review of Different Neuroimaging Methods. *Alcoholism: Clinical and Experimental Research,* 35**,** 1771-1793.
BULLMORE, E. & SPORNS, O. 2009. Complex brain networks: graph theoretical analysis of structural and functional systems. *Nat Rev Neurosci,* 10**,** 186-98.
CAO, R., WU, Z., LI, H., XIANG, J. & CHEN, J. 2014. Disturbed connectivity of EEG functional networks in alcoholism: a graph-theoretic analysis.
CARDENAS, V. A., GREENSTEIN, D., FOUCHE, J.-P., FERRETT, H., CUZEN, N., STEIN, D. J. & FEIN, G. 2013. Not lesser but Greater fractional anisotropy in adolescents with alcohol use disorders. *NeuroImage: Clinical,* 2**,** 804-809.
CARDENAS, V. A., STUDHOLME, C., MEYERHOFF, D. J., SONG, E. & WEINER, M. W. 2005. Chronic active heavy drinking and family history of problem drinking modulate regional brain tissue volumes. *Psychiatry Research: Neuroimaging,* 138**,** 115-130.
CDC. 2013. *Alcohol and Public Health: Alcohol-Related Disease Impact (ARDI). Average for United States 2006–2010 Alcohol-Attributable Deaths Due to Excessive Alcohol Use.* [Online]. Available: https://nccd.cdc.gov/DPH_ARDI/Default/Report.aspx?T=AAM&P=f6d7eda7-036e-4553-9968-9b17ffad620e&R=d7a9b303-48e9-4440-bf47-070a4827e1fd&M=8E1C5233-5640-4EE8-9247-1ECA7DA325B9&F=&D [Accessed 5/1/2019].
CECCARINI, J., HOMPES, T., VERHAEGHEN, A., CASTEELS, C., PEUSKENS, H., BORMANS, G., CLAES, S. & VAN LAERE, K. 2014. Changes in Cerebral CB₁ Receptor Availability after Acute and Chronic Alcohol Abuse and Monitored Abstinence. *The Journal of Neuroscience,* 34**,** 2822.
CHANRAUD, S., PITEL, A.-L., PFEFFERBAUM, A. & SULLIVAN, E. V. 2011. Disruption of Functional Connectivity of the Default-Mode Network in Alcoholism. *Cerebral Cortex,* 21**,** 2272-2281.
CHENG, H., KELLAR, D., LAKE, A., FINN, P., REBEC, G. V., DHARMADHIKARI, S., DYDAK, U. & NEWMAN, S. 2018. Effects of Alcohol Cues on MRS Glutamate Levels in the Anterior Cingulate. *Alcohol and Alcoholism,* 53**,** 209-215.
CHOI, E. Y., DING, S.-L. & HABER, S. N. 2017. Combinatorial Inputs to the Ventral Striatum from the Temporal Cortex, Frontal Cortex, and Amygdala: Implications for Segmenting the Striatum. *eneuro,* 4**,** ENEURO.0392-17.2017.
CHUMIN, E., J., GOÑI, J., HALCOMB MEREDITH, E., DURAZZO TIMOTHY, C., DZEMIDZIC, M. & YODER KARMEN, K. 2018. Differences in White Matter Microstructure and Connectivity in Nontreatment-Seeking Individuals with Alcohol Use Disorder. *Alcoholism: Clinical and Experimental Research,* 42**,** 889-896.
CLARKE, R. B. C., ADERMARK, L., CHAU, P., SÖDERPALM, B. & ERICSON, M. 2014. Increase in Nucleus Accumbens Dopamine Levels Following Local Ethanol Administration Is Not Mediated by Acetaldehyde. *Alcohol and Alcoholism,* 49**,** 498-504.

CLEMENS, K. J. & HOLMES, N. M. 2018. An extended history of drug self-administration results in multiple sources of control over drug seeking behavior. *Progress in Neuro-Psychopharmacology and Biological Psychiatry,* 87**,** 48-55.
COOK, P. A., BAI, Y., NEDJATI-GILANI, S., SEUNARINE, K. K., HALL, M. G., PARKER, G. J. & ALEXANDER, D. C. 2006. Camino: Open-Source Diffusion-MRI Reconstruction and Processing. *14th Scientific Meeting of the International Society for Magnetic Resonance in Medicine***,** p. 2759.
CORREAS, A., CUESTA, P., LÓPEZ-CANEDA, E., RODRÍGUEZ HOLGUÍN, S., GARCÍA-MORENO, L. M., PINEDA-PARDO, J. A., CADAVEIRA, F. & MAESTÚ, F. 2016. Functional and structural brain connectivity of young binge drinkers: a follow-up study. *Scientific Reports,* 6**,** 31293.
COSGROVE, K. P., MCKAY, R., ESTERLIS, I., KLOCZYNSKI, T., PERKINS, E., BOIS, F., PITTMAN, B., LANCASTER, J., GLAHN, D. C., O'MALLEY, S., CARSON, R. E. & KRYSTAL, J. H. 2014. Tobacco smoking interferes with GABA_A receptor neuroadaptations during prolonged alcohol withdrawal. *Proceedings of the National Academy of Sciences,* 111**,** 18031.
COUPÉ, P., YGER, P., PRIMA, S., HELLIER, P., KERVRANN, C. & BARILLOT, C. 2008. An Optimized Blockwise Nonlocal Means Denoising Filter for 3-D Magnetic Resonance Images. *Medical Imaging, IEEE Transactions on,* 27**,** 425-441.
COURTNEY, K. E., GHAHREMANI, D. G., LONDON, E. D. & RAY, L. A. 2014. The association between cue-reactivity in the precuneus and level of dependence on nicotine and alcohol. *Drug and Alcohol Dependence,* 141**,** 21-26.
CSERVENKA, A. 2016. Neurobiological phenotypes associated with a family history of alcoholism. *Drug and Alcohol Dependence,* 158**,** 8-21.
D'ALESSANDRO, A., BOECKELMANN, I., HAMMWHÖNER, M. & GOETTE, A. 2011. Nicotine, cigarette smoking and cardiac arrhythmia: an overview. *European Journal of Preventive Cardiology,* 19**,** 297-305.
DE BELLIS, M. D., VAN VOORHEES, E., HOOPER, S. R., GIBLER, N., NELSON, L., HEGE, S. G., PAYNE, M. E. & MACFALL, J. 2008. Diffusion tensor measures of the corpus callosum in adolescents with adolescent onset alcohol use disorders. *Alcohol Clin Exp Res,* 32**,** 395-404.
DE WIT, H., METZ, J., WAGNER, N. & COOPER, M. 1990. Behavioral and Subjective Effects of Ethanol: Relationship to Cerebral Metabolism Using PET. *Alcoholism: Clinical and Experimental Research,* 14**,** 482-489.
DELL'ANNO, M. T., PALLOTTINO, S. & FISONE, G. 2013. mGlu5R promotes glutamate AMPA receptor phosphorylation via activation of PKA/DARPP-32 signaling in striatopallidal medium spiny neurons. *Neuropharmacology,* 66**,** 179-186.
DEPARTMENT OF HEALTH AND HUMAN SERVICES. 2015a. *2015–2020 Dietary Guidelines for Americans. 8th Edition. December 2015. Appendix 9.* [Online]. Available: http://health.gov/dietaryguidelines/2015/guidelines/ [Accessed 05/01/2019].
DEPARTMENT OF HEALTH AND HUMAN SERVICES. 2015b. *National Survey on Drug Use and Health* [Online]. Department of Health and Human Sevices. Available: https://www.samhsa.gov/data/sites/default/files/NSDUH-DetTabs-

2015/NSDUH-DetTabs-2015/NSDUH-DetTabs-2015.htm#tab5-6a [Accessed 10 March 2017].
DESERNO, L., BECK, A., HUYS, Q. J. M., LORENZ, R. C., BUCHERT, R., BUCHHOLZ, H.-G., PLOTKIN, M., KUMAKARA, Y., CUMMING, P., HEINZE, H.-J., GRACE, A. A., RAPP, M. A., SCHLAGENHAUF, F. & HEINZ, A. 2015. Chronic alcohol intake abolishes the relationship between dopamine synthesis capacity and learning signals in the ventral striatum. *European Journal of Neuroscience,* 41**,** 477-486.
DOYON, W. M., YORK, J. L., DIAZ, L. M., SAMSON, H. H., CZACHOWSKI, C. L. & GONZALES, R. A. 2003. Dopamine Activity in the Nucleus Accumbens During Consummatory Phases of Oral Ethanol Self-Administration. *Alcoholism: Clinical and Experimental Research,* 27**,** 1573-1582.
DRAGANSKI, B., KHERIF, F., KLOPPEL, S., COOK, P. A., ALEXANDER, D. C., PARKER, G. J., DEICHMANN, R., ASHBURNER, J. & FRACKOWIAK, R. S. 2008. Evidence for segregated and integrative connectivity patterns in the human Basal Ganglia. *J Neurosci,* 28**,** 7143-52.
DROUTMAN, V., READ, S. J. & BECHARA, A. 2015. Revisiting the role of the insula in addiction. *Trends Cogn Sci,* 19**,** 414-20.
DURAZZO, T. C., CARDENAS, V. A., STUDHOLME, C., WEINER, M. W. & MEYERHOFF, D. J. 2007a. Non-treatment-seeking heavy drinkers: Effects of chronic cigarette smoking on brain structure. *Drug and Alcohol Dependence,* 87**,** 76-82.
DURAZZO, T. C., GAZDZINSKI, S. & MEYERHOFF, D. J. 2007b. The neurobiological and neurocognitive consequences of chronic cigarette smoking in alcohol use disorders. *Alcohol and Alcoholism,* 42**,** 174-185.
DURAZZO, T. C., MEYERHOFF, D. J., YODER, K. K. & MURRAY, D. E. 2017. Cigarette smoking is associated with amplified age-related volume loss in subcortical brain regions. *Drug and Alcohol Dependence,* 177**,** 228-236.
DURAZZO, T. C., MON, A., PENNINGTON, D., ABÉ, C., GAZDZINSKI, S. & MEYERHOFF, D. J. 2014a. Interactive effects of chronic cigarette smoking and age on brain volumes in controls and alcohol-dependent individuals in early abstinence. *Addiction Biology,* 19**,** 132-143.
DURAZZO, T. C., PENNINGTON, D. L., SCHMIDT, T. P. & MEYERHOFF, D. J. 2014b. Effects of Cigarette Smoking History on Neurocognitive Recovery Over 8 Months of Abstinence in Alcohol-Dependent Individuals. *Alcoholism: Clinical and Experimental Research,* 38**,** 2816-2825.
EISENHARDT, M., LEIXNER, S., SPANAGEL, R. & BILBAO, A. 2015. Quantification of alcohol drinking patterns in mice. *Addiction Biology,* 20**,** 1001-1011.
ELOFSON, J., GONGVATANA, W. & CAREY, K. B. 2013. Alcohol Use and Cerebral White Matter Compromise in Adolescence. *Addict Behav,* 38**,** 2295-305.
ERRITZOE, D., TZIORTZI, A., BARGIELA, D., COLASANTI, A., SEARLE, G. E., GUNN, R. N., BEAVER, J. D., WALDMAN, A., NUTT, D. J., BANI, M., MERLO-PICH, E., RABINER, E. A. & LINGFORD-HUGHES, A. 2014. In Vivo Imaging of Cerebral Dopamine D3 Receptors in Alcoholism. *Neuropsychopharmacology,* 39**,** 1703.

ESPOSITO, F., PIGNATARO, G., DI RENZO, G., SPINALI, A., PACCONE, A., TEDESCHI, G. & ANNUNZIATO, L. 2010. Alcohol increases spontaneous BOLD signal fluctuations in the visual network. *Neuroimage,* 53**,** 534-43.

ESTRUCH, R., NICOLÁS, J. M., SALAMERO, M., ARAGÓN, C., SACANELLA, E., FERNÁNDEZ-SOLÁ, J. & URBANO-MÁRQUEZ, A. 1997. Atrophy of the corpus callosum in chronic alcoholism. *Journal of the Neurological Sciences,* 146**,** 145-151.

EVERITT, B. J. & ROBBINS, T. W. 2005. Neural systems of reinforcement for drug addiction: from actions to habits to compulsion. *Nature Neuroscience,* 8**,** 1481-1489.

FALK, D. E., YI, H.-Y. & HILLER-STURMHÖFEL, S. 2006. An epidemiologic analysis of co-occurring alcohol and tobacco use and disorders: findings from the National Epidemiologic Survey on Alcohol and Related Conditions. *Alcohol Research & Health: The Journal Of The National Institute On Alcohol Abuse And Alcoholism,* 29**,** 162-171.

FELDMAN, H. M., YEATMAN, J. D., LEE, E. S., BARDE, L. H. F. & GAMAN-BEAN, S. 2010. Diffusion Tensor Imaging: A Review for Pediatric Researchers and Clinicians. *J Dev Behav Pediatr,* 31**,** 346-56.

FIELD, M. & COX, W. M. 2008. Attentional bias in addictive behaviors: a review of its development, causes, and consequences. *Drug Alcohol Depend,* 97**,** 1-20.

FINN, P. R., GUNN, R. L. & GERST, K. R. 2015. The Effects of a Working Memory Load on Delay Discounting in Those with Externalizing Psychopathology. *Clinical psychological science: a journal of the Association for Psychological Science,* 3**,** 202-214.

FORNITO, A., ZALESKY, A. & BREAKSPEAR, M. 2015. The connectomics of brain disorders. *Nature Reviews Neuroscience,* 16**,** 159.

FORTIER, C. B., LERITZ, E. C., SALAT, D. H., LINDEMER, E., MAKSIMOVSKIY, A. L., SHEPEL, J., WILLIAMS, V., VENNE, J. R., MILBERG, W. P. & MCGLINCHEY, R. E. 2014. Widespread Effects of Alcohol on White Matter Microstructure. *Alcoholism: Clinical and Experimental Research,* 38**,** 2925-2933.

FOX, M. D., CORBETTA, M., SNYDER, A. Z., VINCENT, J. L. & RAICHLE, M. E. 2006. Spontaneous neuronal activity distinguishes human dorsal and ventral attention systems. *Proceedings of the National Academy of Sciences,* 103**,** 10046-10051.

FRYER, S. L., JORGENSEN, K. W., YETTER, E. J., DAURIGNAC, E. C., WATSON, T. D., SHANBHAG, H., KRYSTAL, J. H. & MATHALON, D. H. 2013. Differential brain response to alcohol cue distractors across stages of alcohol dependence. *Biological Psychology,* 92**,** 282-291.

GALLEN, C. L., BANIQUED, P. L., CHAPMAN, S. B., ASLAN, S., KEEBLER, M., DIDEHBANI, N. & D'ESPOSITO, M. 2016. Modular Brain Network Organization Predicts Response to Cognitive Training in Older Adults. *PLOS ONE,* 11**,** e0169015.

GAZDZINSKI, S., DURAZZO, T. C., STUDHOLME, C., SONG, E., BANYS, P. & MEYERHOFF, D. J. 2005. Quantitative Brain MRI in Alcohol Dependence: Preliminary Evidence for Effects of Concurrent Chronic Cigarette Smoking on

Regional Brain Volumes. *Alcoholism: Clinical and Experimental Research,* 29**,** 1484-1495.
GERDEMAN, G. L., PARTRIDGE, J. G., LUPICA, C. R. & LOVINGER, D. M. 2003. It could be habit forming: drugs of abuse and striatal synaptic plasticity. *Trends in Neurosciences,* 26**,** 184-192.
GOLDSTEIN, R. Z. & VOLKOW, N. D. 2002. Drug Addiction and Its Underlying Neurobiological Basis: Neuroimaging Evidence for the Involvement of the Frontal Cortex. *American Journal of Psychiatry,* 159**,** 1642-1652.
GONZALES, R. A., JOB, M. O. & DOYON, W. M. 2004. The role of mesolimbic dopamine in the development and maintenance of ethanol reinforcement. *Pharmacology & Therapeutics,* 103**,** 121-146.
GOODSON, C. M., CLARK, B. J. & DOUGLAS, I. S. 2014. Predictors of Severe Alcohol Withdrawal Syndrome: A Systematic Review and Meta-Analysis. *Alcoholism: Clinical and Experimental Research,* 38**,** 2664-2677.
GORKA, S. M., PHAN, K. L. & CHILDS, E. 2018. Acute calming effects of alcohol are associated with disruption of the salience network. *Addict Biol,* 23**,** 921-930.
GRACE, A. A. & BUNNEY, B. S. 1985. Low doses of apomorphine elicit two opposing influences on dopamine cell electrophysiology. *Brain Research,* 333**,** 285-298.
GREICIUS, M. D., KRASNOW, B., REISS, A. L. & MENON, V. 2003. Functional connectivity in the resting brain: A network analysis of the default mode hypothesis. *Proceedings of the National Academy of Sciences,* 100**,** 253-258.
HABER, S. N. 2014. The place of dopamine in the cortico-basal ganglia circuit. *Neuroscience,* 282**,** 248-257.
HABER, SUZANNE N. & BEHRENS, TIMOTHY E. J. 2014. The Neural Network Underlying Incentive-Based Learning: Implications for Interpreting Circuit Disruptions in Psychiatric Disorders. *Neuron,* 83**,** 1019-1039.
HABER, S. N., KIM, K. S., MAILLY, P. & CALZAVARA, R. 2006. Reward-related cortical inputs define a large striatal region in primates that interface with associative cortical connections, providing a substrate for incentive-based learning. *J Neurosci,* 26**,** 8368-76.
HABER, S. N. & KNUTSON, B. 2010. The reward circuit: linking primate anatomy and human imaging. *Neuropsychopharmacology,* 35**,** 4-26.
HAGMANN, P., CAMMOUN, L., GIGANDET, X., MEULI, R., HONEY, C. J., WEDEEN, V. J. & SPORNS, O. 2008. Mapping the Structural Core of Human Cerebral Cortex. *PLoS Biol,* 6**,** e159.
HALL, H., SEDVALL, G., MAGNUSSON, O., KOPP, J., HALLDIN, C. & FARDE, L. 1994. Distribution of D1- and D2-Dopamine Receptors, and Dopamine and Its Metabolites in the Human Brain. *Neuropsychopharmacology,* 11**,** 245-256.
HEINZ, A., SIESSMEIER, T., WRASE, J., BUCHHOLZ, H. G., GRÜNDER, G., KUMAKURA, Y., CUMMING, P., SCHRECKENBERGER, M., SMOLKA, M. N., RÖSCH, F., MANN, K. & BARTENSTEIN, P. 2005. Correlation of Alcohol Craving With Striatal Dopamine Synthesis Capacity and D2/3 Receptor Availability: A Combined [18F]DOPA and [18F]DMFP PET Study in Detoxified Alcoholic Patients. *American Journal of Psychiatry,* 162**,** 1515-1520.
HILLMER, A. T., KLOCZYNSKI, T., SANDIEGO, C. M., PITTMAN, B., ANDERSON, J. M., LABAREE, D., GAO, H., HUANG, Y., DELULIIS, G.,

O'MALLEY, S. S., CARSON, R. E. & COSGROVE, K. P. 2016. Nicotine and Nicotine Abstinence Do Not Interfere with GABAA Receptor Neuroadaptations During Alcohol Abstinence. *Alcoholism: Clinical and Experimental Research,* 40**,** 698-705.

HILLMER, A. T., WOOTEN, D. W., TUDORASCU, D. L., BARNHART, T. E., AHLERS, E. O., RESCH, L. M., LARSON, J. A., CONVERSE, A. K., MOORE, C. F., SCHNEIDER, M. L. & CHRISTIAN, B. T. 2014. The effects of chronic alcohol self-administration on serotonin-1A receptor binding in nonhuman primates. *Drug and Alcohol Dependence,* 144**,** 119-126.

HODGE, C. W., SAMSON, H. H. & CHAPPELLE, A. M. 1997. Alcohol Self-Administration: Further Examination of the Role of Dopamine Receptors in the Nucleus Accumbens. *Alcoholism: Clinical and Experimental Research,* 21**,** 1083-1091.

HOJJATI, S. H., EBRAHIMZADEH, A., KHAZAEE, A. & BABAJANI-FEREMI, A. 2017. Predicting conversion from MCI to AD using resting-state fMRI, graph theoretical approach and SVM. *Journal of Neuroscience Methods,* 282**,** 69-80.

HOLLA, B., PANDA, R., VENKATASUBRAMANIAN, G., BISWAL, B., BHARATH, R. D. & BENEGAL, V. 2017. Disrupted resting brain graph measures in individuals at high risk for alcoholism. *Psychiatry Research: Neuroimaging,* 265**,** 54-64.

HORN, J., SKINNER, H., WANBERG, K. & FOSTER, F. 1984. Alcohol Use Questionnaire (ADS) *Toronto, Canada: Addiction Research Foundation*.

HUDKINS, M., O'NEILL, J., TOBIAS, M. C., BARTZOKIS, G. & LONDON, E. D. 2012. Cigarette smoking and white matter microstructure. *Psychopharmacology,* 221**,** 285-295.

ICHISE, M., LIOW, J.-S., LU, J.-Q., TAKANO, A., MODEL, K., TOYAMA, H., SUHARA, T., SUZUKI, K., INNIS, R. B. & CARSON, R. E. 2003. Linearized Reference Tissue Parametric Imaging Methods: Application to [11C]DASB Positron Emission Tomography Studies of the Serotonin Transporter in Human Brain. *Journal of Cerebral Blood Flow & Metabolism,* 23**,** 1096-1112.

INNIS, R. B., CUNNINGHAM, V. J., DELFORGE, J., FUJITA, M., GJEDDE, A., GUNN, R. N., HOLDEN, J., HOULE, S., HUANG, S. C., ICHISE, M., IIDA, H., ITO, H., KIMURA, Y., KOEPPE, R. A., KNUDSEN, G. M., KNUUTI, J., LAMMERTSMA, A. A., LARUELLE, M., LOGAN, J., MAGUIRE, R. P., MINTUN, M. A., MORRIS, E. D., PARSEY, R., PRICE, J. C., SLIFSTEIN, M., SOSSI, V., SUHARA, T., VOTAW, J. R., WONG, D. F. & CARSON, R. E. 2007. Consensus nomenclature for in vivo imaging of reversibly binding radioligands. *J Cereb Blood Flow Metab,* 27**,** 1533-9.

JACOBUS, J., MCQUEENY, T., BAVA, S., SCHWEINSBURG, B. C., FRANK, L. R., YANG, T. T. & TAPERT, S. F. 2009. White matter integrity in adolescents with histories of marijuana use and binge drinking. *Neurotoxicology and Teratology,* 31**,** 349-355.

JARAMILLO, A. A., RANDALL, P. A., STEWART, S., FORTINO, B., VAN VOORHIES, K. & BESHEER, J. 2018a. Functional role for cortical-striatal circuitry in modulating alcohol self-administration. *Neuropharmacology,* 130**,** 42-53.

JARAMILLO, A. A., VAN VOORHIES, K., RANDALL, P. A. & BESHEER, J. 2018b. Silencing the insular-striatal circuit decreases alcohol self-administration and increases sensitivity to alcohol. *Behav Brain Res,* 348**,** 74-81.
JARBO, K. & VERSTYNEN, T. D. 2015. Converging structural and functional connectivity of orbitofrontal, dorsolateral prefrontal, and posterior parietal cortex in the human striatum. *J Neurosci,* 35**,** 3865-78.
JENKINSON, M., BANNISTER, P., BRADY, M. & SMITH, S. 2002. Improved Optimization for the Robust and Accurate Linear Registration and Motion Correction of Brain Images. *NeuroImage,* 17**,** 825-841.
JENKINSON, M., BECKMANN, C. F., BEHRENS, T. E. J., WOOLRICH, M. W. & SMITH, S. M. 2012. FSL. *NeuroImage,* 62**,** 782-790.
JENKINSON, M. & SMITH, S. 2001. A global optimisation method for robust affine registration of brain images. *Medical Image Analysis,* 5**,** 143-156.
JENNISON, K. M. 2004. The Short-Term Effects and Unintended Long-Term Consequences of Binge Drinking in College: A 10-Year Follow-Up Study. *The American Journal of Drug and Alcohol Abuse,* 30**,** 659-684.
JEUB, L. G. S., SPORNS, O. & FORTUNATO, S. 2018. Multiresolution Consensus Clustering in Networks. *Scientific Reports,* 8**,** 3259.
KALIVAS, P. W. & VOLKOW, N. D. 2005. The Neural Basis of Addiction: A Pathology of Motivation and Choice. *American Journal of Psychiatry,* 162**,** 1403-1413.
KALMAN, D., MORISSETTE, S. B. & GEORGE, T. P. 2005. Co-Morbidity of Smoking in Patients with Psychiatric and Substance Use Disorders. *The American Journal on Addictions,* 14**,** 106-123.
KHALILI-MAHANI, N., ZOETHOUT, R. M., BECKMANN, C. F., BAERENDS, E., DE KAM, M. L., SOETER, R. P., DAHAN, A., VAN BUCHEM, M. A., VAN GERVEN, J. M. & ROMBOUTS, S. A. 2012. Effects of morphine and alcohol on functional brain connectivity during "resting state": a placebo-controlled crossover study in healthy young men. *Hum Brain Mapp,* 33**,** 1003-18.
KIM, D.-J., SKOSNIK, P. D., CHENG, H., PRUCE, B. J., BRUMBAUGH, M. S., VOLLMER, J. M., HETRICK, W. P., O'DONNELL, B. F., SPORNS, O., PUCE, A. & NEWMAN, S. D. 2011. Structural Network Topology Revealed by White Matter Tractography in Cannabis Users: A Graph Theoretical Analysis. *Brain Connectivity,* 1**,** 473-483.
KONRAD, A., VUCUREVIC, G., LORSCHEIDER, M., BERNOW, N., THUMMEL, M., CHAI, C., PFEIFER, P., STOETER, P., SCHEURICH, A. & FEHR, C. 2012. Broad disruption of brain white matter microstructure and relationship with neuropsychological performance in male patients with severe alcohol dependence. *Alcohol Alcohol,* 47**,** 118-26.
LANCICHINETTI, A. & FORTUNATO, S. 2012. Consensus clustering in complex networks. *Scientific Reports,* 2**,** 336.
LAVIOLETTE, S. R. & VAN DER KOOY, D. 2004. The neurobiology of nicotine addiction: bridging the gap from molecules to behaviour. *Nature Reviews Neuroscience,* 5**,** 55.
LEHERICY, S., DUCROS, M., VAN DE MOORTELE, P. F., FRANCOIS, C., THIVARD, L., POUPON, C., SWINDALE, N., UGURBIL, K. & KIM, D. S.

2004. Diffusion tensor fiber tracking shows distinct corticostriatal circuits in humans. *Ann Neurol,* 55**,** 522-9.

LIAO, Y., TANG, J., DENG, Q., DENG, Y., LUO, T., WANG, X., CHEN, H., LIU, T., CHEN, X., BRODY, A. L. & HAO, W. 2011. Bilateral Fronto-Parietal Integrity in Young Chronic Cigarette Smokers: A Diffusion Tensor Imaging Study. *PLOS ONE,* 6**,** e26460.

LIN, F., WU, G., ZHU, L. & LEI, H. 2013. Heavy smokers show abnormal microstructural integrity in the anterior corpus callosum: A diffusion tensor imaging study with tract-based spatial statistics. *Drug and Alcohol Dependence,* 129**,** 82-87.

LIN, F., WU, G., ZHU, L. & LEI, H. 2014. Altered brain functional networks in heavy smokers. *Addiction Biology,* 20**,** 809-819.

LINGFORD-HUGHES, A., REID, A. G., MYERS, J., FEENEY, A., HAMMERS, A., TAYLOR, L. G., ROSSO, L., TURKHEIMER, F., BROOKS, D. J., GRASBY, P. & NUTT, D. J. 2010. A [11C]Ro15 4513 PET study suggests that alcohol dependence in man is associated with reduced α5 benzodiazepine receptors in limbic regions. *Journal of Psychopharmacology,* 26**,** 273-281.

LITHARI, C., KLADOS, M. A., PAPPAS, C., ALBANI, M., KAPOUKRANIDOU, D., KOVATSI, L., BAMIDIS, P. D. & PAPADELIS, C. L. 2012. Alcohol Affects the Brain's Resting-State Network in Social Drinkers. *PLOS ONE,* 7**,** e48641.

LOGAN, J., FOWLER, J. S., VOLKOW, N. D., WANG, G. J., DING, Y. S. & ALEXOFF, D. L. 1996. Distribution volume ratios without blood sampling from graphical anaysis of PET data. *J Cereb Blood Flow Metab,* 14**,** 995-1010.

LOVINGER, D. M., WHITE, G. & WEIGHT, F. F. 1989. Ethanol inhibits NMDA-activated ion current in hippocampal neurons. *Science,* 243**,** 1721.

MAIER-HEIN, K. H., NEHER, P. F., HOUDE, J.-C., CÔTÉ, M.-A., GARYFALLIDIS, E., ZHONG, J., CHAMBERLAND, M., YEH, F.-C., LIN, Y.-C., JI, Q., REDDICK, W. E., GLASS, J. O., CHEN, D. Q., FENG, Y., GAO, C., WU, Y., MA, J., RENJIE, H., LI, Q., WESTIN, C.-F., DESLAURIERS-GAUTHIER, S., GONZÁLEZ, J. O. O., PAQUETTE, M., ST-JEAN, S., GIRARD, G., RHEAULT, F., SIDHU, J., TAX, C. M. W., GUO, F., MESRI, H. Y., DÁVID, S., FROELING, M., HEEMSKERK, A. M., LEEMANS, A., BORÉ, A., PINSARD, B., BEDETTI, C., DESROSIERS, M., BRAMBATI, S., DOYON, J., SARICA, A., VASTA, R., CERASA, A., QUATTRONE, A., YEATMAN, J., KHAN, A. R., HODGES, W., ALEXANDER, S., ROMASCANO, D., BARAKOVIC, M., AURÍA, A., ESTEBAN, O., LEMKADDEM, A., THIRAN, J.-P., CETINGUL, H. E., ODRY, B. L., MAILHE, B., NADAR, M. S., PIZZAGALLI, F., PRASAD, G., VILLALON-REINA, J. E., GALVIS, J., THOMPSON, P. M., REQUEJO, F. D. S., LAGUNA, P. L., LACERDA, L. M., BARRETT, R., DELL'ACQUA, F., CATANI, M., PETIT, L., CARUYER, E., DADUCCI, A., DYRBY, T. B., HOLLAND-LETZ, T., HILGETAG, C. C., STIELTJES, B. & DESCOTEAUX, M. 2017. The challenge of mapping the human connectome based on diffusion tractography. *Nature Communications,* 8**,** 1349.

MANJÓN, J. V., COUPÉ, P., CONCHA, L., BUADES, A., COLLINS, D. L. & ROBLES, M. 2013. Diffusion Weighted Image Denoising Using Overcomplete Local PCA. *PLoS ONE,* 8**,** e73021.

MARTINEZ, D., GIL, R., SLIFSTEIN, M., HWANG, D.-R., HUANG, Y., PEREZ, A., KEGELES, L., TALBOT, P., EVANS, S., KRYSTAL, J., LARUELLE, M. & ABI-DARGHAM, A. 2005. Alcohol Dependence Is Associated with Blunted Dopamine Transmission in the Ventral Striatum. *Biological Psychiatry,* 58**,** 779-786.

MATSON, L. M. & GRAHAME, N. J. 2013. Pharmacologically relevant intake during chronic, free-choice drinking rhythms in selectively bred high alcohol-preferring mice. *Addiction Biology,* 18**,** 921-929.

MAWLAWI, O., MARTINEZ, D., SLIFSTEIN, M., BROFT, A., CHATTERJEE, R., HWANG, D., HUANG, Y., SIMPSON, N., NGO, K., HEERTUM, R. & LARUELLE, M. 2001. Imaging Human Mesolimbic Dopamine Transmission With Positron Emission Tomography: I. Accuracy and Precision of D2 Receptor Parameter Measurements in Ventral Striatum. *Journal of Cerebral Blood Flow & Metabolism,* 21**,** 1034-1057.

MELDRUM, B. S. 2000. Glutamate as a Neurotransmitter in the Brain: Review of Physiology and Pathology. *The Journal of Nutrition,* 130**,** 1007S-1015S.

MELIS, M., CAMARINI, R., UNGLESS, M. A. & BONCI, A. 2002. Long-Lasting Potentiation of GABAergic Synapses in Dopamine Neurons after a Single In Vivo Ethanol Exposure. *The Journal of Neuroscience,* 22**,** 2074.

MIGLIORINI, R., STEWART, J. L., MAY, A. C., TAPERT, S. F. & PAULUS, M. P. 2013. What do you feel? Adolescent drug and alcohol users show altered brain response to pleasant interoceptive stimuli. *Drug and Alcohol Dependence,* 133**,** 661-668.

MONNIG, M. A., CAPRIHAN, A., YEO, R. A., GASPAROVIC, C., RUHL, D. A., LYSNE, P., BOGENSCHUTZ, M. P., HUTCHISON, K. E. & THOMA, R. J. 2013. Diffusion tensor imaging of white matter networks in individuals with current and remitted alcohol use disorders and comorbid conditions. *Psychology of Addictive Behaviors,* 27**,** 455-465.

MONNIG, M. A., THAYER, R. E., CAPRIHAN, A., CLAUS, E. D., YEO, R. A., CALHOUN, V. D. & HUTCHISON, K. E. 2014. White matter integrity is associated with alcohol cue reactivity in heavy drinkers. *Brain and Behavior,* 4**,** 158-170.

MONNIG, M. A., YEO, R. A., TONIGAN, J. S., MCCRADY, B. S., THOMA, R. J., SABBINENI, A. & HUTCHISON, K. E. 2015. Associations of White Matter Microstructure with Clinical and Demographic Characteristics in Heavy Drinkers. *PLoS ONE,* 10**,** e0142042.

MOOS, R. H. & MOOS, B. S. 2006. Rates and predictors of relapse after natural and treated remission from alcohol use disorders. *Addiction (Abingdon, England),* 101**,** 212-222.

MORI, S., CRAIN, B. J., CHACKO, V. P. & VAN ZIJL, P. C. M. 1999. Three-dimensional tracking of axonal projections in the brain by magnetic resonance imaging. *Annals of Neurology,* 45**,** 265-269.

MUCHA, P. J., RICHARDSON, T., MACON, K., PORTER, M. A. & ONNELA, J.-P. 2010. Community Structure in Time-Dependent, Multiscale, and Multiplex Networks. *Science,* 328**,** 876.

MÜLLER-OEHRING, E. M., SCHULTE, T., FAMA, R., PFEFFERBAUM, A. & SULLIVAN, E. V. 2009. Global–Local Interference is Related to Callosal Compromise in Alcoholism: A Behavior-DTI Association Study. *Alcoholism: Clinical and Experimental Research,* 33**,** 477-489.

MUNRO, C. A., MCCAUL, M. E., OSWALD, L. M., WONG, D. F., ZHOU, Y., BRASIC, J., KUWABARA, H., KUMAR, A., ALEXANDER, M., YE, W. & WAND, G. S. 2006. Striatal Dopamine Release and Family History of Alcoholism. *Alcoholism: Clinical and Experimental Research,* 30**,** 1143-1151.

NAQVI, N. H., GAZNICK, N., TRANEL, D. & BECHARA, A. 2014. The insula: a critical neural substrate for craving and drug seeking under conflict and risk. *Ann N Y Acad Sci,* 1316**,** 53-70.

NEWMAN, M. E. J. 2006. Modularity and community structure in networks. *Proceedings of the National Academy of Sciences,* 103**,** 8577.

NGUYEN-LOUIE, T. T., SIMMONS, A. N., SQUEGLIA, L. M., ALEJANDRA INFANTE, M., SCHACHT, J. P. & TAPERT, S. F. 2018. Earlier alcohol use onset prospectively predicts changes in functional connectivity. *Psychopharmacology,* 235**,** 1041-1054.

O'MALLEY, P. M. 2004. Maturing out of problematic alcohol use. *Alcohol Research & Health,* 28**,** 202-204.

OBERLIN, B. G., ALBRECHT, D. S., HERRING, C. M., WALTERS, J. W., HILE, K. L., KAREKEN, D. A. & YODER, K. K. 2015a. Monetary discounting and ventral striatal dopamine receptor availability in nontreatment-seeking alcoholics and social drinkers. *Psychopharmacology (Berl),* 232**,** 2207-16.

OBERLIN, B. G., DZEMIDZIC, M., TRAN, S. M., SOEURT, C. M., ALBRECHT, D. S., YODER, K. K. & KAREKEN, D. A. 2013. Beer flavor provokes striatal dopamine release in male drinkers: mediation by family history of alcoholism. *Neuropsychopharmacology,* 38**,** 1617-24.

OBERLIN, B. G., DZEMIDZIC, M., TRAN, S. M., SOEURT, C. M., O'CONNOR, S. J., YODER, K. K. & KAREKEN, D. A. 2015b. Beer self-administration provokes lateralized nucleus accumbens dopamine release in male heavy drinkers. *Psychopharmacology,* 232**,** 861-870.

OLDS, J. & MILNER, P. 1954. Positive reinforcement produced by electrical stimulation of septal area and other regions of rat brain. *Journal of Comparative and Physiological Psychology,* 47**,** 419-427.

OLIVA, I. & WANAT, M. J. 2019. Operant Costs Modulate Dopamine Release to Self-Administered Cocaine. *The Journal of Neuroscience,* 39**,** 1249.

ONOR, I. O., STIRLING, D. L., WILLIAMS, S. R., BEDIAKO, D., BORGHOL, A., HARRIS, M. B., DARENSBURG, T. B., CLAY, S. D., OKPECHI, S. C. & SARPONG, D. F. 2017. Clinical Effects of Cigarette Smoking: Epidemiologic Impact and Review of Pharmacotherapy Options. *International Journal of Environmental Research and Public Health,* 14.

PALACIOS, J. M., CAMPS, M., CORTÉS, R. & PROBST, A. Mapping dopamine receptors in the human brain. *In:* OBESO, J. A., HOROWSKI, R. & MARSDEN, C. D., eds. Continuous Dopaminergic Stimulation in Parkinson's Disease, 1988// 1988 Vienna. Springer Vienna, 227-235.

PARENT, A. & HAZRATI, L.-N. 1995. Functional anatomy of the basal ganglia. I. The cortico-basal ganglia-thalamo-cortical loop. *Brain Research Reviews,* 20**,** 91-127.
PATENAUDE, B., SMITH, S. M., KENNEDY, D. N. & JENKINSON, M. 2011. A Bayesian model of shape and appearance for subcortical brain segmentation. *NeuroImage,* 56**,** 907-922.
PFEFFERBAUM, A., ADALSTEINSSON, E. & SULLIVAN, E. V. 2006a. Dysmorphology and microstructural degradation of the corpus callosum: Interaction of age and alcoholism. *Neurobiology of Aging,* 27**,** 994-1009.
PFEFFERBAUM, A., ADALSTEINSSON, E. & SULLIVAN, E. V. 2006b. Supratentorial Profile of White Matter Microstructural Integrity in Recovering Alcoholic Men and Women. *Biological Psychiatry,* 59**,** 364-372.
PFEFFERBAUM, A., LIM, K. O., DESMOND, J. E. & SULLIVAN, E. V. 1996. Thinning of the Corpus Callosum in Older Alcoholic Men: A Magnetic Resonance Imaging Study. *Alcoholism: Clinical and Experimental Research,* 20**,** 752-757.
PFEFFERBAUM, A., ROSENBLOOM, M., ROHLFING, T. & SULLIVAN, E. V. 2009. Degradation of association and projection white matter systems in alcoholism detected with quantitative fiber tracking. *Biol Psychiatry,* 65**,** 680-90.
PFEFFERBAUM, A., ROSENBLOOM, M. J., CHU, W., SASSOON, S. A., ROHLFING, T., POHL, K. M., ZAHR, N. M. & SULLIVAN, E. V. 2014. White matter microstructural recovery with abstinence and decline with relapse in alcohol dependence interacts with normal ageing: a controlled longitudinal DTI study. *The Lancet Psychiatry,* 1**,** 202-212.
PFEFFERBAUM, A. & SULLIVAN, E. V. 2002. Microstructural but Not Macrostructural Disruption of White Matter in Women with Chronic Alcoholism. *NeuroImage,* 15**,** 708-718.
PFEFFERBAUM, A., SULLIVAN, E. V., HEDEHUS, M., ADALSTEINSSON, E., LIM, K. O. & MOSELEY, M. 2000. In Vivo Detection and Functional Correlates of White Matter Microstructural Disruption in Chronic Alcoholism. *Alcoholism: Clinical and Experimental Research,* 24**,** 1214-1221.
PFEIFER, P., TÜSCHER, O., BUCHHOLZ, H. G., GRÜNDER, G., VERNALEKEN, I., PAULZEN, M., ZIMMERMANN, U. S., MAUS, S., LIEB, K., EGGERMANN, T., FEHR, C. & SCHRECKENBERGER, M. 2017. Acute effect of intravenously applied alcohol in the human striatal and extrastriatal D2/D3 dopamine system. *Addiction Biology,* 22**,** 1449-1458.
POMERLEAU, C. S., CARTON, S. M., LUTZKE, M. L., FLESSLAND, K. A. & POMERLEAU, O. F. 1994. Reliability of the fagerstrom tolerance questionnaire and the fagerstrom test for nicotine dependence. *Addictive Behaviors,* 19**,** 33-39.
RAB, A., ROWE, S. M., RAJU, S. V., BEBOK, Z., MATALON, S. & COLLAWN, J. F. 2013. Cigarette smoke and CFTR: implications in the pathogenesis of COPD. *American Journal of Physiology-Lung Cellular and Molecular Physiology,* 305**,** L530-L541.
RENTERIA, R., MAIER, E. Y., BUSKE, T. R. & MORRISETT, R. A. 2017. Selective alterations of NMDAR function and plasticity in D1 and D2 medium spiny neurons in the nucleus accumbens shell following chronic intermittent ethanol exposure. *Neuropharmacology,* 112**,** 164-171.

ROBINSON, T. E., GORNY, G., MITTON, E. & KOLB, B. 2001. Cocaine self-administration alters the morphology of dendrites and dendritic spines in the nucleus accumbens and neocortex. *Synapse,* 39**,** 257-266.
ROBINSON, T. E. & KOLB, B. 1997. Persistent Structural Modifications in Nucleus Accumbens and Prefrontal Cortex Neurons Produced by Previous Experience with Amphetamine. *The Journal of Neuroscience,* 17**,** 8491.
ROMBERGER, D. J. & GRANT, K. 2004. Alcohol consumption and smoking status: the role of smoking cessation. *Biomedicine & Pharmacotherapy,* 58**,** 77-83.
ROMINGER, A., CUMMING, P., XIONG, G., KOLLER, G., BÖNING, G., WULFF, M., ZWERGAL, A., FÖRSTER, S., REILHAC, A., MUNK, O., SOYKA, M., WÄNGLER, B., BARTENSTEIN, P., LA FOUGÈRE, C. & POGARELL, O. 2012. [18F]fallypride PET measurement of striatal and extrastriatal dopamine D2/3 receptor availability in recently abstinent alcoholics. *Addiction Biology,* 17**,** 490-503.
RON, D. & BARAK, S. 2016. Molecular mechanisms underlying alcohol-drinking behaviours. *Nature Reviews Neuroscience,* 17**,** 576.
ROSENBLOOM, M. J., SASSOON, S. A., FAMA, R., SULLIVAN, E. V. & PFEFFERBAUM, A. 2008. Frontal Callosal Fiber Integrity Selectively Predicts Coordinated Psychomotor Performance in Chronic Alcoholism. *Brain imaging and behavior,* 2**,** 74-83.
RUBINOV, M. & SPORNS, O. 2010. Complex network measures of brain connectivity: Uses and interpretations. *NeuroImage,* 52**,** 1059-1069.
SACKS, J. J., GONZALES, K. R., BOUCHERY, E. E., TOMEDI, L. E. & BREWER, R. D. 2015. 2010 National and State Costs of Excessive Alcohol Consumption. *American Journal of Preventive Medicine,* 49**,** e73-e79.
SAMSON, H. H., PFEFFER, A. O. & TOLLIVER, G. A. 1988. Oral Ethanol Self-administration in Rats: Models of Alcohol-Seeking Behavior. *Alcoholism: Clinical and Experimental Research,* 12**,** 591-598.
SAMSON, H. H., TOLLIVER, G. A., HARAGUCHI, M. & HODGE, C. W. 1992. Alcohol Self-Administration: Role of Mesolimbic Dopamine. *Annals of the New York Academy of Sciences,* 654**,** 242-253.
SAVJANI, R. R., VELASQUEZ, K. M., THOMPSON-LAKE, D. G. Y., BALDWIN, P. R., EAGLEMAN, D. M., DE LA GARZA II, R. & SALAS, R. 2014. Characterizing white matter changes in cigarette smokers via diffusion tensor imaging. *Drug and Alcohol Dependence,* 145**,** 134-142.
SEELEY, W. W., MENON, V., SCHATZBERG, A. F., KELLER, J., GLOVER, G. H., KENNA, H., REISS, A. L. & GREICIUS, M. D. 2007. Dissociable Intrinsic Connectivity Networks for Salience Processing and Executive Control. *The Journal of neuroscience: the official journal of the Society for Neuroscience,* 27**,** 2349-2356.
SEGOBIN, S., RITZ, L., LANNUZEL, C., BOUDEHENT, C., VABRET, F., EUSTACHE, F., BEAUNIEUX, H. & PITEL, A.-L. 2015. Integrity of white matter microstructure in alcoholics with and without Korsakoff's syndrome. *Human Brain Mapping,* 36**,** 2795-2808.

SHEN, X., TOKOGLU, F., PAPADEMETRIS, X. & CONSTABLE, R. T. 2013. Groupwise whole-brain parcellation from resting-state fMRI data for network node identification. *NeuroImage,* 82**,** 403-415.
SHOKRI-KOJORI, E., TOMASI, D., WIERS, C. E., WANG, G. J. & VOLKOW, N. D. 2016. Alcohol affects brain functional connectivity and its coupling with behavior: greater effects in male heavy drinkers. *Molecular Psychiatry,* 22**,** 1185.
SILVERI, M. M., DAGER, A. D., COHEN-GILBERT, J. E. & SNEIDER, J. T. 2016. Neurobiological signatures associated with alcohol and drug use in the human adolescent brain. *Neuroscience & Biobehavioral Reviews,* 70**,** 244-259.
SJOERDS, Z., STUFFLEBEAM, S. M., VELTMAN, D. J., VAN DEN BRINK, W., PENNINX, B. W. J. H. & DOUW, L. 2017. Loss of brain graph network efficiency in alcohol dependence. *Addiction Biology,* 22**,** 523-534.
SMITH, S. M. 2002. Fast robust automated brain extraction. *Human Brain Mapping,* 17**,** 143-155.
SMITH, S. M., JENKINSON, M., JOHANSEN-BERG, H., RUECKERT, D., NICHOLS, T. E., MACKAY, C. E., WATKINS, K. E., CICCARELLI, O., CADER, M. Z., MATTHEWS, P. M. & BEHRENS, T. E. J. 2006. Tract-based spatial statistics: Voxelwise analysis of multi-subject diffusion data. *NeuroImage,* 31**,** 1487-1505.
SMITH, S. M. & NICHOLS, T. E. 2009. Threshold-free cluster enhancement: Addressing problems of smoothing, threshold dependence and localisation in cluster inference. *NeuroImage,* 44**,** 83-98.
SOARES, J. M., MARQUES, P., ALVES, V. & SOUSA, N. 2013. A hitchhiker's guide to diffusion tensor imaging. *Front Neurosci,* 7.
SPORNS, O. & BETZEL, R. F. 2016. Modular Brain Networks. *Annu Rev Psychol,* 67**,** 613-40.
STANGL, B. L., VATSALYA, V., ZAMETKIN, M. R., COOKE, M. E., PLAWECKI, M. H., O'CONNOR, S. & RAMCHANDANI, V. A. 2017. Exposure-Response Relationships during Free-Access Intravenous Alcohol Self-Administration in Nondependent Drinkers: Influence of Alcohol Expectancies and Impulsivity. *International Journal of Neuropsychopharmacology,* 20**,** 31-39.
STEFANI, A., CHEN, Q., FLORES-HERNANDEZ, J., JIAO, Y., REINER, A. & SURMEIER, D. J. 1998. Physiological and Molecular Properties of AMPA/Kainate Receptors Expressed by Striatal Medium Spiny Neurons. *Developmental Neuroscience,* 20**,** 242-252.
SULLIVAN, E. V., HARRIS, R. A. & PFEFFERBAUM, A. 2010. Alcohol's effects on brain and behavior. *Alcohol research & health: the journal of the National Institute on Alcohol Abuse and Alcoholism,* 33**,** 127-143.
SUN, Y., WANG, G.-B., LIN, Q.-X., LU, L., SHU, N., MENG, S.-Q., WANG, J., HAN, H.-B., HE, Y. & SHI, J. 2015. Disrupted white matter structural connectivity in heroin abusers. *Addiction Biology,* 22**,** 184-195.
SURMEIER, D. J., DING, J., DAY, M., WANG, Z. & SHEN, W. 2007. D1 and D2 dopamine-receptor modulation of striatal glutamatergic signaling in striatal medium spiny neurons. *Trends in Neurosciences,* 30**,** 228-235.
SUTHERLAND, M. T., RIEDEL, M. C., FLANNERY, J. S., YANES, J. A., FOX, P. T., STEIN, E. A. & LAIRD, A. R. 2016. Chronic cigarette smoking is linked with

structural alterations in brain regions showing acute nicotinic drug-induced functional modulations. *Behavioral and Brain Functions,* 12**,** 16.

TANG, Y.-Y., POSNER, M. I., ROTHBART, M. K. & VOLKOW, N. D. 2015. Circuitry of self-control and its role in reducing addiction. *Trends in Cognitive Sciences,* 19**,** 439-444.

TAPERT, S. F., CHEUNG, E. H., BROWN, G. G. & ET AL. 2003. Neural response to alcohol stimuli in adolescents with alcohol use disorder. *Archives of General Psychiatry,* 60**,** 727-735.

TAPERT, S. F. & SCHWEINSBURG, A. D. 2005. The human adolescent brain and alcohol use disorders. *Recent Dev Alcohol,* 17**,** 177-97.

TAPERT, S. F., SCHWEINSBURG, A. D., BARLETT, V. C., BROWN, S. A., FRANK, L. R., BROWN, G. G. & MELOY, M. J. 2004. Blood oxygen level dependent response and spatial working memory in adolescents with alcohol use disorders. *Alcohol Clin Exp Res,* 28**,** 1577-86.

TELESFORD, Q. K., LAURIENTI, P. J., FRIEDMAN, D. P., KRAFT, R. A. & DAUNAIS, J. B. 2013. The Effects of Alcohol on the Nonhuman Primate Brain: A Network Science Approach to Neuroimaging. *Alcoholism: Clinical and Experimental Research,* 37**,** 1891-1900.

THIRUCHSELVAM, T., WILSON, A. A., BOILEAU, I. & LE FOLL, B. 2017. A Preliminary Investigation of the Effect of Acute Alcohol on Dopamine Transmission as Assessed by [11C]-(+)-PHNO. *Alcoholism: Clinical and Experimental Research,* 41**,** 1112-1119.

TINAZ, S., LAURO, P. M., GHOSH, P., LUNGU, C. & HOROVITZ, S. G. 2017. Changes in functional organization and white matter integrity in the connectome in Parkinson's disease. *NeuroImage: Clinical,* 13**,** 395-404.

TOMASI, D. & VOLKOW, N. D. 2014. Mapping Small-World Properties through Development in the Human Brain: Disruption in Schizophrenia. *PLOS ONE,* 9**,** e96176.

TRIVEDI, R., BAGGA, D., BHATTACHARYA, D., KAUR, P., KUMAR, P., KHUSHU, S., TRIPATHI, R. P. & SINGH, N. 2013. White matter damage is associated with memory decline in chronic alcoholics: a quantitative diffusion tensor tractography study. *Behav Brain Res,* 250**,** 192-8.

TZIORTZI, A. C., HABER, S. N., SEARLE, G. E., TSOUMPAS, C., LONG, C. J., SHOTBOLT, P., DOUAUD, G., JBABDI, S., BEHRENS, T. E., RABINER, E. A., JENKINSON, M. & GUNN, R. N. 2014. Connectivity-based functional analysis of dopamine release in the striatum using diffusion-weighted MRI and positron emission tomography. *Cereb Cortex,* 24**,** 1165-77.

UMHAU, J. C., ZHOU, W., THADA, S., DEMAR, J., HUSSEIN, N., BHATTACHARJEE, A. K., MA, K., MAJCHRZAK-HONG, S., HERSCOVITCH, P., SALEM, N., JR., URISH, A., HIBBELN, J. R., CUNNANE, S. C., RAPOPORT, S. I. & HIRVONEN, J. 2013. Brain Docosahexaenoic Acid [DHA] Incorporation and Blood Flow Are Increased in Chronic Alcoholics: A Positron Emission Tomography Study Corrected for Cerebral Atrophy. *PLOS ONE,* 8**,** e75333.

VAN DEN HEUVEL, M. P. & SPORNS, O. 2013. Network hubs in the human brain. *Trends in Cognitive Sciences,* 17**,** 683-696.

VAN DEN HEUVEL, M. P., SPORNS, O., COLLIN, G. & ET AL. 2013. Abnormal rich club organization and functional brain dynamics in schizophrenia. *JAMA Psychiatry,* 70**,** 783-792.

VENGELIENE, V., BILBAO, A., MOLANDER, A. & SPANAGEL, R. 2008. Neuropharmacology of alcohol addiction. *British Journal of Pharmacology,* 154**,** 299-315.

VERDEJO-ROMÁN, J., VILAR-LÓPEZ, R., NAVAS, J. F., SORIANO-MAS, C. & VERDEJO-GARCÍA, A. 2016. Brain reward system's alterations in response to food and monetary stimuli in overweight and obese individuals. *Human Brain Mapping,* 38**,** 666-677.

VINCENT, J. L., KAHN, I., SNYDER, A. Z., RAICHLE, M. E. & BUCKNER, R. L. 2008. Evidence for a Frontoparietal Control System Revealed by Intrinsic Functional Connectivity. *Journal of Neurophysiology,* 100**,** 3328.

VOLKOW, N. D., HITZEMANN, R., WOLF, A. P., LOGAN, J., FOWLER, J. S., CHRISTMAN, D., DEWEY, S. L., SCHLYER, D., BURR, G., VITKUN, S. & HIRSCHOWITZ, J. 1990. Acute effects of ethanol on regional brain glucose metabolism and transport. *Psychiatry Research: Neuroimaging,* 35**,** 39-48.

VOLKOW, N. D., KIM, S. W., WANG, G.-J., ALEXOFF, D., LOGAN, J., MUENCH, L., SHEA, C., TELANG, F., FOWLER, J. S., WONG, C., BENVENISTE, H. & TOMASI, D. 2013. Acute alcohol intoxication decreases glucose metabolism but increases acetate uptake in the human brain. *NeuroImage,* 64**,** 277-283.

VOLKOW, N. D., MULLANI, N., GOULD, L., ADLER, S. S., GUYNN, R. W., OVERALL, J. E. & DEWEY, S. 1988. Effects of acute alcohol intoxication on cerebral blood flow measured with PET. *Psychiatry Research,* 24**,** 201-209.

VOLKOW, N. D., WANG, G.-J., SHOKRI KOJORI, E., FOWLER, J. S., BENVENISTE, H. & TOMASI, D. 2015. Alcohol Decreases Baseline Brain Glucose Metabolism More in Heavy Drinkers Than Controls But Has No Effect on Stimulation-Induced Metabolic Increases. *The Journal of Neuroscience,* 35**,** 3248.

VOLKOW, N. D., WANG, G. J., FRANCESCHI, D., FOWLER, J. S., THANOS, P. P., MAYNARD, L., GATLEY, S. J., WONG, C., VEECH, R. L., KUNOS, G. & KAI LI, T. 2006. Low doses of alcohol substantially decrease glucose metabolism in the human brain. *Neuroimage,* 29**,** 295-301.

VOLKOW, N. D., WANG, G. J., MAYNARD, L., FOWLER, J. S., JAYNE, B., TELANG, F., LOGAN, G., DING, Y., GATLEY, S. J., HITZERMANN, R., WONG, C. & PAPPAS, N. 2002. Effects of alcohol detoxification on dopamine D2 receptors in alcoholics: a preliminary study. *Psychiatry Research: Neuroimaging,* 116**,** 163-172.

VOSSEL, S., GENG, J. J. & FINK, G. R. 2014. Dorsal and Ventral Attention Systems: Distinct Neural Circuits but Collaborative Roles. *The Neuroscientist,* 20**,** 150-159.

WANG, G. J., VOLKOW, N. D., ROQUE, C. T., CESTARO, V. L., HITZEMANN, R. J., CANTOS, E. L., LEVY, A. V. & DHAWAN, A. P. 1993. Functional importance of ventricular enlargement and cortical atrophy in healthy subjects and alcoholics as assessed with PET, MR imaging, and neuropsychologic testing. *Radiology,* 186**,** 59-65.

WANG, R., BENNER, T., SORENSEN, A. G. & WEDEEN, V. J. 2007. Diffusion Toolkit: A Software Package for Diffusion Imaging Data Processing and Tractography. *Proc. Intl. Soc. Mag. Reson. Med.,* 15:3720.

WANG, Z., SUH, J., LI, Z., LI, Y., FRANKLIN, T., O'BRIEN, C. & CHILDRESS, A. R. 2015. A hyper-connected but less efficient small-world network in the substance-dependent brain. *Drug and Alcohol Dependence,* 152**,** 102-108.

WAXMAN, S. G. 1980. Determinants of conduction velocity in myelinated nerve fibers. *Muscle & Nerve,* 3**,** 141-150.

WEERTS, E. M., WAND, G. S., KUWABARA, H., MUNRO, C. A., DANNALS, R. F., HILTON, J., FROST, J. J. & MCCAUL, M. E. 2011. Positron Emission Tomography Imaging of Mu- and Delta-Opioid Receptor Binding in Alcohol-Dependent and Healthy Control Subjects. *Alcoholism: Clinical and Experimental Research,* 35**,** 2162-2173.

WERNER, C. T., MURRAY, C. H., REIMERS, J. M., CHAUHAN, N. M., WOO, K. K. Y., MOLLA, H. M., LOWETH, J. A. & WOLF, M. E. 2017. Trafficking of calcium-permeable and calcium-impermeable AMPA receptors in nucleus accumbens medium spiny neurons co-cultured with prefrontal cortex neurons. *Neuropharmacology,* 116**,** 224-232.

WETHERILL, R. R., BAVA, S., THOMPSON, W. K., BOUCQUEY, V., PULIDO, C., YANG, T. T. & TAPERT, S. F. 2012. Frontoparietal connectivity in substance-naïve youth with and without a family history of alcoholism. *Brain Research,* 1432**,** 66-73.

WHO 2014. *Global status report on alcohol and health*, World Health Organization.

WHO, W. H. O. 2017. WHO Report on the Global TObacco Epidemic, 2017: monitoring tobacco use and prevention policies.

WILLARD, S. S. & KOOCHEKPOUR, S. 2013. Glutamate, glutamate receptors, and downstream signaling pathways. *International journal of biological sciences,* 9**,** 948-959.

WINSTON, G. P. 2012. The physical and biological basis of quantitative parameters derived from diffusion MRI. *Quantitative Imaging in Medicine and Surgery; Vol 2, No 4 (December 2012): Quantitative Imaging in Medicine and Surgery*.

WOZNIAK, J. R., MUELLER, B. A., BELL, C. J., MUETZEL, R. L., HOECKER, H. L., BOYS, C. J. & LIM, K. O. 2012. Global Functional Connectivity Abnormalities in Children with Fetal Alcohol Spectrum Disorders. *Alcoholism: Clinical and Experimental Research,* 37**,** 748-756.

XIAO, C., SHAO, X. M., OLIVE, M. F., GRIFFIN III, W. C., LI, K.-Y., KRNJEVIĆ, K., ZHOU, C. & YE, J.-H. 2008. Ethanol Facilitates Glutamatergic Transmission to Dopamine Neurons in the Ventral Tegmental Area. *Neuropsychopharmacology,* 34**,** 307.

YEH, P. H., SIMPSON, K., DURAZZO, T. C., GAZDZINSKI, S. & MEYERHOFF, D. J. 2009. Tract-Based Spatial Statistics (TBSS) of diffusion tensor imaging data in alcohol dependence: abnormalities of the motivational neurocircuitry. *Psychiatry Res,* 173**,** 22-30.

YEO, B. T., KRIENEN, F. M., SEPULCRE, J., SABUNCU, M. R., LASHKARI, D., HOLLINSHEAD, M., ROFFMAN, J. L., SMOLLER, J. W., ZÖLLEI, L., POLIMENI, J. R., FISCHL, B., LIU, H. & BUCKNER, R. L. 2011. The

organization of the human cerebral cortex estimated by intrinsic functional connectivity. *Journal of Neurophysiology,* 106**,** 1125-1165.

YIM, H. J., SCHALLERT, T., RANDALL, P. K. & GONZALES, R. A. 1998. Comparison of Local and Systemic Ethanol Effects on Extracellular Dopamine Concentration in Rat Nucleus Accumbens by Microdialysis. *Alcoholism: Clinical and Experimental Research,* 22**,** 367-374.

YODER, K. K., ALBRECHT, D. S., DZEMIDZIC, M., NORMANDIN, M. D., FEDERICI, L. M., GRAVES, T., HERRING, C. M., HILE, K. L., WALTERS, J. W., LIANG, T., PLAWECKI, M. H., O'CONNOR, S. & KAREKEN, D. A. 2016. Differences in IV alcohol-induced dopamine release in the ventral striatum of social drinkers and nontreatment-seeking alcoholics. *Drug and Alcohol Dependence,* 160**,** 163-169.

YODER, K. K., ALBRECHT, D. S., KAREKEN, D. A., FEDERICI, L. M., PERRY, K. M., PATTON, E. A., ZHENG, Q.-H., MOCK, B. H., O'CONNOR, S. J. & HERRING, C. M. 2011a. Reliability of striatal [11C]raclopride binding in smokers wearing transdermal nicotine patches. *European Journal of Nuclear Medicine and Molecular Imaging,* 39**,** 220-225.

YODER, K. K., ALBRECHT, D. S., KAREKEN, D. A., FEDERICI, L. M., PERRY, K. M., PATTON, E. A., ZHENG, Q. H., MOCK, B. H., O'CONNOR, S. & HERRING, C. M. 2011b. Test-retest variability of [11C]raclopride-binding potential in nontreatment-seeking alcoholics. *Synapse,* 65**,** 553-61.

YODER, K. K., CONSTANTINESCU, C. C., KAREKEN, D. A., NORMANDIN, M. D., CHENG, T. E., O'CONNOR, S. J. & MORRIS, E. D. 2007. Heterogeneous effects of alcohol on dopamine release in the striatum: a PET study. *Alcohol Clin Exp Res,* 31**,** 965-73.

YODER, K. K., KAREKEN, D. A., SEYOUM, R. A., O'CONNOR, S. J., WANG, C., ZHENG, Q.-H., MOCK, B. & MORRIS, E. D. 2005. Dopamine D2 Receptor Availability is Associated with Subjective Responses to Alcohol. *Alcoholism: Clinical and Experimental Research,* 29**,** 965-970.

YU, D., YUAN, K., CHENG, J., GUAN, Y., LI, Y., BI, Y., ZHAI, J., LUO, L., LIU, B., XUE, T. & LU, X. 2018. Reduced Thalamus Volume May Reflect Nicotine Severity in Young Male Smokers. *Nicotine & Tobacco Research,* 20**,** 434-439.

ZAHR, N. M., MAYER, D., VINCO, S., ORDUNA, J., LUONG, R., SULLIVAN, E. V. & PFEFFERBAUM, A. 2008. In Vivo Evidence for Alcohol-Induced Neurochemical Changes in Rat Brain Without Protracted Withdrawal, Pronounced Thiamine Deficiency, or Severe Liver Damage. *Neuropsychopharmacology,* 34**,** 1427.

ZAHR, N. M. & PFEFFERBAUM, A. 2017. Alcohol's Effects on the Brain: Neuroimaging Results in Humans and Animal Models. *Alcohol Research: Current Reviews,* 38**,** 183-206.

ZAKINIAEIZ, Y., SCHEINOST, D., SEO, D., SINHA, R. & CONSTABLE, R. T. 2017. Cingulate cortex functional connectivity predicts future relapse in alcohol dependent individuals. *NeuroImage: Clinical,* 13**,** 181-187.

ZALESKY, A., FORNITO, A. & BULLMORE, E. T. 2010. Network-based statistic: Identifying differences in brain networks. *NeuroImage,* 53**,** 1197-1207.

ZALESKY, A., PANTELIS, C., CROPLEY, V. & ET AL. 2015. Delayed development of brain connectivity in adolescents with schizophrenia and their unaffected siblings. *JAMA Psychiatry,* 72**,** 900-908.

ZHANG, R., JIANG, G., TIAN, J., QIU, Y., WEN, X., ZALESKY, A., LI, M., MA, X., WANG, J., LI, S., WANG, T., LI, C. & HUANG, R. 2015. Abnormal white matter structural networks characterize heroin-dependent individuals: a network analysis. *Addiction Biology,* 21**,** 667-678.

ZHANG, X., SALMERON, B. J., ROSS, T. J., GENG, X., YANG, Y. & STEIN, E. A. 2011. Factors underlying prefrontal and insula structural alterations in smokers. *NeuroImage,* 54**,** 42-48.

ZHANG, Y., BRADY, M. & SMITH, S. 2001. Segmentation of brain MR images through a hidden Markov random field model and the expectation-maximization algorithm. *IEEE Transactions on Medical Imaging,* 20**,** 45-57.

ZHONG, J., SHI, H., SHEN, Y., DAI, Z., ZHU, Y., MA, H. & SHENG, L. 2016. Voxelwise meta-analysis of gray matter anomalies in chronic cigarette smokers. *Behavioural Brain Research,* 311**,** 39-45.

ZORICK, T., OKITA, K., MANDELKERN, M. A., LONDON, E. D. & BRODY, A. L. 2019. Effects of Citalopram on Cue-Induced Alcohol Craving and Thalamic D2/3 Dopamine Receptor Availability. *International Journal of Neuropsychopharmacology,* 22**,** 286-291.

ZORLU, N., ÇAPRAZ, N., OZTEKIN, E., BAGCI, B., DI BIASE, M. A., ZALESKY, A., GELAL, F., BORA, E., DURMAZ, E., BEŞIROĞLU, L. & SARıÇIÇEK, A. 2017. Rich club and reward network connectivity as endophenotypes for alcohol dependence: a diffusion tensor imaging study. *Addiction Biology,* 0.

ZORLU, N., GELAL, F., KUSERLI, A., CENIK, E., DURMAZ, E., SARICICEK, A. & GULSEREN, S. 2013. Abnormal white matter integrity and decision-making deficits in alcohol dependence. *Psychiatry Research: Neuroimaging,* 214**,** 382-388.

ZOU, Y., MURRAY, D. E., DURAZZO, T. C., SCHMIDT, T. P., MURRAY, T. A. & MEYERHOFF, D. J. 2017. Effects of abstinence and chronic cigarette smoking on white matter microstructure in alcohol dependence: Diffusion tensor imaging at 4 T. *Drug and Alcohol Dependence,* 175**,** 42-50.

Curriculum Vitae

Evgeny Jenya Chumin

Education

Aug. 2014 – Sept. 2019	Ph.D. Medical Neurosciences Graduate Program Indiana University-Purdue University, Indianapolis, IN
Aug. 2009 – May 2014	B.S. Neuroscience and Psychology Concentrations: Behavioral Neuroscience and Psychology of Addictions Minors: Biology and Chemistry Indiana University-Purdue University Indianapolis, Indianapolis, IN

Research

Graduate

Apr. 2015 – Current

Graduate Student; Laboratory of Dr. Karmen Yoder, Ph.D.
Dept. of Radiology and Imaging Sciences, IUSM

- Research into the neurobiology of alcoholism in currently drinking human populations, using diffusion and functional magnetic resonance imaging and positron emission tomography.

Jan. 2015 – Apr. 2015

Rotation Student; Laboratory of Dr. Christopher Lapish, Ph.D. Dept. of Psychology, IUPUI

- Computational modeling of rodent delayed discounting behavior.

Oct. 2014 – Jan. 2015

Rotation Student; Laboratory of Dr. David Kareken, Ph.D., ABPP, Dept. of Neurology, IUSM

- Functional magnetic resonance and positron emission tomography image processing.
- Positron emission tomography data quality control procedure development.

Undergraduate

May 2013 – Aug. 2014

Undergraduate Research Assistant; Laboratory of Dr. Karmen Yoder, Ph.D., Dept. of Radiology and Imaging Sciences, IUSM

- Research into relationships of galvanic skin response and dopamine tone in fibromyalgia.
- Comparative analysis of semi quantitative metrics and kinetic modeling in [^{11}C]raclopride positron emission tomography.

May 2012 – May 2013	Undergraduate Research Assistant; Laboratory of Dr. Cristine Czachowski, Ph.D., Dept. of Psychology, IUPUI • Assisted with experimental procedures in research on neurotransmitter specific roles in alcohol seeking and intake, in the basolateral amygdala of the rat.
Jan. 2012 – May 2012	Undergraduate Research Assistant; Laboratory of Dr. Robert Stewart, Ph.D., Dept. of Psychology, IUPUI • Scored behavioral assessments of anxiety in rodents (elevated plus maze, open field, and multivariate concentric square field).

Honors, Awards, Fellowships

2018	Student Merit Travel Award	41st Annual Research Society on Alcoholism Scientific Meeting
2018	Travel Grant	Graduate Student and Professional Government
2017	Larry Kays Fellowship	IU School of Medicine
2017	Best Project Award	Hackathon on Brain Connectomics; 5th Indiana Neuroimaging Symposium
2017	Gill Best Image Award	The Linda & Jack Gill Center for Biomedical Sciences Gill Symposium & Awards
2017	Student Merit Travel Award	40th Annual Research Society on Alcoholism Scientific Meeting
2016	Student Merit Travel Award	39th Annual Research Society on Alcoholism Scientific Meeting
2016	Young Investigator Award	11th International Symposium on Functional NeuroReceptor Mapping of the Living Brain
2015	Paul & Carole Stark Neuroscience Fellowship	Stark Neurosciences Research Institute, IUSM
2014	Robert I. Long Outstanding Undergraduate	Indiana Univ.-Purdue Univ. Indianapolis
2013, 2014	School of Science Deans List	Indiana Univ.-Purdue Univ. Indianapolis
2014	IUPUI Chapter President	Psi Chi National Honor Society
2013	Psychology Club Vice-President	Indiana Univ.-Purdue Univ. Indianapolis
2013	Undergraduate Research Summer Internship	Stark Neurosciences Research Institute, IUSM

2012, 2013	Undergraduate Research Opportunities Grant	Indiana Univ.-Purdue Univ. Indianapolis

Professional Societies

2016-	Research Society on Alcoholism
2015-2016	Society for Nuclear Medicine and Molecular Imaging
2011-2015	American Psychological Association
2013-	Psi Chi National Honor Society

Peer-Reviewed Publications

** Indicates co-first author*

Chumin EJ*, Grecco GG*, Dzemidzic M, Cheng H, Finn P, Sporns O, Newman SD, Yoder KK. (2019) Alterations in White Matter Microstructure and Connectivity in Young Adults with Alcohol Use Disorder. *Alcoholism Clinical and Experimental Research.* 2019 Apr 12. https://doi.org/10.1111/acer.14048

Halcomb ME, Dzemidzic M, **Chumin EJ**, Goñi J, Yoder KK. (2019) Aberrations of Anterior Insular Cortex Functional Connectivity in Nontreatment-Seeking Alcoholics. *Psychiatry Research: Neuroimaging.* 2019 Feb 28. DOI: 10.1016/j.pscychresns.2018.12.016

Chumin EJ, Goñi J, Halcomb ME, Durazzo TC, Džemidžić M, Yoder KK. (2018) Differences in White Matter Microstructure and Connectivity in Nontreatment-Seeking Individuals with Alcohol Use Disorder. *Alcoholism Clinical and Experimental Research.* 2018 Mar 15. DOI: 10.1111/acer.13629

Albrecht DS, MacKie PJ, Kareken DA, Hutchins GD, **Chumin EJ**, Christian BT, Yoder KK. (2015) Differential dopamine function in fibromyalgia. *Brain Imaging and Behavior.* 2015 Oct 24. PMID: 26497890.

Manuscripts in Preparation

Chumin EJ, Dzemidzic M, Harezlak J, Durazzo TC, Goñi J, Yoder KK. Differences in Consensus Community Structure in Cigarette Smokers with and without Alcohol Use Disorder. *In preparation.*

Grecco GG, **Chumin EJ,** Dzemidzic M, Cheng H, Finn P, Newman SD, Yoder KK. Relationship Between Local White Matter Microstructure and Anterior Cingulate Cortex Metabolites: A Multimodal Imaging Approach to Alcohol Use Disorder. *In preparation.*

Abstracts

Z Lin, M Dzemidzic, **E Chumin**, E Lungwitz, J Harezlak, B Oberlin. *Alcohol-Money Compared to Money Discounting Increases Functional Connectivity in Heavy Drinkers.* Organization for Human Brain Mapping Annual Meeting, Roma, Italy, June 2019.

EJ Chumin, ME Halcomb, M Dzemidzic, KK Yoder. *Differential Relationship of White Matter Integrity and Striatal Dopamine in Active Alcohol Use Disorder and Social Drinking Individuals.* 42nd Annual Meeting of Research Society on Alcoholism, Minneapolis, MN, June 2019.

EJ Chumin, M Dzemidzic, KK Yoder. *Associations of Structural Brain Connectivity with Severity of Alcohol Dependence in an Active Alcohol Dependent Sample.* 42nd Annual Meeting of Research Society on Alcoholism, Minneapolis, MN, June 2019.

TJ Collins, **EJ Chumin,** JD West, M Dzemidzic, KK Yoder. *Comparison of Relative Cerebral Blood Flow in Nontreatment-Seeking Alcoholics and Social Drinkers.* 42nd Annual Meeting of Research Society on Alcoholism, Minneapolis, MN, June 2019.

KK Yoder, **EJ Chumin,** M Dzemidzic, KL Hile, ME Halcomb, MH Plaweki, SJ O'Connor, SM Mustafi, YC Wu. *Intravenous Infusions of Saline and Alcohol Increase Axonal Density: Diffusion Weighted Magnetic Resonance Imaging with Neurite Orientation Dispersion and Density Modeling.* 42nd Annual Meeting of Research Society on Alcoholism, Minneapolis, MN, June 2019.

EA Lungwitz, Z Lin, M Dzemidzic, YI Shen, CR Carron, **EJ Chumin,** J Harezlak, BG Oberlin. *Brain Connectivity Metrics with Discounting and Sensation Seeking Behaviors Implicate Salience, Default Mode, and Attentional Networks in Heavy Drinkers.* 42nd Annual Meeting of Research Society on Alcoholism, Minneapolis, MN, June 2019.

ME Halcomb, BG Oberlin, **EJ Chumin,** M Dzemidzic, KK Yoder. *Integrating Delay Discounting and Functional Connectivity Findings in Nontreatment-Seeking Alcoholics.* 42nd Annual Meeting of Research Society on Alcoholism, Minneapolis, MN, June 2019.

ME Halcomb, M Džemidžić, J Goñi, **EJ Chumin**, KK Yoder. *Seed-Based Analysis of Resting State Functional Connectivity in the Default Mode and Salience Networks in Nontreatment-Seeking Alcoholics.* 41st Annual Meeting of Research Society on Alcoholism, San Diego, CA, June 2018.

GG Grecco, **EJ Chumin**, M Džemidžić, H Cheng, PR Finn, SD Newman, KK Yoder. *Preliminary Evidence for White Matter Microstructural Differences in Young Individuals with Alcohol Use Disorder.* 41st Annual Meeting of Research Society on Alcoholism, San Diego, CA, June 2018.

EJ Chumin, M Džemidžić, J Goñi, ME Halcomb, KK Yoder. *Consensus Community Structure Differences in Currently Smoking and Drinking Alcohol Use Disorder Individuals.* 41st Annual Meeting of Research Society on Alcoholism, San Diego, CA, June 2018.

EJ Chumin, GG Grecco, H Cheng, PR Finn, O Sporns, SD Newman, KK Yoder. *Preliminary Assessment of Structural Network Modularity in Young Individuals with Alcohol Use Disorder.* 41st Annual Meeting of Research Society on Alcoholism, San Diego, CA, June 2018.

EJ Chumin, M Džemidžić, J Goñi, ME Halcomb, KK Yoder. *Structural Network Segregation and Integration in Cigarette Dependence Independent of Comorbid Alcoholism.* International School and Conference on Network Science Meeting, Indianapolis, IN, June 2017.

EJ Chumin, M Džemidžić, ME Halcomb, TC Durazzo, J Goñi, KK Yoder. *Potential Additive Adverse Effects of Cigarette and Alcohol Dependence on White Matter Microstructure*. 40th Annual Meeting of Research Society on Alcoholism, Denver, CO, June 2017.

ME Halcomb, M Džemidžić, J Goñi, **EJ Chumin,** KK Yoder. *Seed-Based Analysis of Resting State Functional Connectivity in Nontreatment Seeking Alcoholics.* 40th Annual Meeting of Research Society on Alcoholism, Denver, CO, June 2017.

KK Yoder, SM Mustafi, **EJ Chumin,** KL Hile, ME Halcomb, MH Plawecki, SJ O'Connor, M Džemidžić, YC Wu. *Effects of Acute Alcohol Intoxication on Neurite Orientation Dispersion and Density Indices.* 40th Annual Meeting of Research Society on Alcoholism, Denver, CO, June 2017.

EJ Chumin, J Goñi, ME Halcomb, TC Durazzo, M Džemidžić, KK Yoder. *Altered Connectivity Through Areas of Compromised White Matter Microstructure in Comorbid Cigarette and Alcohol Dependence.* Greater Indiana Society for Neuroscience, Indianapolis, IN, March 2017.

EJ Chumin, ME Halcomb, JA Contreras, M Džemidžić, J Goñi, KK Yoder. *Preliminary Assessment of the Influence of Corticostriatal Structural Connectivity on Striatal [^{11}C]raclopride Availability in Social Drinkers and Nontreatment-Seeking Alcoholics.* 11th International Symposium on Functional NeuroReceptor Mapping of the Living Brain, Boston, MA, July 2016.

M Halcomb, **E Chumin,** J Contreras, J Goñi, M Džemidžić, KK Yoder. *Relationships Between Corticostriatal Functional Connectivity and Striatal [^{11}C]raclopride Availability in Social Drinkers and Nontreatment-Seeking Alcoholics.* 11th International Symposium on Functional NeuroReceptor Mapping of the Living Brain, Boston, MA, July 2016.

EJ Chumin, JA Contreras, M Džemidžić, ME Halcomb, J Goñi, KK Yoder. *Differential Structural Connectivity in Nontreatment-seeking Alcoholics*. 39th Annual Meeting of Research Society on Alcoholism, New Orleans, LA, June 2016.

M Halcomb, **E Chumin,** J Contreras, J Goñi, M Džemidžić, KK Yoder. *Altered Within- and Between Network Functional Connectivity as a Function of Drinking Status.* 39th Annual Meeting of Research Society on Alcoholism, New Orleans, LA, June 2016.

EJ Chumin, JA Contreras, M Džemidžić, ME Halcomb, J Goñi, KK Yoder. *Differential Structural Connectivity in Nontreatment-seeking Alcoholics.* Indianapolis Society for Neuroscience, Indianapolis, IN, March 2016.

JA Contreras, J Goñi, SL Rishacher, E Amico, JD West, **E Chumin**, BC McDonald, MR Farlow, O Sporns, AJ Saykin. *Mapping Cognitive Complaint Index onto Resting State Networks in Prodromal Stages of Alzheimer's disease*. Indianapolis Society for Neuroscience. Indianapolis, IN, March 2016.

M Halcomb, **E Chumin,** J Contreras, J Goñi, M Džemidžić, KK Yoder. *Altered Within- and Between Network Functional Connectivity as a Function of Drinking Status.* Indianapolis Society for Neuroscience, Indianapolis, IN, March 2016.

BG Oberlin, M Džemidžić, **EJ Chumin**, TA Myint, CM Soeurt, SJ O'Connor, KK Yoder, DA Kareken. *Alcohol Flavor Cue Prediction Error Induces Dopamine Release in Male Drinkers.* 38th Annual Meeting of Research Society on Alcoholism, San Antonio, TX, June 2015.

EJ Chumin, PR Territo, S Persohn, N Liu, BP McCarthy, AA Riley, X-M Xu, GD Hutchins, KK Yoder. *Variance of [^{18}F]FDG and [^{64}Cu]PTSM Uptake in a Mouse Brain.* IUPUI Research Day, Indianapolis, IN, April 2015.

EJ Chumin, DA Albrecht, KK Yoder. *Analysis of Galvanic Skin Response: Potential Relationships to Stimulus Responsivity and Brain Dopamine Signal.* The Linda and Jack Gill Center for Biomolecular Science Symposium, Bloomington, IN, September 2015.

EJ Chumin, CL Czachowski. *Neurotransmitter Specific Roles in the Basolateral Amygdala and Their Effect on Ethanol-Seeking and Intake.* Indianapolis Society for Neuroscience, Indianapolis, IN, October 2013.

Research Support

NIH F31 AA025518 (Chumin, PI; Yoder, Sponsor; Kareken, Co-Sponsor) 03/2018 – 07/2019
Cortical Connectivity in Alcoholism. This proposal aims to understand how structural connectivity of reward pathways relates to drinking behaviors and brain dopamine tone. Mr. Chumin is responsible for image processing and data extraction and analysis. Dr. Yoder is responsible for overseeing data acquisition, image processing, and data extraction and analysis, and training Mr. Chumin in these processes and techniques.
NIAAA AA07462 (Czachowski PI). Alcohol Training Grant. 05/2017 – 02/2018

Professional Development

Courses

- Diffusion Imaging in Python (DIPY) Workshop (2019); Organizer: Dr. Eleftherios Garyfallidis
- Mind Research Network SPM fMRI Course (2018); Instructors: Drs. Vince Calhoun, Tor Wager, & Kent Kiehl
- Grant Writers' Seminar and Workshop (2016); Instructor: Dr. John D. Robertson
- PET Pharmacokinetics (2016); Organizer: Dr. Roger N. Gunn
- PET101 – Basics of Positron Emission Tomography; Instructor: Dr. Karmen Yoder
- Statistical Methods in Brain Imaging; Instructor: Dr. Yaroslaw Harezlak
- Scientific Writing from the Reader's Perspective; Instructor: Dr. George Gopen
- Advanced Scientific Writing from the Reader's Perspective; Instructor: Dr. George Gopen

Compliance Training, Human Subjects Research

- 2016 CITI - Biomedical Researcher/Responsible Conduct of Research
- 2016 CITI - Good Clinical Practice Stage 1
- 2019 HIPPA Certification

Conference Attendance

- 42nd Annual Meeting of Research Society on Alcoholism. Minneapolis, MN, USA. June 21-26, 2019.
- 41st Annual Meeting of Research Society on Alcoholism. San Diego, CA, USA. June 16-20, 2018.
- 40th Annual Meeting of Research Society on Alcoholism. Denver, CO, USA. June 24-28, 2017.
- International School and Conference on Network Science. Indianapolis, IN, USA. June 19-23, 2017.
- 11th International Symposium on Functional NeuroReceptor Mapping of the Living Brain. Boston, MA, USA. July 13-16, 2016.
- 39th Annual Meeting of Research Society on Alcoholism. New Orleans, LA, USA. June 26-29, 2016.
- Society for Nuclear Medicine and Molecular Imaging Annual Meeting. Baltimore, MD, USA. June 6-10, 2015.

Scientific Service

- President (2016-2018): Medical Neuroscience Graduate Student Organization.